INFORMATION TO USERS

This manuscript has been reproduced from the microfilm master. UMI films the text directly from the original or copy submitted. Thus, some thesis and dissertation copies are in typewriter face, while others may be from any type of computer printer.

The quality of this reproduction is dependent upon the quality of the copy submitted. Broken or indistinct print, colored or poor quality illustrations and photographs, print bleedthrough, substandard margins, and improper alignment can adversely affect reproduction.

In the unlikely event that the author did not send UMI a complete manuscript and there are missing pages, these will be noted. Also, if unauthorized copyright material had to be removed, a note will indicate the deletion.

Oversize materials (e.g., maps, drawings, charts) are reproduced by sectioning the original, beginning at the upper left-hand corner and continuing from left to right in equal sections with small overlaps. Each original is also photographed in one exposure and is included in reduced form at the back of the book.

Photographs included in the original manuscript have been reproduced xerographically in this copy. Higher quality 6" x 9" black and white photographic prints are available for any photographs or illustrations appearing in this copy for an additional charge. Contact UMI directly to order.

UMI

A Bell & Howell Information Company
300 North Zeeb Road, Ann Arbor MI 48106-1346 USA
313/761-4700 800/521-0600

Hierarchical models of fishing behavior by factory trawlers in a midwater-trawl fishery for Pacific hake (*Merluccius productus*)

by

Martin William Dorn

A dissertation submitted in partial fulfillment
of the requirement for the degree of

Doctor of Philosophy

University of Washington

1998

Approved by Gordon R. Swartzman
Chairperson of Supervisory Committee

Program authorized
to offer degree School of Fisheries

Date March 12, 1998

Doctoral Dissertation

In presenting this dissertation in partial fulfillment of the requirements for the Doctoral Degree at the University of Washington, I agree that the Library shall make its copies freely available for inspection. I further agree that extensive copying of this dissertation is allowable only for scholarly purposes, consistent with "fair use" as prescribed in the U.S. Copyright Law. Requests for copying or reproduction of this dissertation may be referred to University Microfilms, 1490 Eisenhower Place, P.O. Box 975, Ann Arbor, MI 48106, to whom the author has granted "the right to reproduce and sell (a) copies of the manuscript in microform and/or (b) printed copies of the manuscript made from microform."

Signature Martin Dunn

Date March 12, 1998

University of Washington

Abstract

Hierarchical models of fishing behavior by factory trawlers in a midwater-trawl fishery for Pacific hake (*Merluccius productus*)

by Martin W. Dorn

Chairperson of Supervisory Committee:
Research Professor Gordon L. Swartzman
School of Fisheries

The fishing behavior of factory trawlers in the Pacific hake (*Merluccius productus*) fishery at different spatio-temporal scales was studied using several modeling techniques. In Chapter 1, a Markov decision process model was developed for the scheduling of fishing operations on a factory trawler. Stochastic dynamic programming was used to obtain the optimal controls for setting and retrieving the net. The optimal controls generally consisted of a bin threshold that signals the vessel to start fishing and a catch threshold that signals the vessel to stop fishing. A range of simple "rule of thumb" strategies generated nearly as much net revenue as the optimal control, indicating that the reward surface is flat in the region of the optimal control.

In Chapter 2, a statistical analysis was conducted of mesoscale (5-50 km) movement patterns of factory trawlers. Generalized additive models (GAM) were used to examine influence of the catch rates of prior hauls on the distance between successive hauls. Results of GAM models suggested that deviations from the expected catch rate influence the decision to move from a local foraging area, as expected from optimization models of animal foraging. These decisions appeared to be based on relatively short time

frames, such that information from only the most recent 1-2 hauls in the area are utilized. In addition, results indicated that the presence of other fishing vessels operating nearby reduces the probability that a vessel will leave an area.

In Chapter 3, a simulation model was developed for an individual factory trawler. The model integrated the results of the above analyses in a hierarchical model of decision-making at different spatio-temporal scales. Decision-making occurred at two scales: 1) choosing an area within which fishing will be conducted, and 2) scheduling haul setting and retrievals while fishing within an area. A novel aspect of the model was a procedure, based on the Kalman filter, for modeling information about local fish densities gained by searching and fishing. The simulation model was used to identify the optimal decision rules, and to evaluate the usefulness of indices derived from factory trawler catch data to monitor population abundance trends.

TABLE OF CONTENTS

LIST OF FIGURES

LIST OF TABLES

ACKNOWLEDGMENTS

I thank my supervisory committee, Drs. Gordon Swartzman, Ana Parma, Ray Hilborn, Robert Francis and Joe Rutledge, for their guidance during the course of my studies and research. I am especially indebted to committee chairperson Dr. Gordon Swartzman for his steadying influence and long-term commitment to this project. I am grateful to Drs. Richard Marasco, Anne Hollowed, and Richard Methot of the Alaska Fisheries Science Center, Resource Ecology and Fisheries Management Division, for providing me with the financial support, facilities, and time to conduct this research.

Portions of the manuscript were reviewed by Anne Hollowed, Daniel Kimura, Martin Loefflad, Joseph Terry, Jimmie Traynor, Marianne Vignaux, and Neal Williamson. I thank them for their insights and comments. Chris Wilson and Ed Nunnallee generously provided unpublished acoustic survey data. I thank Dr. Michiyo Shima for advice and encouragement. Finally, I thank the officers and crew of the factory trawlers *Alaska Ocean* and *American Triumph* for making me feel welcome and giving me the opportunity to observe their fishing operations.

INTRODUCTION

Fishing is an ecological interaction between a predator and a prey species. Because of the ecological basis of fishing, experiments and theoretical work on the foraging behavior of animal predators provide the conceptual framework for interpreting the behavior of fishing vessels. However, before models of animal foraging are applied to fishery problems, the similarities and differences between fishing vessels and animal predators needs to be considered carefully. For commercial fishing, the operational unit of predation is the fishing vessel, not an individual organism. Fishing vessels are powered by internal combustion engines, so they do not depend on the energy content of their prey for their continued activity. Because they are man-made, their entry and exit from the fishery is not limited by biological rates of increase and decrease.

Commercial fishing is also a technologically-advanced activity that operates in an economic setting. Fishing technology has followed two main paths of development. The first path is technology that increases the efficiency of fish capture and processing: the design of vessels, nets, and machinery. The second is technology that extends human sensory ability. Modern fishing vessels are equipped with an array of electronic sensing devices such as radar, echo-sounders, global positioning systems, and net recorders. These sensing devices give fishermen the ability to recognize objects and navigate in the marine environment--sensory and orientation abilities similar to those of marine mammals, such as cetaceans, which have evolved these abilities over evolutionary time scales.

A general frame of reference for the study of fishing behavior was advocated by the pioneering work of Allen and McGlade (1986):

> *"Fishing is one of the few remaining examples in the world today of ancestral hunting activities in humans... Fishing represents a fascinating "case study" of the much more general and wider issues of adaptiveness, creativity, and learning. This is interesting not only for itself and the role that new methods can play in managing such a vital industry, but also because of the general principles it raises. Within a problem having fairly clear boundaries, all the great questions of our relationship to nature, the problem of managing a complex system, and of finding a balance between risk and yield, are posed, and hopefully from this type of work, a new understanding will emerge in both particular and general cases".*

In many respects, the factory trawlers in the Pacific hake fishery represent the ultimate achievement of fishing technology. The advanced technology of these vessels, including hydraulic winches to set and retrieve extremely large nets, automated filleting machines, flash freezers, freezer holds, fish meal plants, electronic echosounders, and GPS navigation and plotting equipment, enables them to efficiently catch and process large quantities of fish (up to 500 metric tons per day). Because of this exceptional fishing power, factory trawlers can have significant impacts, both ecologically and economically. Management of fisheries involving factory trawlers must be based on sound scientific

understanding of how these vessels operate. Management actions that ignore the constraints and tradeoffs under which fishing vessels operate may fail to achieve their intended purposes, or may have unforseen adverse consequences.

This dissertation promotes the view that fishing behavior results from a decision process based on uncertain information about a stochastic environment. The decisions made by fishermen depend on the spatial and temporal scale at which they assess the environment. Models and analyses of fishing behavior have focused on the problem of patch selection by fishing vessels (Hilborn and Ledbetter 1979, Mangel and Clark 1983, Lane 1989, Gillis et al. 1993). The historical focus on patch selection has left other aspects of fishing strategy unexamined. Recent ecological models of animal foraging have emphasized the hierarchical character of decisions made by foraging animals (Holling 1992). A decision hierarchy appropriate for trawlers consists of at least four levels: 1) the decision to participate in a fishery, 2) the selection of a patch or fishing grounds on which to operate, 3) the scheduling of fishing operations within that patch, and 4) decisions associated with fishing depth, trawling speed, and compass bearing while actively fishing. Each level has a characteristic spatial and temporal scale. Decisions on which fishery to participate in are made annually with a spatial scale ~1,000 km; patch selections are made for periods ranging from several days to several weeks with a spatial scale of ~10-50 km. Decision-making within a patch affects behavior over shorter intervals and smaller spatial scales.

In this dissertation, the fishing behavior of factory trawlers at different spatio-temporal scales was investigated using several modeling techniques. In Chapter 1, a

Markov decision process model was developed for the scheduling of fishing operations on a factory trawler while operating within a mesoscale aggregation fish. Stochastic dynamic programming was used to obtain the optimal controls for setting and retrieving the net. A simple prototype, where the random catch increment while fishing is an independent draw from a single probability distribution, was analyzed. Results from forward simulations of a vessel following the optimal control are compared with at-sea observer data for the 1991-95 hake fishery and simple "rules of thumb" that mimic the more complex optimal controls. More complex and realistic models with correlated catch increments and diel patterns in the catch increments are developed and analyzed. Potential changes in fishing behavior and net revenue during a temporary ban on night fishing in 1992 were investigated using the model with a diel trend in the catch increments.

In Chapter 2, several statistical analyses focused on the mesoscale characteristics of the environment (5-50 km), and vessel movement at these spatial scales. The analyses of vessel movement presented in this chapter are motivated by a contribution to optimal patch foraging theory by Arditi and Dacorogna (1985, 1988). The appropriate spatial scale at which to assess vessel movement patterns is identified by geostatistical analysis that assesses the spatial continuity of Pacific hake using data from acoustic resource assessment surveys conducted by the NOAA research vessel *Miller Freeman* during July-September of 1992 and 1995 (Dorn et al. 1994; Wilson and Guttormsen 1997). Then, using fishery data collected by at-sea observers, models are fit to the haul-by-haul catch rates of the factory trawler fleet during 1991-95 using time of day and vessel as predictor variables. The residuals from this model are then used in a generalized additive model

(GAM) to predict the probability of movement from a foraging area. Other variables are also assessed in the model. Finally, the results are compared with other studies of spatial correlation and fishing behavior, and recommendations are offered about further research into fishing behavior.

In Chapter 3, a simulation model was developed for an individual factory trawler. The model integrated the results of the analyses in Chapters 1 and 2 in a hierarchical model of decision-making at different spatio-temporal scales. The model was used to explore several concepts that provide new insight into fishing behavior. A central theme of the model was the role of decision-making at different spatio-temporal scales. Decision-making occurred at two scales: 1) choosing an area within which fishing will be conducted, and 2) scheduling haul setting and retrievals while fishing within an area. These decisions were considered to be state-dependent, with the state consisting of both the internal state of the vessel, represented by the amount of fish in holding bins and the amount of fish already in the net, and the external state of the environment, represented by the density of Pacific hake in the area.

A novel feature of the model was a procedure based on the Kalman filter for modeling expert knowledge about local fish densities gained by searching and fishing. Information about local fish density is processed by the fisherman, and retained in memory as a spatial representation, or a "map." Although the spatial structure of the map and the updating procedures are quite simple in the model presented in this chapter, the concept is general and can be extended to other kinds of information available to the fisherman about local fish densities. The simulation model was used to identify the optimal decision rules,

to explore the relationship between mean fish density and various aspects of vessel performance, and to evaluate the usefulness of indices derived from factory trawler catch data to monitor population abundance trends.

Each chapter of this dissertation was written to stand on its own as an independent paper. Chapter 1 is cited elsewhere in the dissertation as Dorn (1998); Chapter 2 is cited as Dorn (1997). When submitted for publication, each paper included a short introductory section that provided background information on the factory trawler fleet and the Pacific hake population. Rather than to repeat the same information in each chapter, this section has been moved forward to the introduction and follows this paragraph.

Factory Trawlers and Pacific Hake

U.S. factory trawlers are a recent and influential component of the fishing fleet off the west coast of North America. Since 1990, these vessels have accounted for more than one million metric tons (t) of groundfish catch per year from off the West Coast and in Alaskan waters (NMFS 1996). The at-sea processors in the Pacific hake fishery have onboard surimi (minced fish flesh) production capacity, and were designed to fish primarily for walleye pollock (*Theragra chalcogramma*) in Alaska fisheries. Generally, these vessels also have the capacity to produce frozen fillet blocks and have a fish meal plant that processes the waste from the making of surimi. Although some fishing companies have several boats participating in the hake fishery, most vessels are from different companies. There are two classes of at-sea processors in the Pacific hake fishery: factory trawlers, which catch and process their own fish, and motherships, which process

deliveries from catcherboats, but do not fish on their own.

During 1991-95, an average of 14 factory trawlers and five motherships participated in the Pacific hake at-sea fishery each year, with an average aggregate catch of 150,000 metric tons (t) per year. The factory trawlers in the Pacific hake fishery are large vessels (length 275-375 ft), carry a crew of 70-100, and are capable of trips lasting several months. Between 50% and 70% of the crew is engaged in surimi production. Several work shifts man the processing factory 24 h per day. Midwater trawls (mean trawl opening 90 x 55 m) are used exclusively for Pacific hake. The fishery is managed using an annual harvest guideline (i. e., quota), with a separate allocation reserved for the shore-based processing sector. The at-sea fishery operates as a "derby" fishery where all vessels compete for the fleet-wide quota. The American fishery for Pacific hake is a recent development. As the opportunities to fish for pollock were cut back due to increases in the size of the fleet, other species became viable alternatives. In 1991, these vessels entirely displaced the joint venture fishery for Pacific hake, dramatically changing the character of the at-sea fishery. Prior to 1991, the fishery lasted for as long as 6 mo. Currently, the at-sea fishery closes 3-4 wk after the annual opening date of April 15.

As is usual with targeted midwater trawling, catches in the hake fishery are extremely pure, with bycatch typically amounting to less than 3% of the total catch by weight. The most common bycatch species are pelagic rockfishes and mackerels: yellowtail rockfish (*Sebastes flavidus*), widow rockfish (*Sebastes entomelas*), Pacific ocean perch (*Sebastes alutus*), jack mackerel (*Trachurus symmetricus*), and Pacific mackerel (*Scomber japonicus*). The bycatch is either discarded at sea or diverted to the

fish meal plant. Although the bycatch of chinook salmon (*Oncorhynchus tshawytscha*) is low (4,000-6,000 fish per year), it is an important concern due to the extremely low abundance of many West Coast chinook salmon populations. Several West Coast chinook salmon runs are listed as endangered under terms of the U.S. Endangered Species Act (Waples et al. 1991; Fisher 1994).

Pacific hake form aggregations of sufficient density to support fishing activity along the continental shelf break from northern California to Vancouver Island. The affinity of Pacific hake for the shelf break habitat produces a fishing region that is much narrower in its east-west dimension than its north-south dimension. The north-south range of fishing is 750 km, while the fishery is conducted over bottom depths ranging from 150 m to 600 m, an area that is between 10 km and 30 km wide. Interspersed regions of high and low density extend along the entire coast. Certain features along the shelf break tend to support higher densities of Pacific hake (e.g., Heceta Bank off central Oregon, Willapa-Guide Canyons off southwest Washington, and Juan de Fuca Canyon off Cape Flattery). In general, areas of high hake density are not persistent features, and so will have to be detected by the vessel before they can be exploited. From the perspective of the fisherman, the key spatial characteristics of the hake population are 1) a narrow elongated region of potential occurrence, and 2) transient fishable aggregations of 15-30 km in size that can be fished multiple times.

CHAPTER 1 - FINE-SCALE FISHING STRATEGIES OF FACTORY TRAWLERS

INTRODUCTION

Although the use of catch per unit effort (CPUE) to monitor the abundance of fish stocks has a long history (Smith 1988), researchers have only recently begun to consider fishing behavior as a legitimate subject for investigation (Hilborn and Ledbetter 1979, Gillis et al. 1995a). This emerging field of study is not as concerned with the time-honored objective of indexing abundance as it is with gaining a better understanding of the principles that govern fishing behavior. Much of this research has been guided by ecological models of optimal patch selection by animal foragers (Gillis et al. 1993), although economic aspects of fishing strategy have occasionally been studied (Lane 1989). Markov decision process models (or stochastic dynamic programming models) have proven to be useful tools for studying fishing behavior as a particular case of a general class of optimal foraging problems in behavioral ecology (Mangel and Clark 1988). Ultimately, this research has the promise of developing new techniques for interpreting fishing experience in a less restrictive way to monitor the abundance of fish populations. Operational models of fishing also have immediate practical applications in evaluating the consequences of management actions on the fishing industry. Management actions that ignore the constraints and tradeoffs under which fishing vessels operate may fail to achieve

their intended purposes, or may have unforseen adverse consequences (Gillis et al. 1995a).

The choices available to fishermen of fishing strategy depend on the spatial and temporal scales of their assessment of the environment. Models and analyses of fishing strategy have mainly focused on the problem of patch selection by fishing vessels (Hilborn and Ledbetter 1979, Lane 1989, Gillis et al. 1993), leaving other important aspects of fishing behavior unexamined. Recent ecological models of animal foraging have emphasized the hierarchical character of decisions made by foraging animals (Holling 1992). A decision hierarchy appropriate for trawlers consists of at least four levels: 1) the decision to participate in a fishery, 2) the selection of a patch or fishing grounds on which to operate, 3) the scheduling of fishing operations within that patch, and 4) decisions associated with fishing depth, trawling speed, and compass bearing while actively fishing. Each level has a characteristic spatial and temporal scale. Decisions on which fishery to participate in are made annually with a spatial scale ~1,000 km; patch selections are made for periods ranging from several days to several weeks with a spatial scale of ~10-50 km (Fig. 1.1). Decision-making within a patch affects behavior over shorter intervals and smaller spatial scales.

Models with different temporal and spatial scales can shed light on different aspects of fishing behavior. This chapter adopts a fine-scale focus to develop a model for decision-making over short periods of time by fishing vessels operating within a large-scale aggregation of fish. At this level of detail, it is reasonable to suppress the spatial aspects of foraging and focus exclusively on time scheduling problems. On trawlers, an important component of decision making at this scale is the temporal scheduling of two

events: setting the net, which initiates fishing, and retrieving the net, which ends fishing. A factory trawler will seek to maintain the flow of fish from holding bins into the factory by starting to fish when the amount of fish in the bins becomes low. If the vessel waits too long to start fishing, there is a risk that the factory will run out of fish before the next haul can be landed. If the vessel starts to fish too soon, it may catch fish for which there is no space in the holding bins. While fishing, the vessel must decide whether to continue fishing or to retrieve the net with the fish already caught. If the vessel continues to fish for too long, it may capture so many fish that retrieval is difficult and fish are damaged during retrieval, lowering product quality.

This research is motivated by a series of events that occurred in 1992. Based on an analysis which suggested that chinook salmon bycatch was higher at night, the Pacific Fishery Management Council (PFMC) established a night closure for the 1992 hake fishery extending from midnight to one hour after official sunrise. At-sea processors objected to the night fishing ban, contending that the night closure disrupted fishing and processing operations. In response to these concerns and to a re-analysis of the salmon bycatch which suggested that bycatch rates were not significantly higher at night, the Council limited the night closure to south of 42°N lat., leaving most of the fishing grounds open to fishing at night. Evidently, factory trawlers considered night fishing important, despite lower catch rates (the catch rate at night is approximately one-third of the catch rate during the day) and possibly higher bycatch rates. The reasons for this are unclear. One possibility is that the factory trawlers were unable to catch enough fish during daylight hours to keep the factory operating at night, forcing shutdowns that reduced

efficiency. However, not enough was known about daily fishing operations on a factory trawler to evaluate whether fishing at night was necessary for a profitable operation. To explore these hypotheses required the development of new analytical tools.

Here I present a Markov decision process model for the scheduling of net setting and retrievals for a factory trawler. The model will be used to study how the state of the factory trawler influences decision-making, as measured by the tons of unprocessed catch in holding bins and the amount of fish in the net when the vessel is fishing. Since factory trawlers process their catch onboard, optimization models where the fishing vessel maximizes the landed value of catch are not appropriate for studying the fine-scale aspects of decision-making. Such vessels are constrained by their daily processing capacity, so an increase in daily catch above a certain level would not result in a corresponding increase in daily production. Here I assume that the objective of the factory trawler is to maximize the daily net revenue, which implies that they are risk-neutral (Squires and Kirkley 1991).

Although the major focus in this chapter is on optimal strategies, recent studies on foraging behavior of animals suggests that animals do not generally act according to predictions of optimal foraging models and are as likely to employ simple "rules of thumb" to guide their foraging activities (Kareiva et al. 1989). In addition, the reward surface is often flat, suggesting that a wide range of strategies can result in close to the maximum reward. To explore these possibilities, a section of this chapter uses forward simulation of the fishing process to test simple "rules of thumb" against the optimal strategies.

The subsequent sections of the chapter are organized as follows. The Markov decision process model is developed, and the dynamic programming algorithm used to

obtain the optimal controls is described. An analysis of a simple prototype is presented, and the results from simulations of a vessel following the optimal control are compared with at-sea observer data and some simple "rules of thumb" that mimic the more complex optimal controls. The simple prototype assumes that the random catch increment is an independent draw from a single probability distribution. Subsequent sections consider more complex and realistic models with correlated catch increments and diel patterns in catch increments. The question of whether a ban on night fishing significantly reduces net revenue is examined using the model with a diel trend in the catch increments. Finally, the implications of the model results are discussed and the major conclusions are briefly summarized.

METHODS

Model development

Markov decision process models are discrete time representations of continuous time processes. The sequence of events that occur at each time step is as follows. First, the state of the vessel is observed. Based on the observed state, a decision is made whether to fish or not. Next, a random catch increment is generated according to a given probability distribution. The reward is then calculated and added to previous rewards. Finally, the state equations update the state to the next step. If the next step is the final period, then the terminal reward is added to the previous rewards and the process stops; otherwise, the same sequence of events is repeated for the next time step. The model was configured to increment time in 15 min steps, which gave the model sufficient resolution

to capture the pattern of net setting, fishing, and net retrieval that make up the daily schedule on a factory trawler.

The state of the fishing vessel at each time step k consists of three variables: the weight of unprocessed fish on board, x_k, the weight of fish currently in the net, c_k, and a ship status indicator variable, s_k, which keeps track of the current activity of the vessel. States $s_k = 1, 2$ occur in sequence after the decision to retrieve the net. The second state in the sequence, $s_k = 2$, is needed because once the vessel begins hauling back, it is committed to completing this activity during the following time step. In state $s_k = 3$, the vessel is able to fish, but not yet doing so. In state $s_k = 4$ the vessel is actively fishing. With these dynamics, the catch is added to the fish in the bins 45 min after the decision to stop fishing. Fish begin entering the net 15 min following the decision to start fishing. The state variables x_k and c_k are observable at each time step, implying that fish bins can be monitored periodically, and that the vessel can monitor the catch already in the net while fishing. This assumption is reasonable because net telemetry on a factory trawler typically includes headrope-mounted side-scan sonar, which detects fish entering the net, and net tension indicators, which trigger as the net fills with fish.

In each time step, the weight of fish in the bins, x_k, decreases by the quantity the factory processes in a time step, p. In vessel state $s_k = 2$, the catch is added to the fish in the bins at the end of the time step. The state dynamics for the weight of fish in the net, c_k, depends on the ship status. If the vessel is fishing, the weight of fish in the net increases by a catch increment, w_k, drawn from a known non-negative probability distribution. During a haul-back sequence ($s_k = 1, 2$), the weight of fish in the net

remains constant, $c_{k-1} = c_k$. When the vessel is not fishing ($s_k = 3$), $c_{k-1} = 0$.

The decision set is $u_k \in \{0, 1\}$, where $u_k = 0$ is the decision not to fish, and $u_k = 1$ is the decision to fish. During the haul-back sequence ($s_k = 1, 2$), the vessel is committed to completing the sequence, reducing the decision set to the single element $u_k \in \{0\}$. Although this model is conceptually straightforward, considerable detail is needed to treat the haul-back and net-setting sequences realistically. The state transitions may be easier to follow as listed in Table 1.

The state equations (Table 1) are subject to the constraints $0 \le x_k \le x_{max}$, and $0 \le c_k \le c_{max}$, where x_{max} is the maximum capacity of the fish bins, and c_{max} is the maximum capacity of the net. The need for a constraint on the weight of fish in the bins is obvious, and could be achieved by spilling fish from a net that has been retrieved, or by discarding some of the fish already in the bins to make more space. A constraint on the maximum amount of fish in the net is a reasonable requirement, but awkward to model. If a vessel continues to fish when $c_k = c_{max}$ and catch does not increase, then a potentially viable strategy might be to fill the net with fish, then delay the decision to haul back until some later time. In reality, this strategy would not be possible. Consequently, when $c_k = c_{max}$ the decision set was reduced to the single element $u_k \in \{0\}$ so that the vessel would not have the option of continuing to fish. Vessels avoid overfilling the net, and the model ought to include this behavior. This was done by adding a penalty for oversize catches which will be described shortly.

The random catch increments were modeled with a Δ-distribution, which specifies the probability of a zero catch and models the nonzero values with a log-normal

distribution (Pennington 1983). Although the robustness of the use of this distribution to estimate abundance indices from survey data has been questioned (Smith 1990), the Δ-distribution was used here only for modeling. The mean of Δ-distribution was set equal to the mean fishery catch rate in the at-sea fishery in 1993, while the probability of a zero catch increment and the coefficient of variation (CV) of the Δ-distribution were obtained from the acoustically measured density of hake during the 1992 NMFS acoustic survey (Dorn et al. 1994). The purpose of this two-step process was to obtain a parametric probability distribution that approximated the catches per 15 min time step that would be encountered by a factory trawler in the Pacific hake fishery. For the optimization model, the Δ-distribution was discretized so that possible catch increments were even multiples of the processing rate (p = 4.0 t per 15 min time step) from zero to 200 t. The state variables x_k and c_k were discretized in the same way so that no interpolation was needed to update the state to the next time step.

The reward per time step is the value of surimi and fish meal produced during that time step, minus costs and penalties. The positive part of the reward is the processing rate multiplied by conversion factor, ρ, which converts raw fish weight to product value. It is assumed that product value does not depend on the intrinsic characteristics of the fish (i.e., size or sex), or on how long the fish have been held before processing. Although Pacific hake are highly perishable, a vessel that processes its catches sequentially would hold fish for a maximum of $x_{max}\ p^{-1}$ h (about 12 h for most factory trawlers). Declines in product quality are relatively slight over this interval. The activity costs of the vessel, $\kappa(s_k, u_k)$

depend on vessel status and on the decision, u_k. There are three different costs, a per time step cost while fishing, κ_f, a per time step cost while not fishing, κ_{nf}, and a per time step cost while the vessel is setting or retrieving the net, κ_{sr}.

Penalties can be incurred for discarded fish, ν_1, and for oversize catches, ν_2. Discards occur only when the net is retrieved and the total catch is greater than the remaining space in the bins. Under current management policy, no financial penalties are incurred by a vessel for discarded fish. However, discard is subtracted from the quota so that the total amount of fish available to the fishery is reduced by a corresponding amount. Furthermore, fishermen may have other motives for avoiding discard, such as ethical concerns about fully utilizing the catch, and a desire to gain advantage in political settings where decisions are made about how to allocate the catch between user groups. The penalty for oversize catches is imposed for catches above a threshold, c_{thresh}. Large catches are hazardous to the deck crew, damage fish, and increase the likelihood of equipment failure. These would impose additional costs or reduce revenue. The net reward during a time step, g_k, is given by

$$g_k(x_k, c_k, s_k, u_k) = \begin{cases} \rho \min(p, x_k) - \kappa(s_k, u_k) - (\nu_1 + \nu_2) & \text{if } s_k = 2 \\ \rho \min(p, x_k) - \kappa(s_k, u_k) & \text{otherwise} \end{cases},$$

except for the final step, where $g_T(x_T) = \rho x_T$. The penalties ν_1 and ν_2 are incurred only when the catch is added to the fish already in the bins ($s_k = 2$), and are given by

$$v_1 = \begin{cases} \gamma_1(x_{k+1} - x_{\max}) & \text{if } x_{k+1} > x_{\max} \\ 0 & \text{otherwise} \end{cases},$$

$$v_2 = \begin{cases} \gamma_2(c_k - c_{thresh})^2 & \text{if } c_k > c_{thresh} \\ 0 & \text{otherwise} \end{cases},$$

where γ_1 and γ_2 are penalty weights that specify the relative importance of the penalties for discard and oversize catches, respectively. The influence of these weights on decision-making will be examined later. The penalty for discard, v_1, increases linearly with an increase in discard. The penalty for oversize catches, v_2, is quadratic above the threshold, modeling the escalating difficulties of handling larger catches. The use of a quadratic function to model these difficulties was based on interviews with observers and limited personal observations on fishing vessels. The most significant problem with large tows reported by fishermen is the decline in product quality due to compression of fish in codends as they are hauled out of the water.

Solving the optimization problem

Assume that the vessel fishes for T time steps, with T arbitrarily large. The objective of the vessel is to maximize the total expected reward over this period. The total

expected reward, J, as a function of the initial states x_0, c_0, and s_0 is given by

$$J(x_0,c_0,s_0|u_0,u_1,u_2,\ldots,u_{T-1})$$

$$= \underset{w_k,\, k\,=\,0,\ldots,T-1}{E} \left\{ g_T(x_T) + \sum_{k=0}^{T-1} g_k(x_k,c_k,s_k,u_k) \right\}.$$

The expected reward will depend on the sequence of decisions $u_0,u_1,u_2,\ldots,u_{T-1}$ made over this period. To solve the optimization problem, we seek a control law, a sequence of functions $\pi = \{\mu_0,\mu_1,\ldots,\mu_{T-1}\}$, where μ_k defines the decision u_k for any vessel state at step k: $u_k = \mu_k(x_k,c_k,s_k)$. A control law is a plan of action, determined in advance, that specifies the decision for every possible state of the vessel. The optimal control law π^* is the element of the set of feasible control laws Π that maximizes expected reward:

$$J_0^*(x_0,c_0,s_0) = J(x_0,c_0,s_0|\pi^*)$$

$$= \max_{\pi\,\in\,\Pi} \underset{w_k,\, k\,=\,0,\ldots,T-1}{E} \left\{ g_T(x_T) + \sum_{k=0}^{T-1} g_k(x_k,c_k,s_k,\mu_k) \right\},$$

where $J_0^*(x_0,c_0,s_0)$ is the maximum expected reward for the entire period. To solve this problem the dynamic programming algorithm is used (Bertsekas 1987). The dynamic

programming algorithm is based on the Bellman optimality principle, which states that a control law that is optimal for the entire period must also be optimal starting from some intermediate step. It is therefore possible to solve the optimization problem for the next to last time step and then work backwards in time toward the initial time step to obtain the optimal control law for the entire period. The recursive equations are given by

$$J_T^* = g_T(x_T) ,$$

$$J_k^*(x_k, c_k, s_k) = \max_{u_k(s_k)} \; E_{w_k} \left\{ g_k(x_k, c_k, s_k, u_k) \right.$$

$$\left. + J_{k+1}^*\left[x_{k+1}(x_k, c_k, s_k, u_k), c_{k+1}(c_k, s_k, u_k, w_k), s_{k+1}(s_k, u_k) \right] \right\} ,$$

where $J_k^*(x_k, c_k, s_k)$ is the maximum expected reward starting at the kth time step.

For the models considered in this chapter the optimal control law becomes stationary as the recursive equations get further away from the final step. In the results, I focus on stationary control laws rather than time-dependent controls, which become important only when little time remains before the closure of the fishery. A stationary control law was approached within 100-200 time steps (~ 1-2 days) moving backwards in time before the terminal time step. However, time-dependent controls may be important in assessing regulations, particularly fishing closures.

Parameter values for a simple prototype

To investigate fishing strategy in the at-sea Pacific hake fishery, the optimization model was configured with parameters representative of a typical factory trawler. For this simple prototype, the random catch increments were generated from a single probability distribution with no serial correlation or trend. Model parameters were estimated from observer data obtained during the 1993 at-sea fishery and from cost and production surveys (Freese et al. 1995). Since all at-sea processors carry observers, the observer database is a complete record of the position, set and retrieval time, and total catch of all hauls by all vessels in the fishery. For some parameters, however, the available data permitted only a rough estimate of the appropriate value; in such cases the sensitivity of the optimal control to the parameter value was assessed. The following parameters were used in the prototype.

1) Total bin capacity: 200 t. Estimates of bin capacity are not available for all factory trawlers. Two hundred t is the mean of five bin capacities recorded by observers in the 1993 hake fishery.

2) Maximum net capacity: 160 t. The maximum of observed catches in 1993 was 161 t. Observer logbooks record instances where hauls ~150-170 t could not be brought up the stern ramp, and some of the catch had to be discarded.

3) Processing rate: 4.0 t per 15 min time step. At this processing rate the vessel could process 384 t/d, which is the 84th percentile of the catch per day during the 1993 fishery. Since daily catches should not greatly exceed the daily processing capacity, this processing rate is a reasonable approximation. No direct observations of factory processing rates are available.

4) Revenue per ton of hake catch (includes both surimi and fish meal) ($): 260. (Freese et al. 1995.)

5) Costs ($). An estimate of the cost of operating a factory trawler is 80,000 per day (833 per time step) (Freese et al. 1995). The model provides for three different per time step costs: a cost incurred while fishing, κ_f, a cost incurred while not fishing, κ_{nf}, and a cost incurred while setting or retrieving the net κ_{sr}. Based on fuel consumption, the potential for equipment failure or damage, and the crew's activity level, a ranking of the costs $\kappa_{nf} < \kappa_f < \kappa_{sr}$ is reasonable. For the simple prototype, the values $\kappa_{nf} = 800$, $\kappa_f = 840$, and $\kappa_{sr} = 880$ were used.

6) Penalty weight for discards ($): 130. With this penalty weight, a ton of discard incurs a penalty equal to one-half the revenue that it would have produced. If Pacific hake were managed using an individual transferrable quota system (ITQ) where discards are counted against the quota, the penalty for discard would be equal to the revenue that it would have produced. Here some intent to avoid

discard is assumed, but less than would be expected under an ITQ system.

7) Penalty weight for oversize catches ($): 0.722. With this penalty weight, the penalty incurred by a catch equal to the net capacity (160 t) is equal to the revenue generated by 10 t of unprocessed catch. A catch smaller than 100 t incurs no penalty. This threshold is the 93rd percentile of the observed haul weight for factory trawlers in the 1993 at-sea fishery.

Parameter values for the Δ-distribution of random catch increments were obtained from two sources: the catch rates in the 1993 at-sea fishery and acoustically measured densities of hake along transects during the 1992 NMFS acoustic survey. The best way to estimate these parameters would be to use the catch by 15 min time steps in the fishery. Collecting this information would require the installation of a calibrated echosounder on a fishing vessel. With the fisheries data that are available, catch rates can be calculated only for entire tows (total catch/haul duration). The mean of these catch rates is appropriate to use for the mean of the Δ-distribution, but the CV and the probability of a zero catch would be higher for 15 min time steps than the catch rate for entire tows. The mean catch per 15 min time step in the at-sea fishery in 1993 during the day (06:00-20:00) (all times are in Pacific Daylight Time) was 13.9 t per 15 min (CV = 1.18), while at night the mean catch rate was 5.0 t per 15 min (CV = 1.00). The day catch rate of 14.0 t per 15 min was used as the mean of the probability distribution of catch increments for the basic prototype.

The acoustically-measured densities of hake along transects during the 1992 NMFS acoustic survey were used to obtain the CV and the probability of a zero catch increment. These data consisted of mean acoustic densities for 1 nmi transect segments with bottom depths between 150 and 600 m from 43°00'N to 48°15'N (n =377). This region corresponded to the area where the at-sea fleet fished in 1993. Since mean towing speed in the at-sea hake fishery is 4.0 knots, a vessel transits approximately 1 nmi in 15 min. Mean acoustic densities were converted to nominal catches for 15 min time steps by assuming that a midwater trawl captures all the fish in the water column and calculating the area swept by a net with 90 m horizontal opening in 1 nmi of trawling. Since fishing is not random within the area where the fishery operates, this approach may misrepresent the distribution of potential catch increments. However, out of the limited alternatives available, this method was considered to be the most reliable.

The empirical distribution of acoustic hake densities was right-skewed and contained 7.7% zero observations (mean = 9.4 t per 15 min interval, CV (coefficient of variation) = 1.5). A Kolmogorov-Smirnov test (using the critical values by Lilliefors (1967)) indicated that the logarithm of the non-zero observations differed significantly from a normal distribution ($\alpha = 0.05$). This significant result was due to the presence of seven small non-zero values. The Kolmogorov-Smirnov test for the logarithm of values > 0.135 was not significant, and quantile-quantile plots against a normal distribution indicated that a lognormal distribution was appropriate for catch increments > 0.135 t per 15 min. Since rounding these smaller values down to zero does not substantially change the mean and the coefficient of variation, a Δ-distribution was considered an appropriate

parametric distribution to model these data. The probability of a zero catch increment was estimated as 36/377=0.095. Conversion formulas in Pennington (1983) were used with the CV of the acoustic data (1.5) and the mean fishery catch rate (14.0 t per 15 min time step) to obtain the mean and standard deviation of the log-normal distribution for the non-zero part of the distribution.

The final step consisted of obtaining a discrete probability distribution for catches of 0, 4, 8, ... , 160 t as required by the dynamic programming algorithm. This was obtained by summing the probability mass between the bin limits. The bin limits were located at the midpoints of adjacent values of 0, 4, 8, ... , 160 t on a log scale. The bin boundary between zero and 4 t was arbitrarily set at 2 t. Two additional stochastic models for the catch increments are developed in subsequent sections, a model with first-order serial correlation, and a model with diel trends. In both cases, the parameters for the model were obtained in a similar way to the method described above, where the expected catch increment was obtained from fishery catch rate data, and other parameters (i.e., variance, probability of zero catches) were estimated with acoustic survey data.

RESULTS

Description of the stationary optimal control for a simple prototype

The dynamic programming algorithm for the simple prototype reached a stationary optimal control (SOC) in 86 time steps (~22 h). Decisions are possible in two ship states, $s_k = 3$, when the vessel is not fishing, and $s_k = 4$, when the vessel is fishing. For $s_k = 3$, the optimal control indicates the appropriate decision of whether to start fishing

or not for each of the possible bin levels. For $s_k = 4$, the SOC divides the state space into two regions: a region where the optimal control is to continue fishing, and a region where the optimal control is to begin retrieving the net. The fishing region occupies the quadrant of the state space where both the catch in the net (c_k) and weight of fish in the bins (x_k) is low (Fig. 1.2). The important characteristics of the SOC are as follows. First, there is a bin threshold, such that when the weight of fish in the bins drops to the threshold, (56 t for the simple prototype) the vessel should start fishing. Second, the upper margin of fishing region below the bin threshold is flat, indicating that when the catch in the net increases above a catch threshold (52 t for the simple prototype), the optimal control is to cease fishing independent of the weight of fish in the bins. Finally, there is a notch in the fishing region where the weight of fish in bins is low and the catch in the net is between 24 and 52 t. The notch causes the vessel to retrieve the net before reaching the catch threshold and provides additional protection against running out of fish to process.

The sensitivity of the SOC to model parameters was examined by obtaining the SOC for a range of values for a particular parameter with all the other parameters held constant. Sensitivity to the following parameters was examined: the penalty for oversize catches; the cost differences between not fishing, fishing, and setting/retrieval; and the penalty for discard (Table 2). The general characteristics of the SOC are robust to variation in these parameters (Fig. 1.3). In particular, the bin threshold is extremely robust to variation in parameter values. Changes in the penalty for oversize catches primarily affect the catch threshold. With a large oversize catch penalty, the vessel adopts a more

cautious strategy, and does not fill the net as full before retrieval (uppermost set of graphs in Fig. 1.3). However, the change in catch threshold is relatively modest, with a difference about 20 t between the low penalty and the high penalty. When cost differences are small, the vessel incurs little additional costs for setting and retrieving the net, resulting in a very low catch threshold. Change in the relative costs of different activities has a substantial effect on the catch threshold (middle set of graphs in Fig. 1.3). As the cost differences increase, the vessel waits until the net is fuller before retrieving it. This would reduce amount of time spend setting and retrieving the net, and thus avoid the higher cost of these activities. The range of discard penalties between zero and the monetary value of the discarded fish had little influence on the SOC. A low discard penalty expands the fishing region, but mostly in a part of the state space that would not be visited in a forward simulation of the state dynamics. With a low discard penalty, the vessels have a higher bin threshold, and fill their nets fuller before retrieving, but only slightly (bottom set of graphs in Fig. 1.3). These results suggest that concern over discarding has a minor effect on the SOC.

Next, the response of a vessel following the SOC to changes in the mean and variance of catch rates was examined. As the mean catch rate increases, the region of the state space where the optimal control is to continue fishing shrinks in size. The bin threshold decreases to less than 50 t for a catch rate of 21 t per interval (top set of graphs in Fig. 1.4). The catch threshold also decreases as the mean catch rate increases. As a result, the vessel spends less time actively fishing when the catch rate is high. In a more realistic setting, a vessel could use this additional time by searching for other high-density

aggregations so that the catch rate would continue to be high in subsequent hauls. When catch rates are low, the vessel must spend all its time fishing, and would have little time to seek out higher density aggregations. Changes in catch rate variance strongly affect the catch threshold (bottom set of graphs in Fig. 1.4). Higher variance (as measured by the CV of the catch rate) produces a decrease in the catch threshold. The bin threshold remains stable as variance in the catch rate changes, suggesting that it is determined by the expected catch rate and not by its variance.

Forward simulation of the optimal control

A forward simulation model of the state dynamics was constructed to examine the behavior of a vessel following the optimal control (Mangel and Clark 1988). The state dynamics and parameters were the same as those used in the optimization model. In addition, the optimal decision table as a function of vessel state was provided to the model. The model was started with $x_0 = 0$, $c_0 = 0$, $s_0 = 3$ and run forward with the vessel following the stationary optimal control. To describe the typical path through the state space, consider a vessel that is not fishing, but has 100 t in its bins. Its path will be to the left along the bottom margin of the state space (Fig. 1.2). When the bin level drops to 56 t, the vessel starts fishing and starts moving upwards in the state space as catch increments are added to the catch already in the net. When the catch in the net exceeds approximately 52 t, the vessel retrieves the net over two time steps and returns to the bottom margin of the state space. The simulated vessel cannot catch 52 t exactly because the decision to continue fishing must be made before the random catch increment is added

to the catch in the net. A vessel may have more control over its catch than results from a discrete time model with 15 min time steps. Nevertheless, the Markov decision process approach requires the use of a discrete time model, and the use of a 15 min time step in the model is reasonable level of accuracy to study decisions relating to setting and retrieving the net. The use of a smaller time step in the model might allow the vessel more control over its catch, but the vessel would still have to decide whether to continue fishing before knowing what it will catch in the next time increment.

Frequency distributions and pairwise scatterplots of haul weight, haul duration, and haul interval (time between successive tows) for a 20,000 time step simulation of the stationary optimal control were examined to determine the haul characteristics of a vessel following the optimal control (Fig. 1.5). The haul weight frequency distribution shows a peak just above the catch threshold of 52 t and an extended right tail to the distribution (Fig. 1.5). Very few tows less than the catch threshold occur in the forward simulation. Haul durations for the forward simulation ranged between 0.25 and 2.75 h and showed a symmetrical distribution (graph B in Fig. 1.5). The haul intervals (time between tows) ranged between 1.0 and 9.8 h and had a mean of 3.2 h (graph C in Fig. 1.5). The distribution of haul intervals is also right-skewed, but does not show a sharp minimum. A haul interval of 1 h is the minimum possible time, and it occurs when the vessel starts fishing immediately. This occurred in approximately 4% of all the hauls made in the forward simulation. Above the catch threshold of 52 t, the haul intervals increased approximately linearly with increasing haul weight (graph D in Fig. 1.5). As haul weight increases, more time is required to reduce the amount of fish in the bins to the bin

threshold. Because the vessel uses a catch threshold to decide when to retrieve the net, haul weights appear independent of haul duration (graph E in Fig. 1.5). Since the basic stochastic assumption of the model is that the catch per time increment is a random variable, without the optimal controller adjusting effort (i.e., haul duration), there would be a positive relationship between catch and effort. Haul intervals are inversely related to haul duration (graph F in Fig. 1.5). When a short duration haul is emptied into the holding bins, the total amount of fish in the bins will be considerably above the level that triggers fishing, so the vessel does not begin fishing immediately. However, if haul duration is long, the bin level will be substantially below the threshold when the net is emptied. As a result, the total amount of fish in the bins will not greatly exceed the bin threshold, and so the vessel will quickly begin fishing again.

Comparison with at-sea observer data

There are considerable obstacles to comparing the simulated optimal control with the statistics of fishing vessels. During a fishing season a vessel will adjust its fishing strategy to changing circumstances. A vessel may encounter fish at different mean densities rather than at a single mean density, as was assumed by the optimization model. The higher level aspects of fishing strategy--patch selection and exploratory fishing--will affect the vessel catch statistics in ways that are difficult to predict. Fishing vessels have different maximum bin capacities, processing rates, and use different nets. Their fishing strategy would likely vary because of these differences. Nevertheless, if the model captures some fundamental aspects of fishing behavior, there should be some

correspondence between a simulation of the optimal control strategy and the qualitative fishing patterns of fishing vessels.

One of the most important predictions of the model that can be assessed with at-sea observer data is the presence of a catch threshold. Frequency distributions were compiled for haul weights in the 1993 fishery during the daylight hours, 06:00-20:00, when the vessel traveled less than 50 km before starting the next haul, and the time between hauls was less than 8 h. These criteria were applied to exclude hauls whose properties might reflect diel changes in fishing strategy or changes in behavior related to movement to new fishing grounds. Frequency distributions of haul weight for individual factory trawlers usually showed a left-truncated distribution with few small values (Fig. 1.6). The range of catch thresholds was from 40 t to 70 t, and corresponded well to the model predictions. Most haul weight distributions showed a scattering of points below the catch threshold. These hauls would not have occurred if the vessel had followed a strict catch threshold strategy. One potential explanation is that vessels adjusted their catch threshold in response to changes in fish density. Later in this chapter, I examine whether serial correlation in catch sequences would produce simulated haul weight distributions with this characteristic.

Since observers do not record the amount of fish in holding bins, it is not possible to examine directly whether fishing vessels use a bin threshold to decide when to start fishing. However, it is possible to address this issue in an indirect way by assuming a nominal processing rate, keeping track of the derived amount of fish in the holding bins by adding in the catches and subtracting the nominal processing rate, and recording the bin

levels when the vessel starts to fish. This procedure was done using data from six factory trawlers for the first 10 d of the 1993 fishery. At the start of the season, no vessel would have fish on board, so the initial state was known. Catches were added to the fish in the bins 45 min after the recorded start of net retrieval. An estimate of the nominal processing rate was obtained by stepping through a range of processing rates, and selecting the processing rate that satisfied the following criteria. First, the maximum tons on board should not greatly exceed 200 t since most vessels have a bin capacity of ~200 t. Second, the nominal processing rate should not result in the factory being out of fish to process a high proportion of time (i.e., greater than 15% of time). The nominal processing rates obtained in this way ranged from 2.9 t per 15 min to 4.9 t per 15 min for the six vessels. The frequency distributions of nominal bin levels when the vessel decided to start fishing showed a right-truncated distribution (Fig. 1.7). This suggests that there is an upper limit to the amount of fish in the bins when the vessel starts fishing. These thresholds ranged from 60-100 t, higher than the bin threshold of 56 t for the SOC. In forward simulations, very few hauls were started when the bin level was below the threshold, yet apparently this occurs frequently to fishing vessels, suggesting that vessels have more difficulty keeping bin levels above the threshold than occurs in the basic prototype. One possibility for this discrepancy is that the probability model for catch increments does not adequately represent the distribution of catch increments in the fishery.

Frequency distributions and pairwise scatterplots of haul weight, haul duration, and haul interval (time between successive tows) for all factory trawlers in the 1993 at-sea fishery (Fig. 1.8) correspond to those for the SOC simulation (Fig. 1.5). As with Figure

1.6, only the daytime catches where the vessel traveled less than 50 km to the next tow were selected as appropriate for comparison to the SOC simulation.

Although combining the catch statistics for different vessels obscures the catch thresholds for the individual vessels, a tendency for most of the hauls to be greater than 40 t is apparent in the frequency distribution for all factory trawlers (graph A in Fig. 1.8). The haul weight distribution has a long right tail of large catches similar to the haul weight distribution for the simulated SOC. Haul duration averaged about 2.0 hours with a scattering of tows of longer length (graph B in Fig. 1.8). The haul intervals showed a different frequency distribution than the SOC (graph C in Fig. 1.8) . There is a sharp peak in the distribution at 1.0-1.5 h, indicating that vessels frequently started fishing again soon after retrieving a net. This does not occur as often in the SOC simulations. A reviewer suggested that fishermen may be genuinely risk-averse about running out of fish to process, and begin fishing sooner than is optimal under assumption of risk-neutrality. Another possibility is that the cost of running out of fish is higher than is assumed in the model.

The pairwise scatterplots generally show similar patterns to the scatterplots for the simulated SOC. Haul interval increases with haul weight above ~50 t (graph D in Fig. 1.8). This pattern suggests that vessels base the decision when to begin fishing on the amount of fish in the bins, since otherwise there would be no relationship between haul interval and haul weight. The haul duration versus haul weight plot (graph E in Fig. 1.8) shows no increase in haul weight with haul duration, similar to the statistics for the simulated SOC. This is a strong indication of decision-making based on the amount of

catch in the net, since haul weight would be expected to increase with haul duration with a random distribution for the catch increments. There is an inverse relationship between haul duration and haul interval (graph F in Fig. 1.8), such that longer tows are followed by shorter haul intervals and vice versa. This also corresponds to the statistics for the simulated SOC.

"Rule of thumb" decision algorithms and the shape of the reward surface

The stationary optimal control is a bin and catch threshold strategy plus some refinements. A bin and catch threshold strategy is the following: start fishing when the weight of fish in the bins is $\leq$ x tons, and stop fishing when the weight of fish in the net is $\geq$ y tons. Kareiva et al. (1989) use the term "rule of thumb" for decision-making algorithms that foragers might plausibly use. Such algorithms may perform nearly as well as an optimal strategy, and may have other advantages--such as simplicity, ease of calculation, and robustness. For the foraging problem examined in this chapter, a bin and catch threshold strategy could be called a "rule of thumb" fishing strategy. Note that this strategy is obtained by abstracting the most important characteristics of the optimal control into a simple set of rules. Simulation of these "rule of thumb" strategies can address two related questions: 1) how well do these algorithms perform relative to the SOC, and 2) how sensitive is the reward (daily net revenue) to the decision-making algorithm. For example, it may be possible to obtain most of the potential reward with many different decision algorithms. If the reward is not particularly sensitive to the decision-making algorithm, this could explain differences in fishing strategy between

vessels.

Forward simulations of "rule of thumb" strategies were used to generate contour plots of net revenue for three different mean catch rates (7.0, 14.0, and 21.0 t per 15 min). A grid of all possible combinations of bin and catch threshold strategies in increments of 4 tons (n = 41 catch levels X 51 bin levels = 2091) was used. For each bin and catch threshold pair, the mean revenue was obtained from 20 simulations of 2,000 time steps, so that each point in the grid was based on simulations roughly equivalent to 20 vessels following that strategy for a 20-d fishery opening for Pacific hake. The region of the reward surface where bin and catch threshold strategies attain greater than 90% of the net revenue of the SOC is fairly broad for each of the mean catch rates (Fig. 1.9). The flat-topped portion of the reward surface is roughly the same size for each of the three catch rates, but its location depends on the catch rate. When the catch rate is low (left panel of Fig. 1.9), maximum revenues occur at high catch and bin thresholds. When the catch rate is high (right panel of Fig. 1.9), higher revenues occur at lower catch and bin thresholds. This pattern is similar to that for the stationary optimal control. A bin and catch threshold strategy that yields close to maximum revenue at one catch rate may not perform as well at other catch rates. Other bin and catch threshold strategies perform well regardless of the catch rate. Strategies that are robust to mean catch rates are favorable strategies because fisherman typically will not know the mean catch rate before starting to fish. The region of overlap between the flat-topped portions of the reward surfaces identifies strategies that are robust to changes in mean catch rate. For example, a bin and catch threshold strategy of a bin threshold of 100 t and a catch threshold of 50 t performs well

regardless of the mean catch rate.

A model with correlated catch increments

To add serial correlation to the sequence of catch increments, the technique of state augmentation was used (Bertsekas 1987). In a Markov model for serial correlation, the additional state variable required is the random catch increment in the previous time step, w_{k-1}. This variable is assumed to be observable by the fishing vessel, which should be possible using net telemetry. For the simple prototype presented earlier, the stochastic part of the model was a single discrete probability distribution, $pr(w_k)$, giving the probability of catch increments from zero to 160 t in 4 t increments. For the serial correlation model, the stochastic component is a probability transition matrix, $pr(w_k|w_{k-1})$, that gives the probability of catch increments from zero to 160 t given the catch increment in the previous time step from zero to 160 t.

Since factory trawlers are unable to make sharp turns while trawling, serial correlation in the sequence of catch increments should be similar to the spatial correlation of fish densities along straight-line transects. Consequently, the transition probabilities for the correlated catch increment model were derived from the density of hake along acoustic transects during the 1992 NMFS acoustic survey. The objective in obtaining a probability transition matrix was to keep the correlation structure as simple as possible, yet still capture the most important characteristics of the hake spatial pattern as it relates to fishing strategy. To estimate the transition probabilities, hake densities for 1 nmi transect

segments (15 min of towing by a factory trawler) were considered as either a part of a low-density region (< 3.0 t per nmi) or a part of a hake aggregation (> 3.0 t per nmi) (3.0 t was used because the mean catch rate in the fishery is about 1.5 times the mean acoustic density, and 2.0 t was the boundary between catch increments of zero and 4 t used in obtaining the discrete probability distribution.). The transition probabilities were $p_{00} = 0.71$, $p_{01} = 0.29$, $p_{10} = 0.17$, $p_{11} = 0.83$, where, for example, p_{01} is the probability of a positive catch increment given a zero catch increment in the previous time step.

A Δ-distribution with mean = 14 and CV = 1.5 was generated for each row in the probability transition matrix. Then the probabilities of zero and non-zero catch were adjusted so that the transition probabilities matched those estimated from the acoustic data. Simulations of the correlated catch increment model show a random pattern of high-density aggregations surrounded by low-density regions. After the vessel decides to begin fishing, the catch increment for the first time step does not enter the net because of the time required to set the net. In the serial correlation model, the probability distribution for this initial catch increment is strictly positive (i.e., no zero catch increments) because a fishing vessel would be unlikely to initiate fishing activities without first detecting fish with the echo sounder.

Because of the simple structure to the transition probabilities, the SOC has two basic patterns, a strategy when the vessel is in the low-density region, and a strategy when the vessel is fishing in an aggregation. When serial correlation is incorporated into the state dynamics, the SOC changes in the following ways. First, the bin threshold increases

from 64 t for a non-correlated model (based on the stationary PDF to the probability transition matrix) to a threshold of 76 t for the correlated catch increment model (Fig. 1.10). Second, when the vessel is in the low-density state, the region of the state space where the optimal control is to fish becomes smaller, so that the vessel ceases fishing operations sooner. For example, if the vessel has between 36 and 56 t in the net, and the vessel encounters a low-density region, it immediately retrieves the net. If there is less than 36 t in the net, the vessel will fish longer before retrieving the net (until approximately 24 t remains in the bins) because the vessel has a probability of 0.29 of encountering another aggregation. At higher levels of serial correlation, the SOC is always to cease fishing immediately if the vessel leaves the aggregation.

Forward simulations of the SOC for correlated catch increments show a catch threshold in the frequency distribution of haul weights similar to that for the random catch increment model (Fig. 1.11). However, a scattering of tows smaller than the catch threshold occurred when the vessel moved from an aggregation to a low-density region. Thus, serial correlation in catch increments could explain the occurrence of small tows in the observer data, which did not occur in the simple prototype with random catches. A reviewer suggested that the small haul weights in the observer data may also be due to uncertainty the estimation of the amount of fish that have accumulated in the net, so that the net is occasionally retrieved with less fish than is expected. There were also more short haul intervals with the correlated catch increment model. The vessel began fishing in the shortest possible time (60 min) in 11% of all tows in the forward simulation of correlated catch increment model, but in only 4% of tows for the model without serial

correlation. This also agrees more closely with at-sea observer data, where hauls intervals ≤ 1.5 h were common.

Diel trends in catch rate and the effect of a ban on night fishing

The diel pattern in fishery catch rates is caused by the behavior of Pacific hake. During the day, Pacific hake form aggregations which occupy a distinct layer 10-20 m thick. This layer ranges in depth from 100 to 300 m and may be close to the bottom on the continental shelf or in midwater off the shelf. At dusk, these aggregations break up as hake disperse to begin actively feeding. Usually there is a vertical component to their movement. At night, hake can be found from the surface to 300 m with no discernable pattern of aggregation. The breakdown of hake aggregations coincides with the dusk movement of macrozooplankton, including euphausiids, the primary prey of Pacific hake. The transitions between day and night distribution patterns occur in about an hour at dawn and dusk.

To include this diel pattern in the model, a variable for the time of day (discretized into 96 states of 15 min duration) was included in the state space. To complete the model, the state dynamics and a probability distribution of catch increments for each of these possible times is needed. To model the state dynamics, the counter for the time of day is simply incremented by 1 from 1 to 96, then returns to 1. Catch distributions from factory trawlers in the 1993 hake fishery were used to obtain the mean catch rate by time of day. From 06:30 to 19:30, a mean catch increment of 14.0 t per 15 min was used, and from 20:30 to 05:30, a mean catch increment of 4.0 t per 15 min was used. The dawn and

dusk transitions occurred linearly in one hour between the mean day and night catch rates. Δ-distributions were generated using the methods described in the simple prototype section for each period. The CV and the probability of a zero catch were the same as the basic prototype and did not vary through the day.

The stationary optimal control was obtained for two models, a model where night fishing was allowed, and a model where fishing was prohibited between midnight and 07:00. A ban on night fishing was easily modeled by reducing the decision set to $u_k = 0$ from 23:15 to 07:00 (the additional 45 min before midnight gave the vessel time to get the net on deck). The stationary optimal control for the non-fishing state ($s_k = 3$) specifies the appropriate bin threshold by time of day. The stationary optimal control for the fishing state ($s_k = 4$) is three-dimensional, with bin level, catch level and time of day as the three dimensions. The general pattern of SOC at each time of day is similar to simpler models already analyzed. The top edge of the fishing region is usually flat-topped, resulting in a catch threshold that is independent of the amount of fish in holding bins. As with the simpler models, there is a notch in the fishing region where catch is high and bin level is low that provides additional protection against running out of fish in the factory. A plot of bin and catch threshold by time of day (Fig. 1.12) captures most of the pattern of the SOC, and avoids having to show many plots to characterize the SOC. For the SOC with night fishing, the bin threshold peaks at ~150 t in the early evening (around 20:00), then declines to a minimum at dawn. When night fishing is closed, the bin threshold is higher throughout the day, and peaks at ~190 t in the early evening. The catch threshold for the model with night fishing is between 50 and 60 t during the day, then increases to ~80 t

when the mean catch increment decreases at nightfall. The catch threshold without night fishing shows a similar pattern, except for a larger increase (to ~100 t) at nightfall.

In forward simulations of the SOC with and without night fishing, the changing catch and bin thresholds through the day cause an increasing trend in the mean amount of fish on board starting from a minimum at dawn and reaching a maximum at dusk (Fig. 1.13). During the night, the mean amount of fish in holding bins decreases. The rate of decrease is more rapid and sustained when night fishing is prohibited. One interesting result is that even when fishing is allowed through the night, the tendency is for the fishing vessel to curtail its fishing activities during the period when the catch rate is low. Apparently, vessels should fish just enough at night to ensure that the fish in holding bins will supply the factory through the night to daybreak when catch rates increase again. Since more time is needed to catch an equivalent amount of fish at night, the cost per ton of catch is higher at night than during the day.

The forward simulations of SOC with and without night fishing, and a "rule of thumb" strategy of a 100 t bin threshold and a 50 t catch threshold were compared to observer data from the 1992 fishery (when night fishing was prohibited), and the 1993 fishery (when night fishing was allowed). The "rule of thumb" strategy was also compared because in previous simulations without a diel trend in catch rates this strategy produced a large percentage of the potential yield regardless of the mean catch rate. Models with and without night fishing result in a peak of fishing activity in the morning, a period of lower activity during the day, followed by an increase at dusk (graph A in Fig. 1.14). An examination of hourly vessel activity for the 1992 and 1993 fisheries also

indicate that a peak in vessel activity occurs in the morning when fishing opens (graph D in Fig. 1.14). However, the peak is much higher in both SOCs. In the 1993 fishery data, the proportion of time spent actively fishing is highest in early hours of the morning, whereas the SOC predicts a decrease in fishing effort early in the morning. This suggests that vessels may not vary their bin threshold through the day as predicted by the SOC. The "rule of thumb" strategy followed throughout the day shows a closer match to the proportion of time spent fishing in the 1993 fishery data (graph A in Fig. 1.14).

The diel trends in haul weight for the SOC (with and without night fishing) are generally similar to the fishery data for the corresponding conditions (graphs B and E in Fig. 1.14). Mean haul weight is highest immediately before dusk because it is advantageous to wait until catch rates decline before retrieving the net. When night fishing is allowed, both the SOC and the fishery data show a decline in haul weight from dusk to midnight, then a gradual increase through the day. When night fishing is banned, the pattern is similar for both the SOC and the fishery data, except for a more rapid decline in haul weight after dusk due to vessels retrieving their nets to comply with the midnight closure. Both the simulated SOCs and the observer data show an increase in haul duration at night (graphs C and F in Fig. 1.14). When night fishing is allowed, haul duration for the SOC increases substantially at night, while the corresponding fishery data shows less of an increase. The 1993 fishery data more closely resembles the "rule of thumb" strategy than the SOC. When night fishing is banned, haul duration begins to increase at dusk, but then declines as vessels retrieve their nets to comply with the midnight closure. This pattern is seen in both the SOC and the 1992 fishery data.

The mean revenue per day in simulations of vessels following different strategies depicts the change in profitability of a factory trawler when night fishing is prohibited. When night fishing is prohibited, a vessel following the SOC can still attain a large fraction (~98%) of the potential daily net revenue (Table 3). The most significant difference when night fishing is banned is that the mean discard increases from 1.7 t per day to 6.8 t per day. This is because the vessel must fill its holding bins closer to capacity before fishing is closed for the day, running the risk of catching too many fish. However, discard rates still remain low, less than 2%, and a manager might be willing to accept this higher level of discard to reduce salmon bycatch rates. The "rule of thumb" strategy works well with night fishing (93% of the mean daily revenue of the SOC), but the performance of this "rule of thumb" strategy degrades substantially when night fishing is closed (21% of mean daily revenue of the SOC). This suggests that the simpler "rule of thumb" strategy may be adequate when night fishing is allowed, but that the vessel may be compelled to adopt a diel strategy of stockpiling fish during the day when night fishing is banned.

DISCUSSION

The analysis of the simple prototype, where the random catch increment was generated from a single probability distribution, showed that the optimal controls generally consist of a bin threshold and a catch threshold. The bin threshold signals the vessel to start fishing and the catch threshold signals the vessel to stop fishing. Although the optimal controls displayed some sensitivity to key parameters of the model, basic

characteristics of the optimal controls were unchanged. Further analyses showed how vessels adjust these controls in response to changes in the mean and variance of the sequence of catch increments entering a net in the water. An exploration of "rule of thumb" strategies showed that the reward surface is flat in the region of the optimal control. As a result, fishing vessels should have considerable flexibility in selecting simple strategies that generate nearly as much net revenue as the optimal controls. Observer data on haul size, haul duration, and haul interval recorded during the 1993 at-sea fishery were consistent with model results showing that fishing vessels should manage their fishing operations using bin and catch thresholds to maximize net profits. The wide range of catch and bin thresholds evident in the data is consistent with the conclusion obtained by modeling "rule of thumb" strategies that vessels have considerable flexibility in selecting strategies.

Two elaborations of the simple prototype, a model with serially correlated catch increments and a model with diel variation in catch rates, presented the vessel with a more complex and realistic environment. The resulting optimal controls accommodated that complexity in intuitively reasonable ways. The model with serial correlation showed that the vessel should have a lower catch threshold in the low-density region, such that the net would be retrieved with fewer fish in it than if the vessel remained in a high-density region throughout the tow. The model with diel variation in catch rates caused the vessel to adjust bin and catch thresholds through the day to stockpile fish during the daylight hours when the catch rate is high, and then to cut back on fishing at night when the catch rate is low and fishing is less profitable. With a ban on night fishing, vessels accumulated fish to

a greater extent during the day, but daily net revenue did not decline significantly.

Diel patterns in the fishery data for 1992 and 1993 were most consistent with a "rule of thumb" strategy consisting of a fixed bin and catch threshold rather than the optimal strategy of stockpiling fish during the daylight hours. However, the performance of this "rule of thumb" strategy degraded substantially in simulations when night fishing was closed. The ability to accommodate a daily shutdown of fishing operations would depend of the bin capacity of the vessel. Vessels with smaller bin capacities may have been be more adversely affected by the night closure than vessels with larger bin capacities. Issues of fairness and equity should be addressed when regulations such as the night closure in 1992 are proposed. These issues were not obvious prior to conducting this research.

Since the model was intentionally kept simple to emphasize the essential characteristics of the time-allocation problem on factory trawlers, fishing vessels may have more behavioral flexibility than the model allows. One example of this flexibility is "short wiring," where a vessel partially retrieves the net so that it is no longer actively fishing. The vessel maintains trawling speed so the fish already captured cannot escape. In the context of the Markov decision process model, allowing vessels to short wire expands the decision set for $s_k = 1$, when the vessel is retrieving the net. Rather than being compelled to move to state $s_k = 2$, as the model now requires, the vessel would have the option of remaining in this state. Limited personal observations suggest that short wiring is a fairly common strategy among factory trawlers in the Pacific hake fishery. Short wiring is helpful because it allows the vessel to reserve its catch until there is room in holding bins

to receive the fish. Experimentation with a model where fishing vessels were allowed to short wire suggested that vessels would only short wire when retrieving the net would result in discard; that is, when $x_k + c_k > x_{max}$. This suggests that short wiring may help vessels manage their discard.

The model developed in this chapter also assumes that the factory processing rate is constant. In reality, a vessel can adjust its processing rate by shutting down a production line or reducing the number of factory workers. There may also be a random component to the processing rate due to unpredictable equipment breakdowns. Machinery for surimi processing operates most efficiently when supplied with a continuous flow of fish, and there may be significant startup costs when restarting a production line after a long shutdown. A strategy to reduce the processing rate would only be employed when catch rates are low and there is some risk of running out of fish. Because vessels in the at-sea hake fishery are all competing for the fishery-wide quota, vessels with low catch rates would be strongly motivated to search for higher densities of fish rather than adjust their processing rate downwards. Consequently, the ability of the vessel to modify its processing rate is unlikely to have a large influence on the general results obtained in this chapter.

An additional assumption of the model is that product value does not depend on the length of time the fish have been held. To model changes in product value over time would require additional state variables and decision options, and would substantially increase the complexity of the SOC. For example, the vessel may decide to discard fish held too long to produce top-grade surimi, a decision which is not now an option in the

model. Although holding time is an important factor in determining the grade of surimi, potential decreases in product value probably do not play a significant role in decision-making at the time scales addressed in the model. Surimi grades are based on color and gel strength. The gel strength of Pacific hake increases for up to 6 h after landing due to stiffening of the muscle tissue, and in pollock fisheries, the fish are typically "aged" for several hours before processing. Price differences for surimi of different grades fluctuates depending on the market, but typically the price range between top-grade surimi and second-grade surimi is 5-10%.

Pacific hake held for less than about 10 h in holding bins, or for less than 24 h in refrigerated seawater tanks produce top-grade surimi (Gregory Peters, Oregon State University Seafood Laboratory, Astoria, Oregon, pers. commun.). About one-third of the at-sea fleet have refrigerated seawater tanks; the rest of the fleet stores unprocessed fish in holding bins. For the simple prototype, 1.0% of the fish were held longer than 10 h before processing in forward simulations of the optimal control (mean holding time = 3.6 h). For the diel model with night fishing, 1.4% of the fish where held longer than 10 h (mean holding time = 4.3 h). However, with a night closure on fishing, 9.5% of the fish are held longer than 10 h before processing. This suggests that under normal conditions (i.e., without a night closure or an equipment breakdown), a vessel would be unlikely to lose revenue due to a decrease in product value. Although a ban on night fishing could reduce product value, it is not obvious how a vessel could change its strategy to improve product value since all the fish processed during the 7 h night closure must be caught earlier in the day.

Gillis et al. (1995b) describe three types of discarding on commercial fishing vessels: capacity-discarding, exclusion-discarding, and high grading. Capacity-discarding is discarding because the vessel has no room in holding bins for the catch, and is the kind of discard that occurs in the model developed in this chapter. Exclusion-discarding is discarding when the species or the size of the fish has no economic value. Since juvenile hake occur mostly off California, south of where the fishery operates, exclusion-discarding of undersized hake is rare. However, all non-hake species are typically discarded. High grading is the discard of marketable fish to leave space for higher-valued fish. In the Pacific hake fishery, high-grading would be unlikely to occur because all marketable hake can be processed into surimi, which has the same value no matter the size of the fish used to produce it.

Gillis et al. (1995b) contend that only with high-grading does discard occur at the discretion of the fishermen. However, they are concerned only with decision-making that occurs after a haul is brought on board. The operational models developed in this chapter suggest that discarding should be viewed within the context of the entire set of decisions that lead to the discard. The analysis of these models indicate that capacity-discarding can occur as an indirect result of decisions made before the discard occurs, but which influence the probability that discard will occur. Factory trawlers can maximize net revenue by keeping the factory continually supplied with fish. If they start to fish when they already have a substantial amount of fish in bins (i.e., a strategy with a large bin threshold), there is a high probability that they will be able catch enough fish to refill the bins before they become empty. However, vessels following this strategy would have a

higher risk of capacity-discarding, since they may occasionally catch so many fish that they have no space in the bins to hold them. The strategy adopted by the fishing vessel can put it in a situation where discarding is unavoidable. If the penalty for discard were to be increased, as would occur if the fishery were managed with ITQs and discard was subtracted from the vessel's quota, vessels would adopt a strategy to avoid those situations. However, some discard during the fishing season may be unavoidable due to the stochastic nature of fishing and the spatial and temporal overlap between economically valuable fish and those species with little or no economic value.

Although observers in the hake fishery do not record the type of discard, they do estimate the total discard by a vessel. Discard is difficult to monitor by observers because it is episodic in nature and can occur in more than one location on the vessel. The estimated discard of hake in the factory trawler fleet declined from 5.5% in 1992 when night fishing was banned to 3.8% in 1993 when night fishing was allowed. This decline in discard corresponds to the model prediction of lower discard when night fishing is allowed. However, this decrease in discard from 1992 to 1993 occurred within the context of a trend of decreasing discard since the large-scale fishery started in 1991. Consequently, it is impossible to separate the effect of the ban on night fishing on discard from the trend of increasing efficiency as the factory trawler fleet becomes more proficient at fishing for hake. An intriguing conclusion the night fishing analysis is that a management action designed to control one problem, the bycatch of salmon, can have consequences that are difficult to predict, and may be as undesirable as the problem the management action was intended to correct. A potential benefit of the modeling

techniques developed in this chapter is the ability to predict consequences of management actions before implementing them. However, the data needed parameterize and test operational models of fishing are not routinely collected. As regulatory environment under which fisheries operate becomes increasingly restrictive, there is an ongoing need to monitor fishing behavior, develop new models, and to test the predictions of those models.

The Markov decision process model developed in this chapter is a projection of the general foraging problem of a fishing vessel into one-dimensional time. While the fishing vessel contends with time-allocation problems, it also has to contend with the spatial aspects of foraging, as in deciding where to start the next haul. When the vessel has found a large-scale aggregation of hake and can obtain an acceptable catch rate, the time-allocation concerns are probably in the forefront since the vessel can quickly reach any location within the aggregation to start the next haul. Approximately 90% of all tows in the 1993 at-sea fishery were located within 18 nmi of the immediately preceding tow--1-1.5 h of running time by the vessel, suggesting that over short periods the spatial aspects of foraging do not act as constraints. When longer periods are involved, the spatial aspects of foraging cannot be ignored. Decisions associated with patch selection (i.e., spatial aspects of foraging) are a step higher in the hierarchy of decisions from the operational models developed in this chapter. At this level, the time scale ranges from one day to one week, and a new set of issues must be addressed. Fine-scale strategy (the operational aspects of fishing) affects decision-making at larger scales by linking fish abundance, as experienced by the fishing vessel as a catch rate, to factory production.

Decision-making at the patch selection level can be separated into two questions:

"when to leave" and "where to go." The "when to leave" question evaluates whether the abundance of fish within the patch can support the processing capacity of the vessel. The model developed in this chapter indicates that vessels saturate rather quickly when catch rates increase above the processing rate. When the catch rate is equal to the factory processing rate, the net revenue of a vessel following the SOC is close to zero. When the catch rate is 1.5 times the factory processing rate, the vessels can obtain 94% of their potential net revenue by following the SOC. At greater than twice the factory processing rate, the vessel can increase its daily surimi production by very little, suggesting that there would be little incentive for a vessel to seek higher catch rates. A catch rate between 1-1.5 times the factory processing rate may prompt the vessel to assess whether to continue fishing in an aggregation. This assessment could take the form of a threshold catch rate that would initiate movement to a new aggregation. The "where to go" aspect of patch selection was not addressed in this chapter, but is a promising area for research. Informal discussions with fishermen and research on other fisheries (Eales and Wilen 1986) suggest that these decisions are based on the fishermen's knowledge of areas historically high in fish density, anecdotal information from other fishing vessels, the location of other vessels, and information gained from searching. Exploring the relative importance and interplay between these various factors is a challenging task

Further progress in modeling fishing behavior may depend on developing alternative models of decision-making or using the techniques of other scientific disciplines. By viewing decision-making as a hierarchial set of choices, it may be possible to address problems at different spatial and temporal scales, yet keep the problem of

manageable size and relevant to actual decision-making processes. A useful alternative perspective could be gained from an anthropological investigation of how fisherman view the environment and their opportunities for decision-making. The technique developed in this chapter of modeling fishing behavior using "rule of thumb" strategies and comparing these strategies with the optimal controls is a tool for simplifying and generalizing successful strategies. Consideration of "rule of thumb" strategies provides broader perspective than can be obtained by studying only the optimal solutions to decision-process models.

Table 1.1. State dynamics on a factory trawler.

Ship status, s_k	Description	Decision, u_k	Updated state	Per period cost, $\kappa(s_k, u_k)$
$s_k = 1$	Haul back	$u_k = 0$	$s_{k+1} = 2$ $x_{k+1} = \max(0, x_k - p)$ $c_{k+1} = c_k$	κ_{sr}
$s_k = 2$	Haul back (catch added to fish in bins)	$u_k = 0$	$s_{k+1} = 3$ $x_{k+1} = \max(0, x_k - p) + c_k$ $c_{k+1} = 0$	κ_{sr}
$s_k = 3$	Vessel able to fish	$u_k = 0$	$s_{k+1} = 3$ $x_{k+1} = \max(0, x_k - p)$ $c_{k+1} = 0$	κ_{nf}
		$u_k = 1$	$s_{k+1} = 4$ $x_{k+1} = \max(0, x_k - p)$ $c_{k+1} = 0$	κ_{sr}
$s_k = 4$	Vessel fishing	$u_k = 0$	$s_{k+1} = 1$ $x_{k+1} = \max(0, x_k - p)$ $c_{k+1} = c_k$	κ_{sr}
		$u_k = 1$	$s_{k+1} = 4$ $x_{k+1} = \max(0, x_k - p)$ $c_{k+1} = c_k + w_k$	κ_f

Table 1.2. Ranges of parameter values used to examine the sensitivity of the optimal control to key parameters.

	Low	Baseline	High
Oversize catch penalty	0.361	0.722	1.444
Cost per time step contrast	κ_{sr} = 810 κ_{nf} = 800 κ_{f} = 805	κ_{sr} = 880 κ_{nf} = 800 κ_{f} = 840	κ_{sr} = 960 κ_{nf} = 800 κ_{f} = 880
Discard penalty	0.0	130.0	260.0

Table 1.3. Mean daily costs and revenue for a 50,000 step forward simulation of the statationary optimal control when the mean catch increment follows a diel pattern. The "rule of thumb" (ROT) strategy is to use a 100 t bin threshold and a 50 t catch threshold throughout the day.

	SOC with night fishing	SOC without night fishing	ROT with night fishing	ROT without night fishing
Total catch per day (t)	383.8	381.5	380.2	321.5
Gross revenue per day	$99,780	$99,199	$98,840	$83,584
Costs per day	$80,087	$79,936	$80,557	$79,572
Discard penalty	-278.6	-1094.2	-376.4	-184.7
Discard per day (t)	1.7	6.8	2.4	1.2
Percent discard	0.45%	1.76%	0.62%	0.36%
Oversize catch penalty	-813.4	-998.7	-648.6	-568.5
Net revenue per day	$19,693	$19,263	$18,282	$4,012

Figure 1.1. Temporal and spatial scales in a hierarchy of decisions made by factory trawlers (adapted from Holling 1992) .

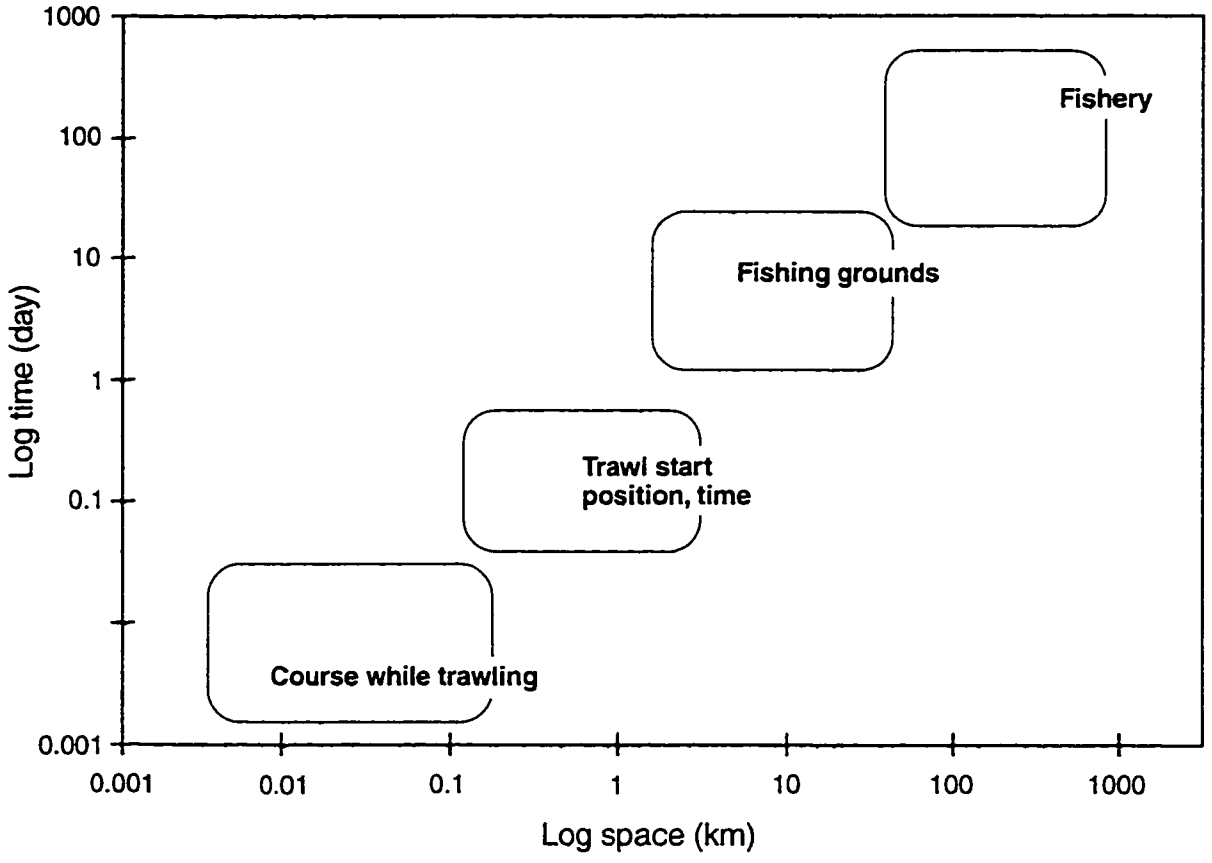
1000
100
10
1
0.1
0.001
Log time (day)
Fishery
Fishing grounds
Trawl start
position, time
Course while trawling
0.001
0.01
0.1
1
10
100
1000
Log space (km)

Figure 1.2. Stationary optimal control for the simple prototype. The shaded area indicates the part of the state space where the optimal control is to continue fishing; the unshaded area where the optimal control is to begin retrieving the net. At the lower edge of the figure the optimal control for $s_k = 3$ (able to fish but not currently fishing) is indicated.

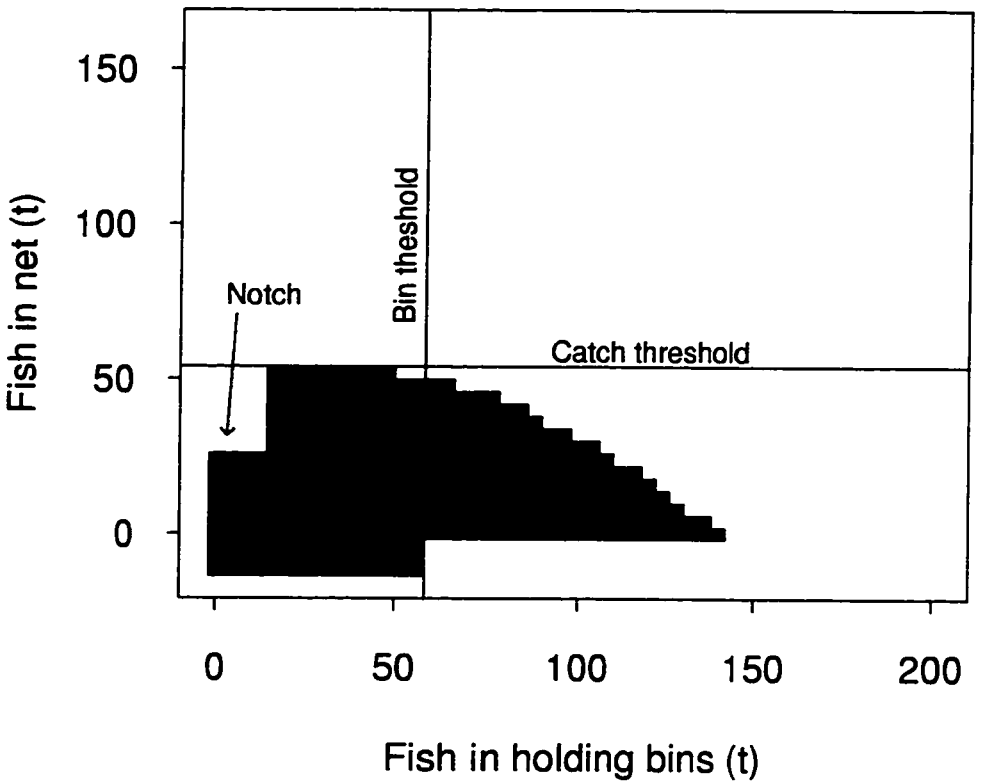
150
100
50
0
Fish in net (t)
Notch
Bin theshold
Catch threshold
0
50
100
150
200
Fish in holding bins (t)

Figure 1.3. Sensitivity of SOC to the model parameters. The lower edge of each figure indicates the optimal control for $s_k = 3$; the main part of the figure indicates the optimal control for $s_k = 4$. The top row of panels show the SOC for a ranges of penalties on oversize catches (>100 t) with all other model parameters held constant. The middle row of panels show the SOC for a range of values for the costs of fishing, not fishing, and setting or retrieving the net. The bottom row of panels show the SOC for a range of discard penalties. Parameter values used to obtain these figures are given in Table 2.

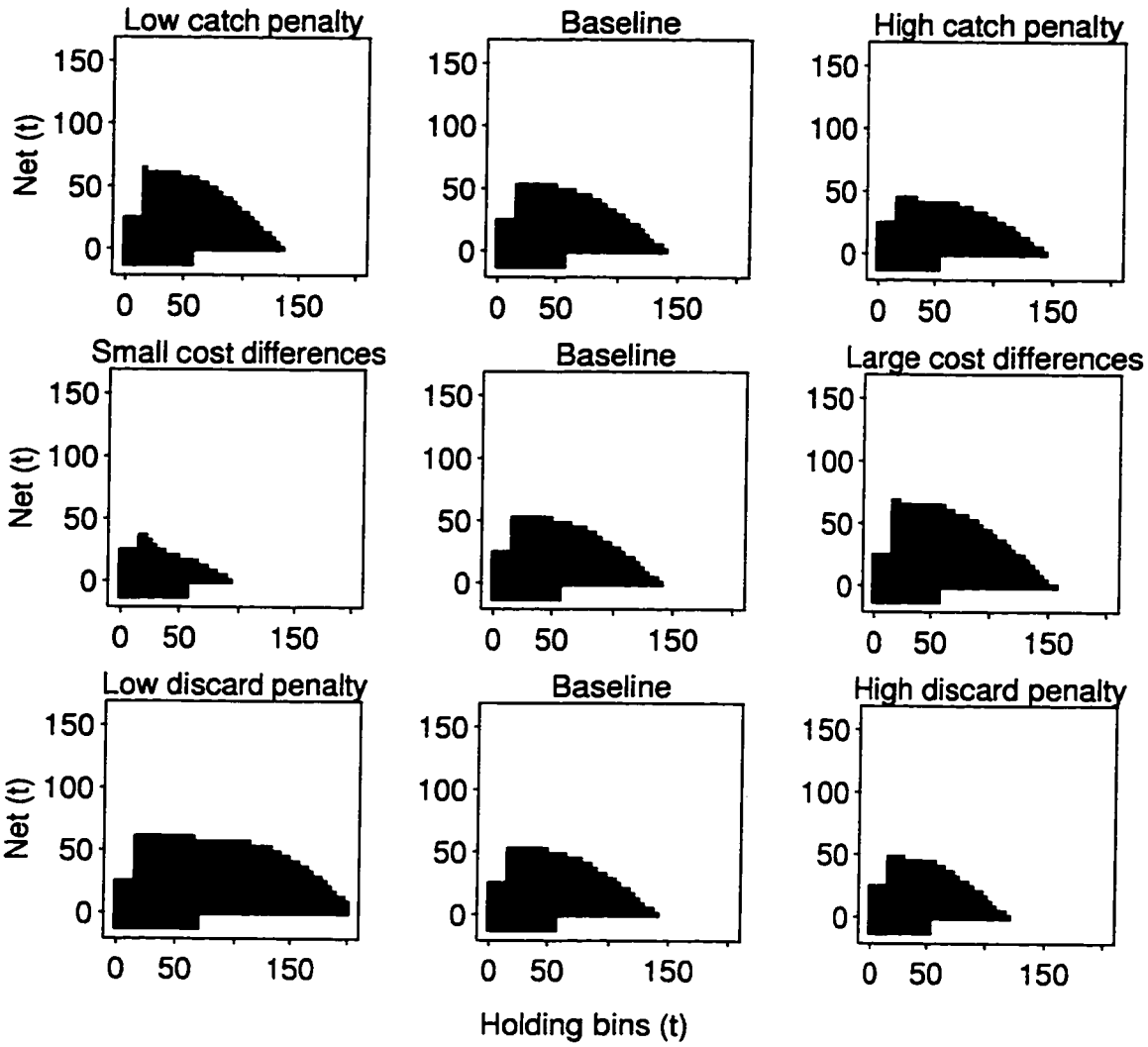
Low catch penalty
Baseline
High catch penalty
Small cost differences
Baseline
Large cost differences
Low discard penalty
Baseline
High discard penalty
Net (t)
Holding bins (t)
0
50
100
150

Figure 1.4. Effect of changes in the mean and CV of catch rate on the SOC. Top panels show the SOC for a range of mean catch rates with the CV fixed at 1.5. Bottom panels show the SOC for a range of CVs with the mean catch rates fixed at 14.0 t per 15 min.

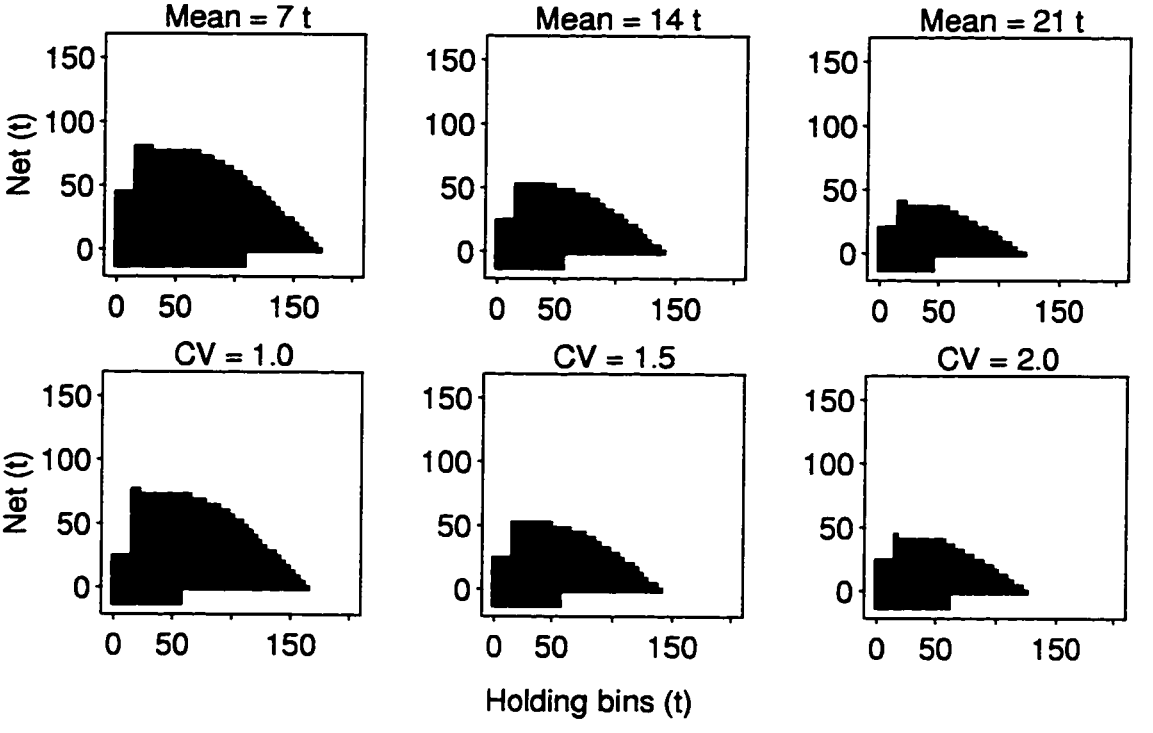
Mean = 7 t
Mean = 14 t
Mean = 21 t
CV = 1.0
CV = 1.5
CV = 2.0
Net (t)
150
100
50
0
0
50
150
Holding bins (t)

Figure 1.5. Summary graphs for a 20,000 step forward simulation of the stationary optimal control. A. Frequency distribution of haul weight. B. Frequency distribution of haul duration. C. Frequency distribution of haul interval. D. Scatterplot of haul interval versus haul weight. E. Scatterplot of haul weight versus haul duration. F. Scatterplot of haul interval versus haul duration. The values for the scatterplots were jittered.

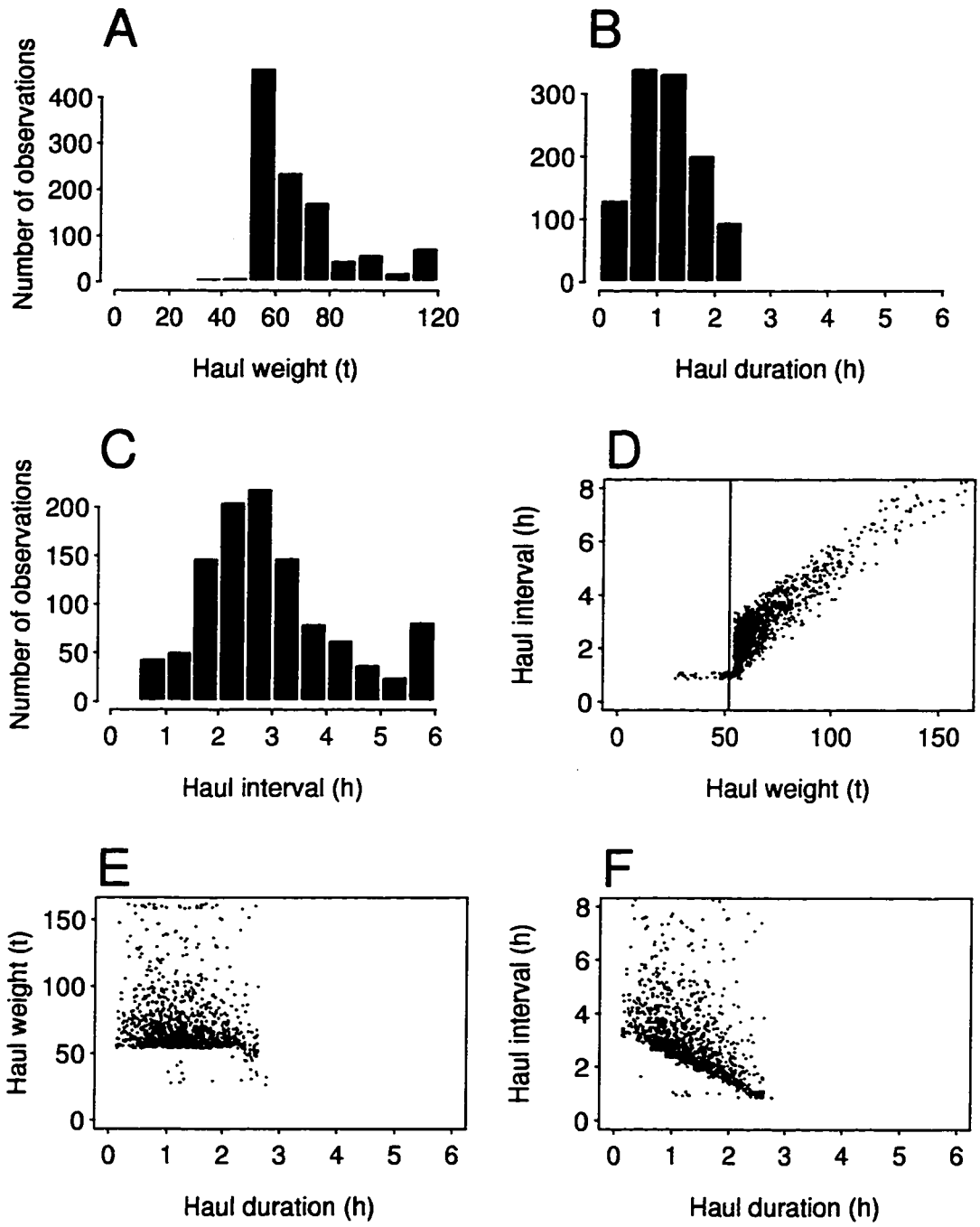
A
Number of observations
400
300
200
100
0
0 20 40 60 80 120
Haul weight (t)
B
300
200
100
0
0 1 2 3 4 5 6
Haul duration (h)
C
Number of observations
200
150
100
50
0
0 1 2 3 4 5 6
Haul interval (h)
D
Haul interval (h)
8
6
4
2
0
0 50 100 150
Haul weight (t)
E
Haul weight (t)
150
100
50
0
0 1 2 3 4 5 6
Haul duration (h)
F
Haul interval (h)
8
6
4
2
0
0 1 2 3 4 5 6
Haul duration (h)

Figure 1.6. Frequency distributions of haul weight for six factory trawlers in the 1993 at-sea Pacific hake fishery. Vessels were given random codes to preserve confidentiality.

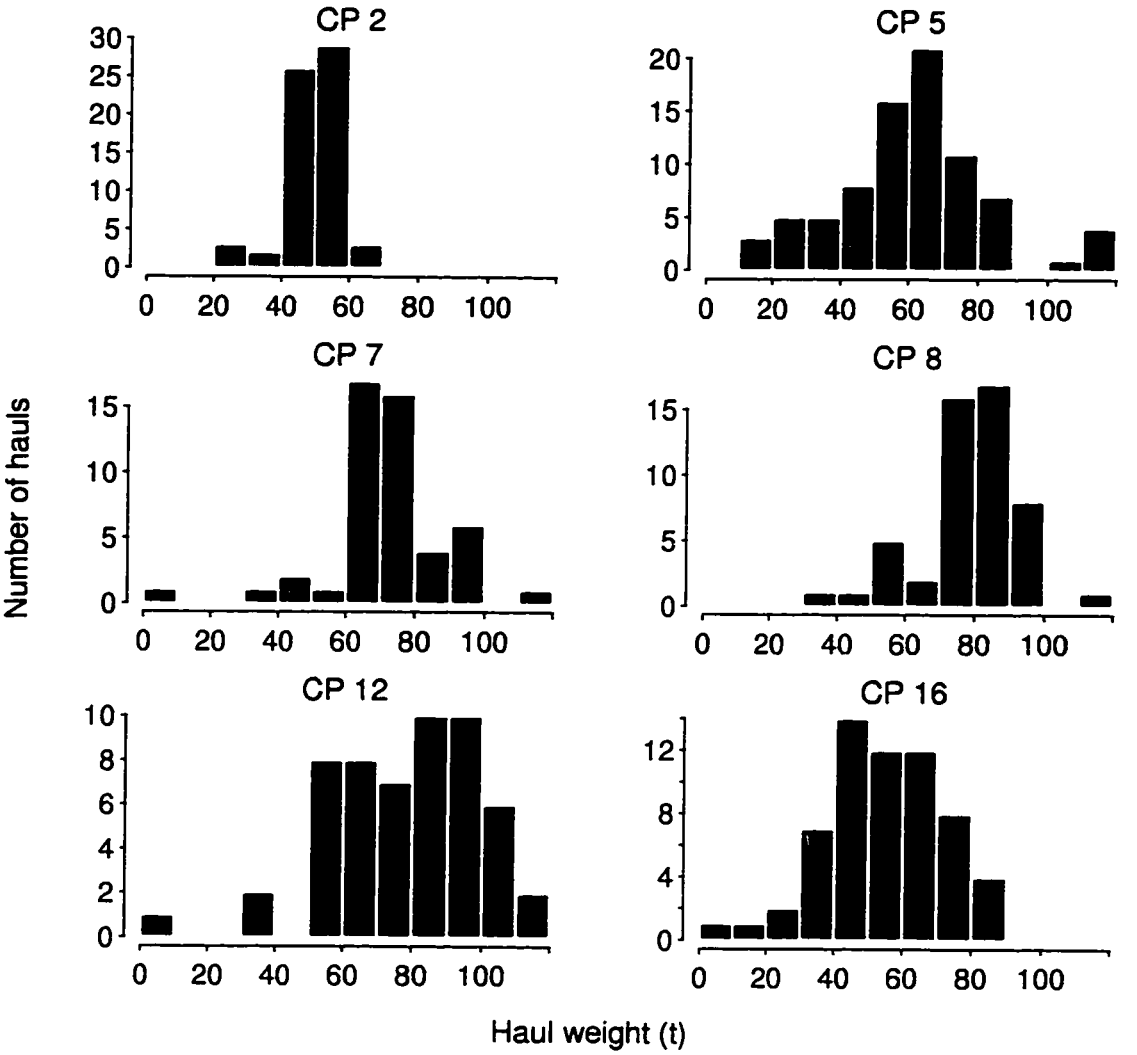
CP 2
CP 5
CP 7
CP 8
CP 12
CP 16
Number of hauls
Haul weight (t)

Figure 1.7. Frequency distributions of bin levels when starting to fish for six factory trawlers in the 1993 at-sea Pacific hake fishery. Vessels were given random codes to preserve confidentiality.

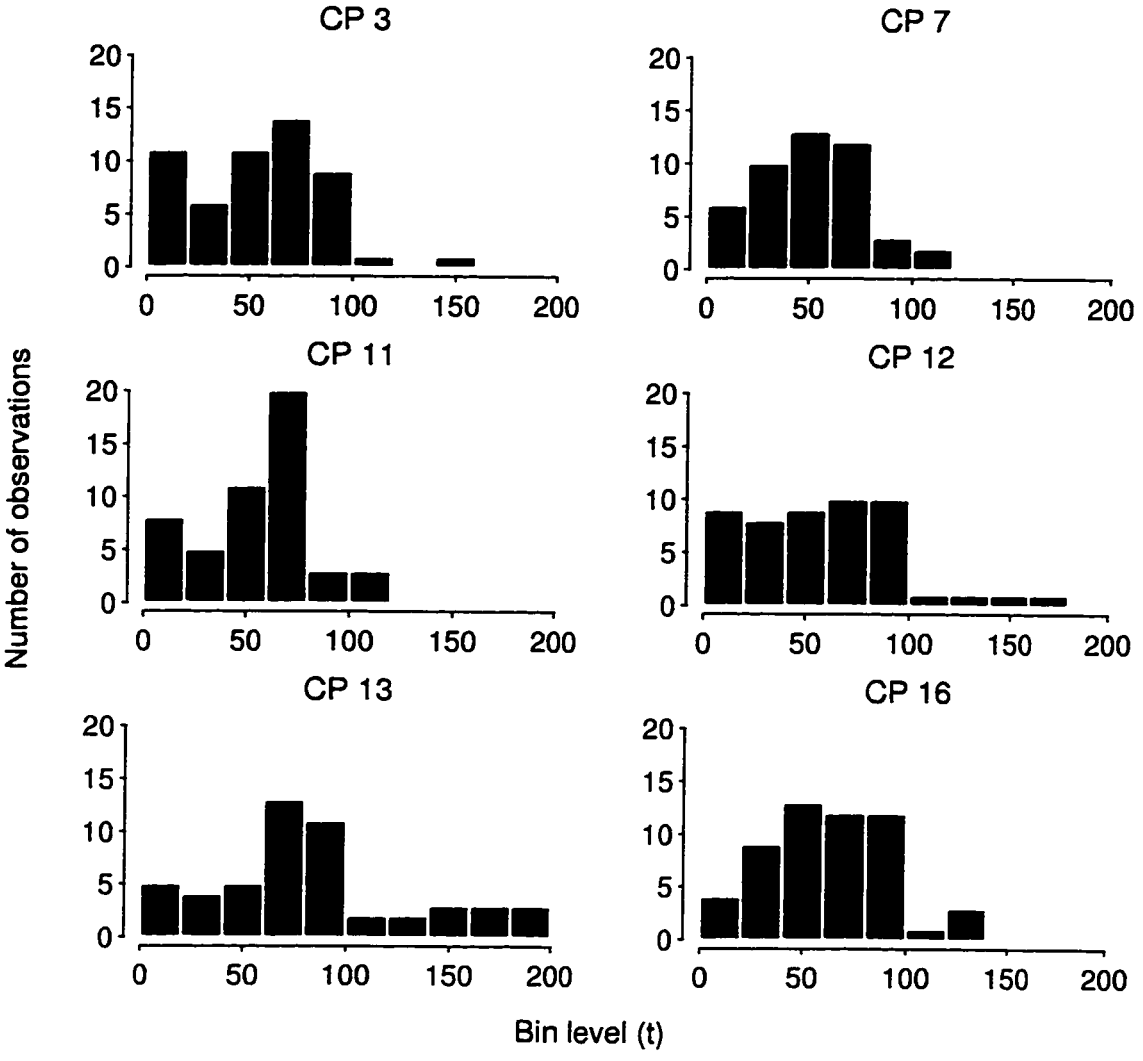
CP 3
CP 7
CP 11
CP 12
CP 13
CP 16
Number of observations
Bin level (t)
0
5
10
15
20
50
100
150
200

Figure 1.8. Summary graphs for observer data collected on factory trawlers during the 1993 Pacific hake fishery. A. Frequency distribution of haul weight. B. Frequency distribution of haul duration. C. Frequency distribution of haul interval. D. Scatterplot of haul interval versus haul weight. E. Scatterplot of haul weight versus haul duration. F. Scatterplot of haul interval versus haul duration. A lowess smooth (Chambers and Hastie 1992) was fit to each scatterplot to bring out the trend in the data.

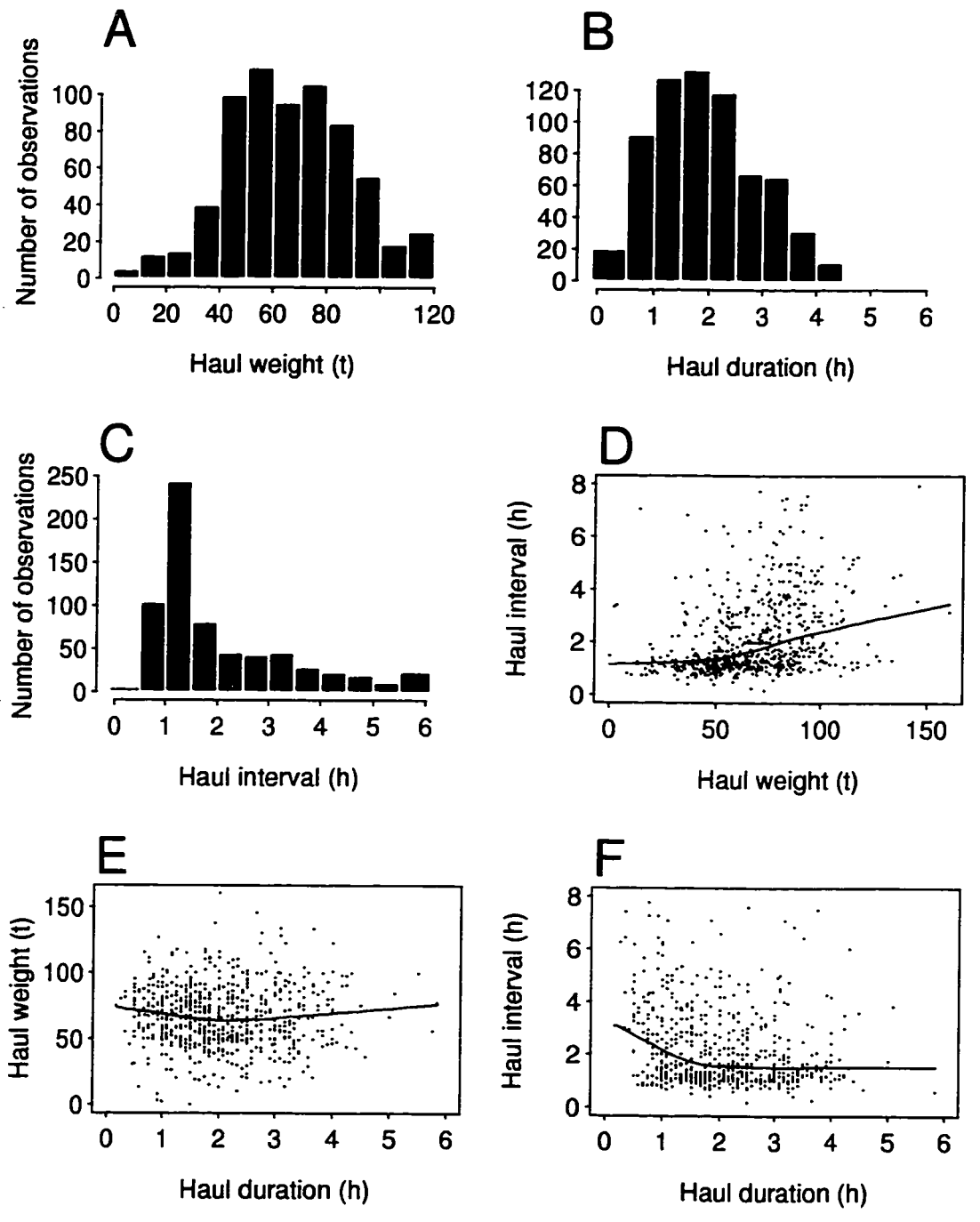
A
Number of observations
0
20
40
60
80
100
120
Haul weight (t)
B
0
20
40
60
80
100
120
0
1
2
3
4
5
6
Haul duration (h)
C
Number of observations
0
50
100
150
200
250
0
1
2
3
4
5
6
Haul interval (h)
D
Haul interval (h)
0
2
4
6
8
0
50
100
150
Haul weight (t)
E
Haul weight (t)
0
50
100
150
0
1
2
3
4
5
6
Haul duration (h)
F
Haul interval (h)
0
2
4
6
8
0
1
2
3
4
5
6
Haul duration (h)

Figure 1.9. Reward surfaces for "rule of thumb" decisions consisting of combinations of bin and catch thresholds for three different mean catch rates. The lowest contour line is where mean daily net revenue is zero. Succeeding contours show the net revenue for the "rule of thumb" strategy as a proportion of the mean net revenue for the SOC. The highest contour line is where the daily net revenue is 90% of the mean net revenue for the SOC.

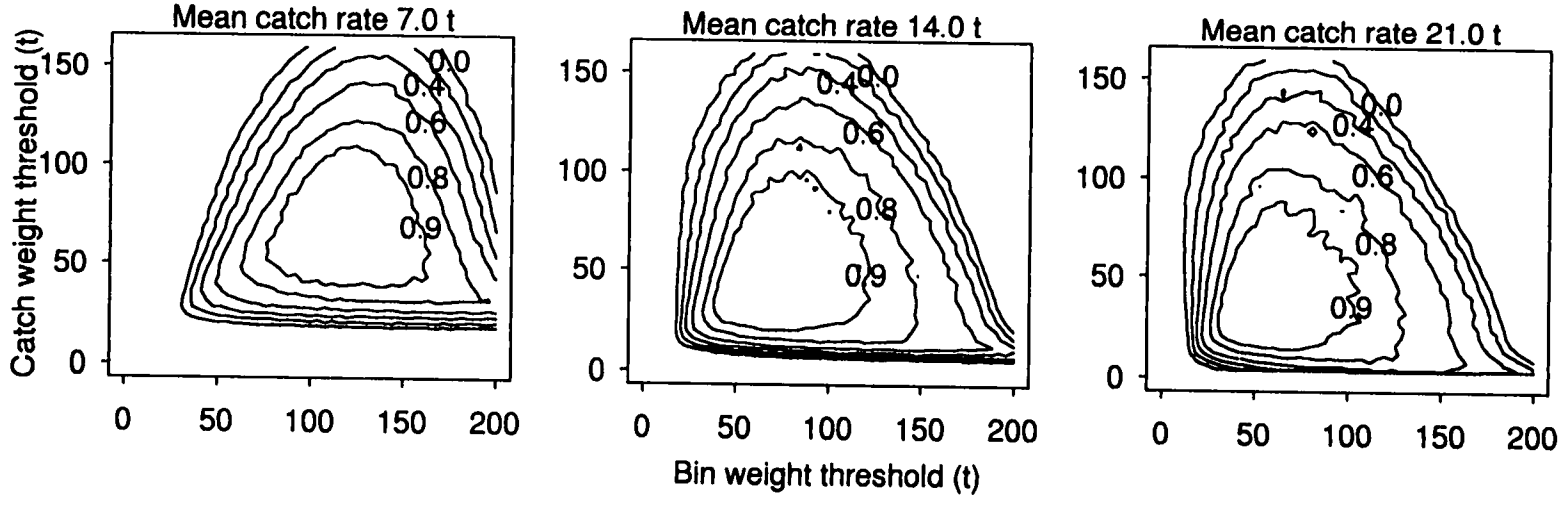
Mean catch rate 7.0 t
Mean catch rate 14.0 t
Mean catch rate 21.0 t
Catch weight threshold (t)
Bin weight threshold (t)
0.0
0.4
0.6
0.8
0.9
0
50
100
150
200

Figure 1.10. Stationary optimal controls for models with random and serially-correlated catch increments. A. SOC for random catch increment model. B. SOC for correlated catch increment model when the vessel is in the low density region. C. SOC for correlated catch increment model when the vessel is in high density region.

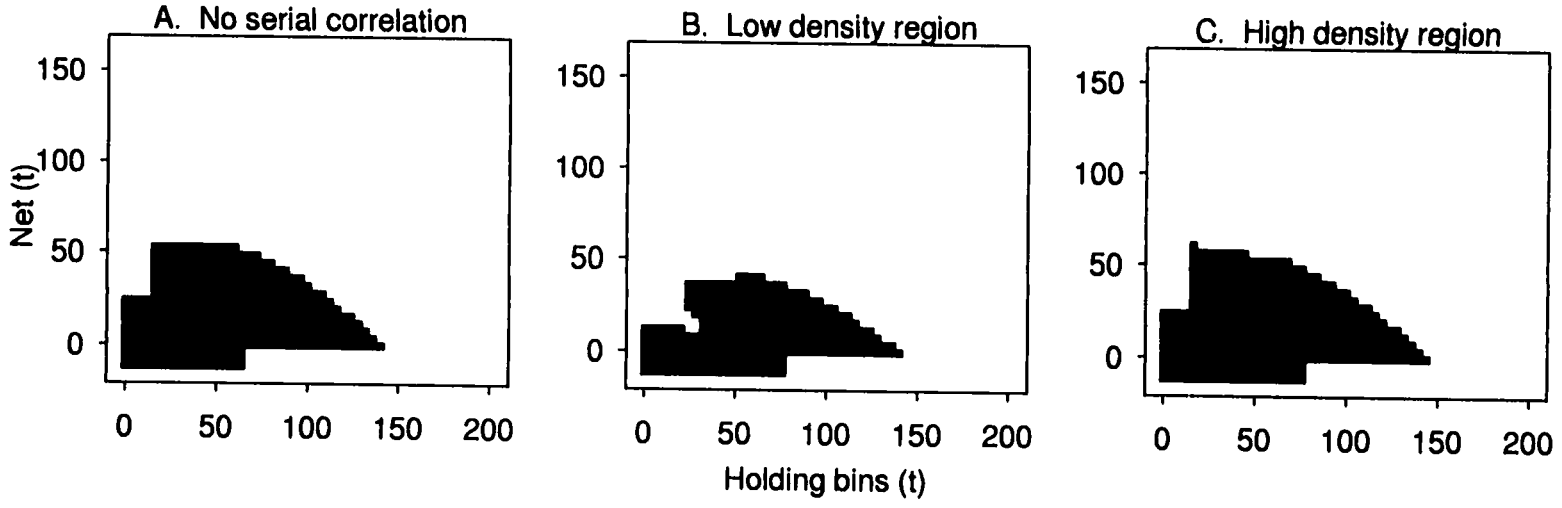
A. No serial correlation
B. Low density region
C. High density region
Net (t)
150
100
50
0
0
50
100
150
200
Holding bins (t)

Figure 1.11. Frequency distribution of haul weight in a forward simulation of the SOC for models with random catch increments, and correlated catch increments.

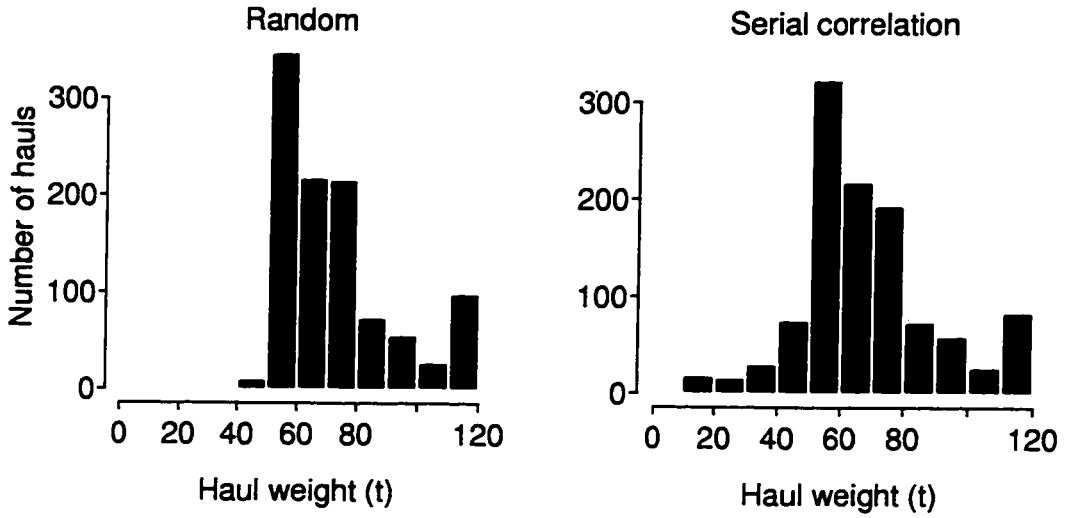
Random
Number of hauls
300
200
100
0
0 20 40 60 80 120
Haul weight (t)
Serial correlation
300
200
100
0
0 20 40 60 80 120
Haul weight (t)

Figure 1.12. Bin and catch thresholds for Markov decision process models with night fishing and without night fishing (between midnight and 07:00). The catch threshold was obtained by averaging the catch thresholds for bin levels from 16 t to the bin threshold.

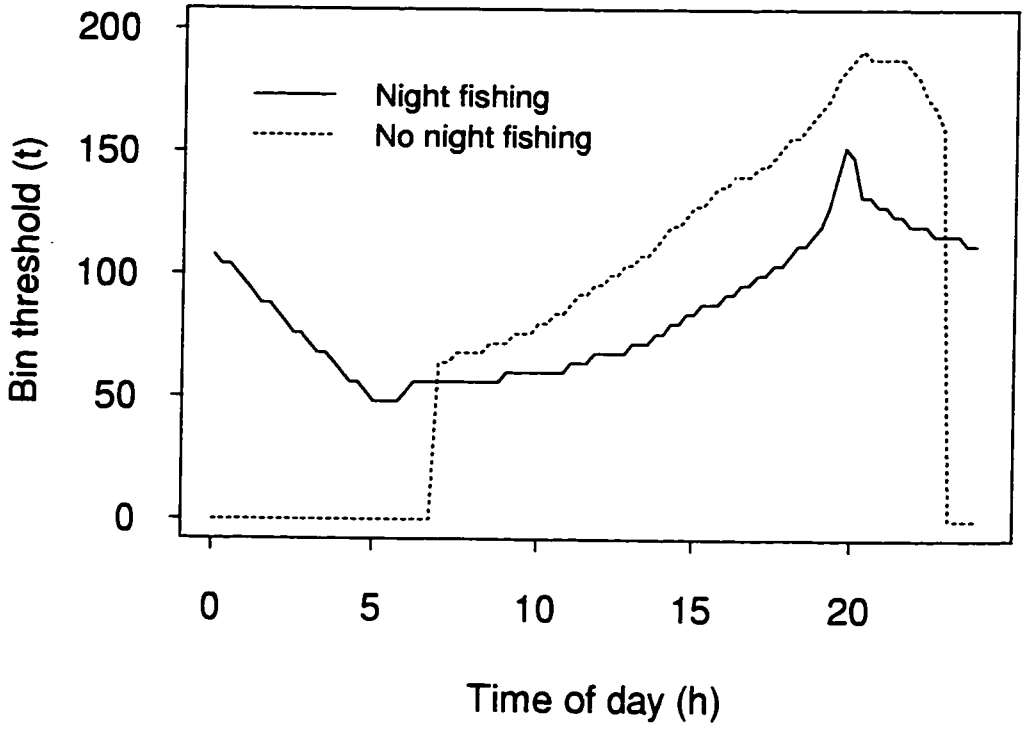
200
150
100
50
0
Bin threshold (t)
Night fishing
No night fishing
0
5
10
15
20
Time of day (h)

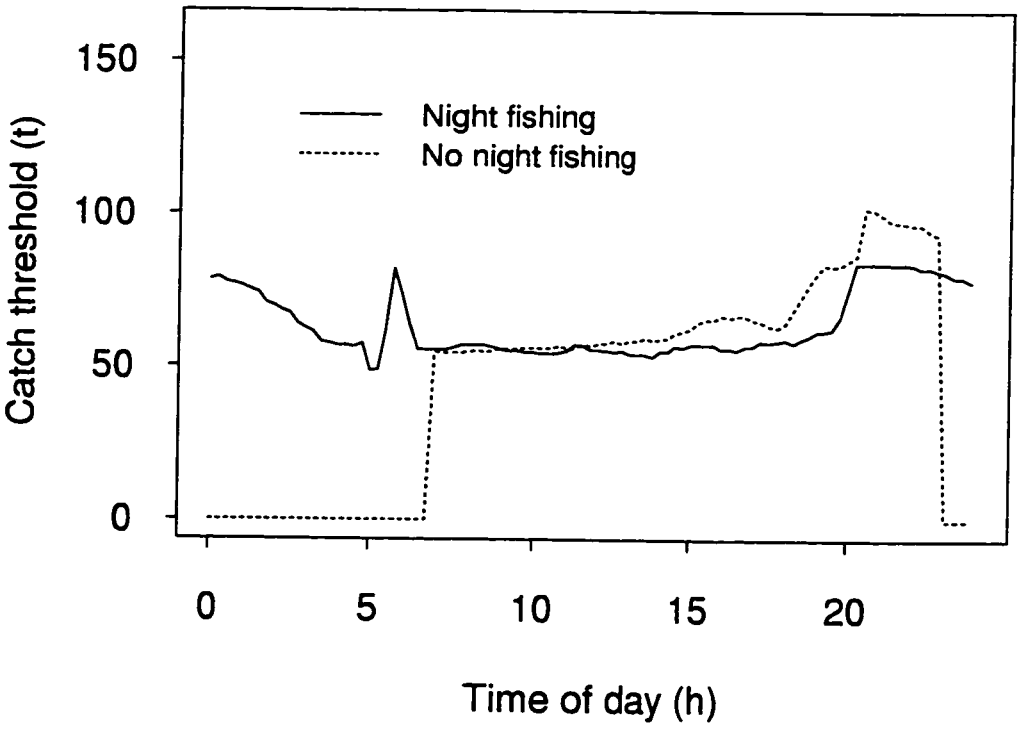
150
100
50
0
Catch threshold (t)
Night fishing
No night fishing
0
5
10
15
20
Time of day (h)

Figure 1.13. Mean tons in holding bins in a forward simulation of the SOC with and without night fishing.

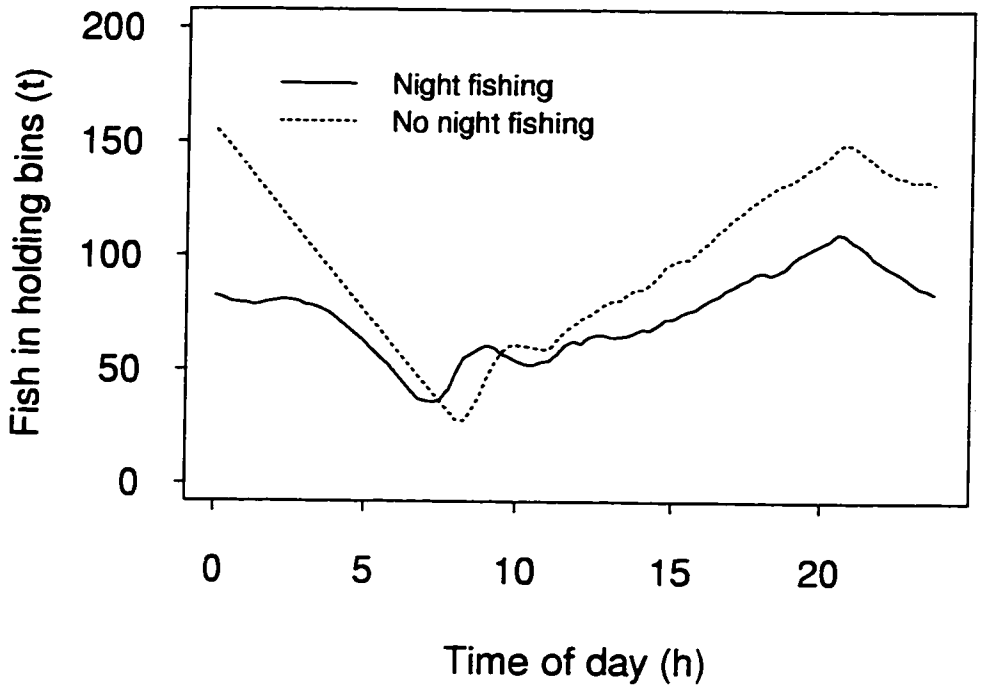
200
150
100
50
0
Fish in holding bins (t)
Night fishing
No night fishing
0
5
10
15
20
Time of day (h)

Figure 1.14. Proportion of the time actively fishing for forward simulations of the SOC with and without night fishing, and a "rule of thumb" (ROT) strategy (panel A). Proportion of the time actively fishing for factory trawlers in the 1992 fishery (night fishing banned) and 1993 fishery (night fishing allowed) (panel D). Mean haul weight and haul duration by time of day for forward simulations of the SOC with and without night fishing, and a "rule of thumb" (ROT) strategy (panels B and C), and for factory trawlers in the 1992 and 1993 at-sea fisheries (panels E and F).

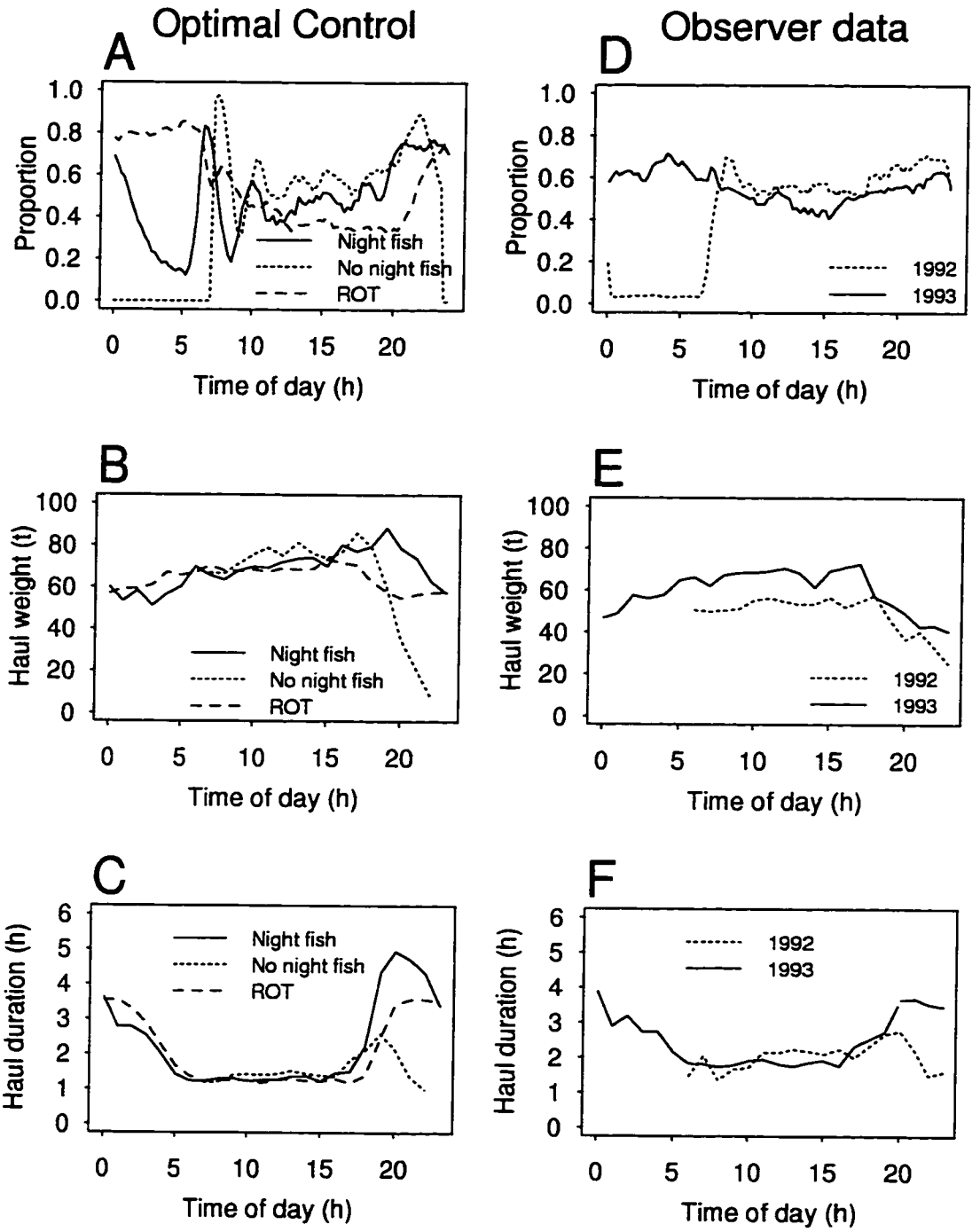
Optimal Control
A
Proportion
1.0
0.8
0.6
0.4
0.2
0.0
Night fish
No night fish
ROT
0
5
10
15
20
Time of day (h)
Observer data
D
Proportion
1992
1993
Time of day (h)
B
Haul weight (t)
100
80
60
40
20
0
Night fish
No night fish
ROT
Time of day (h)
E
Haul weight (t)
1992
1993
Time of day (h)
C
Haul duration (h)
6
5
4
3
2
1
0
Night fish
No night fish
ROT
Time of day (h)
F
Haul duration (h)
1992
1993
Time of day (h)

CHAPTER 2 - MESOSCALE FISHING PATTERNS OF FACTORY TRAWLERS

INTRODUCTION

Factory trawlers, fishing vessels that both catch and process fish, are important in many fisheries worldwide (Garcia and Newton 1995). The advanced technology of these vessels (including hydraulic winches to set and retrieve extremely large nets, automated filleting machines, flash freezers, freezer holds, fish meal plants, electronic echosounders, and GPS navigation and plotting equipment) enables them to efficiently catch and process large quantities of fish (up to 500 metric tons per day). The ability of these vessels to operate independently of port services for extended periods is a significant advantage in harvesting migratory species like Pacific hake (*Merluccius productus*), whose spatial distribution can vary greatly from one year to the next. Since fish can be processed immediately after they are caught, these vessels produce a high-quality product from fish species whose flesh undergoes rapid proteolysis when held at ambient temperatures.

In this chapter, I study the fishing patterns of factory trawlers as an example of the foraging behavior of animal predators. Although a factory trawler is, of course, a complex machine operated by a crew, from the perspective of its role in the ecosystem, it is reasonable to view it as a single agent--a midwater filter feeder that detects prey using echolocation. A similar approach was used by Gillis et al. (1995a, 1995b) to study

discarding behavior in a trawl fishery subject to trip limits. The foraging choices available to these vessels depend on the spatial and temporal scale of their assessment of the environment (Holling 1992). This chapter focuses on the mesoscale characteristics of the environment (5-50 km) and vessel movement at these spatial scales. Since factory trawlers do not return to port regularly to deliver fish to a processing plant, their movement patterns at this scale are assumed to be a pure foraging process. Foraging behavior at this scale can be described as a series of movements between successive trawling locations. The focus of this chapter is to develop statistical models for investigating the factors which influence these movements, in particular, those movements which indicate that the vessel has left the area in which it had been fishing previously.

The analyses of vessel movement presented in this chapter are motivated by a contribution to optimal patch foraging theory by Arditi and Dacorogna (1985, 1988). Their work generalizes the marginal value theorem (Charnov 1976) to habitats with arbitrary prey distributions. Although they limit their consideration to one-dimensional habitats, this is not as restrictive an assumption as it seems. Many fisheries occur within relatively narrow depth limits parallel to the shelf break or the coastline. Arditi and Dacorogna (1988) show that when presented with an arbitrary prey distribution in a habitat, the optimal forager should partition the habitat into contiguous areas of two types, areas in which it is optimal to forage, and areas in which the optimal strategy is to transit as quickly as possible without foraging. In the areas where it is optimal to forage, the forager should move on when the density of prey declines below the critical density that partitioned the habitat into foraging and non-foraging regions (Fig. 2.1). The critical

density is determined by the mean density of prey in the habitat as a whole (similar to the marginal value theorem), and the forager's functional response curve. For a factory trawler, the functional response is the relationship between fish density and surimi production, and is a non-linear function of the capture efficiency of the net, the time required to set and retrieve the net, and the production capacity of the factory (Dorn 1998).

The Arditi and Dacorogna foraging model implies that the forager perceives its habitat as a "behavioral landscape" in which different activities are performed in different regions. This emphasis on the forager's perception is different than the marginal value theorem, where the pattern of the environment is assumed. The model suggests that the "patches" of classic optimal foraging theory may not be intrinsic to the environment, but a result of the forager imposing a particular cognitive structure on the environment. The critical threshold transforms an undifferentiated environment into a mosaic of two types of regions--foraging and non-foraging regions. The characteristic dimensions of those regions will depend on the spatial continuity of the prey population. A prey population with short-range spatial continuity would present the forager with many small patches to exploit. If the spatial correlation of the population extends to wider scales, the patches will be larger and fewer in number. Since the forager alternates between two patterns of movement, small-scale movements within foraging area, and larger scale movements that occur when the forager transits between foraging areas, the spatial continuity of the prey population has important implications for the movement characteristics of the forager.

The transition from the theoretical models of Arditi and Dacorogna (1988) to a

statistical analysis of the effect of catch rates on vessel movement must confront the real complexity of the environment--that is, those important characteristics of the environment not included in the theoretical model. Although the model allows the catch rate to decline in a foraging area only due to fishing activity, in fact, local changes in prey abundance may occur due to a variety of factors, many of them unrelated to fishing activity. Moreover, although the model assumes perfect knowledge of the environment, fishing vessels typically will not know in advance where the regions of high prey density are located. Catch rates for Pacific hake also follow a diel pattern, with the daytime rates about twice as high as nighttime catch rates when hake are dispersed through the water column. Catch rates vary between vessels because of differences in the nets used, vessel horsepower, and other technological characteristics of the vessel. To standardize the catch rates by accounting for the diel trend and differences between vessels in fishing power, a preliminary model was fit to the haul-by-haul catch rate data with time of day and a categorical term for individual vessels as predictor variables. The residuals from this model were used in the analysis of vessel movement patterns. This approach follows Vignaux (1996a, 1996b) who used a similar strategy to assess the spatial structure of fish distribution and to analyze fishing behavior in a trawl fishery off New Zealand.

The statistical analyses presented in this chapter examine the effect of catch rates and other information on the decision to leave an area where the vessel is fishing. One might expect the catch rate of the target species to be the most factor affecting this decision, but other factors, such as the presence of other vessels nearby, may also be important. The first objective of the statistical analysis will be to evaluate the effect of

catch rate of the most recent haul on the decision to leave. Next, the effect of prior catch rates will be evaluated. Previous catches differ from the most recent catch by being further away in space and time from the most recent catch. Since areas of higher than usual hake density are transient, vessels may use a weighting function that assigns more emphasis to catches which are more recent. An exponential weighting model has been used in theoretical work on other foraging situations (McNamara and Houston 1985) and will be evaluated here. In addition, the effect of the presence of other vessels fishing nearby on the decision to move will be evaluated. The presence of other vessels could induce the vessel to remain longer in the area than it would if its decision were based strictly on its own catch rate.

The subsequent sections of the chapter are organized as follows. A geostatistical analysis using data from acoustic resource assessment surveys is used to assess the spatial continuity of Pacific hake. The results of this analysis are used to select the appropriate spatial scale at which to assess vessel movement patterns. Then, using fishery data collected by at-sea observers, models are fit to the haul-by-haul catch rates of the factory trawler fleet during 1991-95 using time of day and vessel as predictor variables. The residuals from this model are then used in a generalized additive model (GAM) to predict the probability of movement from a foraging area. Other variables are also assessed in the model. Finally, the results are compared with other studies of spatial correlation and fishing behavior, and recommendations are offered about further research into fishing behavior.

METHODS

Analysis of Pacific Hake Spatial Pattern

Geostatistical techniques were used to assess the spatial continuity of Pacific hake using data from acoustic resource assessment surveys conducted by the NOAA research vessel *Miller Freeman* during July-September of 1992 and 1995 (Dorn et al. 1994; Wilson and Guttormsen 1997). Acoustic data were collected with a Simrad EK500 scientific echo-sounding system (Bodholt et al. 1989) using a 38 kHz transducer mounted on the vessel's centerboard 9 m below the waterline. Acoustic data were processed on a SUN workstation using Simrad BI500 echo-integration and analysis software (Foote et al. 1991) to exclude non-hake sound-scatterers from the echo integration. The survey design consisted of equally spaced east-west transects extending from 30 m to approximately 1,500 m bottom depth. Transects were spaced 10 nautical miles (nmi.) apart for most of the survey, with higher density transect spacing (5 nmi.) in the Juan de Fuca canyon-La Perouse region (48°-49° N lat.). Survey transects were run only during the daylight hours because hake disperse during the night. The acoustic backscatter attributed to Pacific hake by 0.5 nmi. transect section was converted to fish density using a length-target strength relationship of $TS = 20 \log(length) - 68$ (Traynor 1996). Since 40-60 days are required to conduct a coastwide acoustic survey of Pacific hake, some redistribution of fish would be expected during the survey operations. However, adjacent transects were almost always surveyed within one day, and usually within several hours, so the effect of fish redistribution should be relatively minor at scales less than the transect spacing. To

conduct an analysis of spatial correlation using acoustic survey data, it is necessary to assume that they provide an instantaneous "snapshot" of Pacific hake distribution patterns.

Directional correlograms (Rossi et al. 1992) were estimated for mean hake density by 0.5 nmi. transect section, $z(x_i)$, where x_i is location of the transect section. Separate correlograms were estimated for E-W (east-west) and (N-S) north-south directions, with a directional tolerance of $\pm 45°$. In the E-W direction, binning intervals of 2.5 km were used to a maximum distance of 50 km; in the N-S direction, binning intervals of 10 km were used to a maximum distance of 80 km. Different binning intervals were used because the survey design of parallel E-W transects yields fine-scale information on spatial correlation along the transect in the E-W direction, but relatively coarser information in the N-S direction (Pelletier and Parma 1994). Since the orientation of the shelf break is north-south in the area where the fishery operates, the N-S correlogram measures along-shelf spatial correlation, while the E-W correlogram measures the cross-shelf correlation. In addition, an omnidirectional correlogram was estimated, using the same binning strategy as for the E-W correlogram. The estimation was restricted to acoustic data collected north of 41° N lat. and east of 127° W long., an area that roughly corresponds to the area where the fishery operates. The correlogram is a plot of the lag correlation, $\hat{\rho}(\boldsymbol{h})$, such that

$$\hat{\rho}(\boldsymbol{h}) = \frac{\frac{1}{N(\boldsymbol{h})} \sum_{i=1}^{N(\boldsymbol{h})} \left[z(x_i) - m_{-\boldsymbol{h}} \right] \left[z(x_i + \boldsymbol{h}) - m_{+\boldsymbol{h}} \right]}{s_{-\boldsymbol{h}} \, s_{+\boldsymbol{h}}},$$

where $z(x_i)$ and $z(x_i+\boldsymbol{h})$ are pairs of hake densities separated by vector distance $\boldsymbol{h}$, and $m_{-\boldsymbol{h}}$ and $m_{+\boldsymbol{h}}$ are the means of the initial and terminal points of the vectors used to estimate the lag correlation, and $s_{-\boldsymbol{h}}$ and $s_{+\boldsymbol{h}}$ are the standard deviations of the initial and terminal points. Rossi et al. (1992) call this the non-ergodic correlogram to distinguish it from the more usual spatial correlogram where the global mean is subtracted out, and the global variance is used to scale the covariance. Rossi et al. (1992) recommend this form of the correlogram in ecological applications where non-stationarity in local means and variances is frequently encountered.

To demonstrate how the spatial structure in hake distribution might be perceived by fishing vessels, I estimated structure functions using hake density by 0.5 nmi. transect section. The structure function is a description of the spatial pattern of resources from the perspective of the forager (Mangel and Adler 1994). I applied an indicator transform to hake densities of the form

$$i(x;z) = \begin{cases} 1 & \text{if } z(x) \geq k \\ 0 & \text{if } z(x) < k \end{cases},$$

where the threshold density ($k = 635\ kg\ ha^{-1}$) is the value of hake density such that the median of all acoustic densities greater than the threshold is equal to the median density implied by the catch rates for factory trawlers during the fishery.

To obtain an expected density from the fishery catch rates, the area swept by the net was obtained from the haul duration, towing speed, and the horizontal opening of the

net (= 90 m, the mean net width recorded by several observers). Daylight hauls (between 06:00 and 20:00 Pacific Standard Time) made by factory trawlers during the 1991-95 seasons were used. Since a strong avoidance response has been reported for Pacific hake when encountering midwater trawl nets (Nunnallee 1991), the assumption of 100% capture efficiency is unjustifiable. To estimate the threshold density, I assumed that a commercial midwater trawl would capture 50% of the fish in the water column, and evaluated the sensitivity of the results to this assumption. It should be emphasized that the purpose here was to obtain a rough approximation of the spatial pattern and geographic extent of the regions where fishing would be successful.

The structure function is defined as:

$p(i(x+\boldsymbol{h})=1 \mid i(x)=1)$ = Prob {resource at vector distance $\boldsymbol{h}$ away, given that there is resource at the current point}

$p(i(x+\boldsymbol{h})=1 \mid i(x)=0)$ = Prob {resource at vector distance $\boldsymbol{h}$ away, given that there is no resource at the current point}.

In this definition, the structure function has been generalized from Mangel and Adler (1994) to allow the structure function to vary depending on the direction away from the current point. This broader definition of the structure function makes it possible to consider directional structure functions similar to directional correlograms. To estimate the structure function, the algorithm of Mangel and Adler (1994) was followed,

$$\hat{p}\left(i(x+\boldsymbol{h})=1 \mid i(x)=1\right) = \frac{\sum_{k=1}^{N(\boldsymbol{h})} i(x_k+\boldsymbol{h})\, i(x_k)}{\sum_{k=1}^{N(\boldsymbol{h})} i(x_k)} .$$

Estimation of the structure function used the same binning strategies that were used to estimate the directional correlograms.

Catch Rate Model

NMFS-certified observers are placed on all factory trawlers and motherships in the at-sea fishery. While they are onboard, observers maintain a complete record of the catch weight, duration, set and retrieval times, and retrieval location for each haul made by the vessel. Set location, however, is not recorded, limiting the spatial resolution of estimated distances between trawling locations. A tow that retraced the path of previous tow in reverse direction could have a retrieval location that is greater that 10 km away. Alternatively, two tows that ended at the same location could have trawled towards that location from opposite directions. Since all vessels carry observers, there is a complete record of all hauls for all vessels for the duration of the fishery. This data resides in the NORPAC database, an ORACLE relational database maintained by the North Pacific Observer Program at the Alaska Fisheries Science Center (7600 Sand Point Way NE, BIN C15700, Seattle, WA 98115-0070). The number of hauls in each fishing season by factory trawlers ranged between about 1,000 and 2,000 (Table 2.1).

A generalized additive model (GAM) with Poisson error (Hastie and Tibshirani

1990) was used to standardize the catch rates. This form of GAM has been used in marine ecology applications to analyze trawl survey data (Smith 1990, Swartzman et al. 1992). Poisson regression is a pragmatic choice for "count-like" data where the variance is proportional to the mean (McCullagh and Nelder 1983),

$$E[cr_i] = \mu(\boldsymbol{x}_i)$$

$$Var[cr_i] = \phi\ \mu(\boldsymbol{x}_i)\ ,$$

where cr_i is the catch rate in t hr^{-1} for the ith haul, $\mu(\boldsymbol{x}_i)$ is the expected catch rate of the ith haul as a function of a vector of covariates $\boldsymbol{x}_i$, and ϕ is an overdispersion parameter that models the additional variability in the data relative to the Poisson distribution, where the variance is equal to the mean (Lawless 1987).

The structural part of the model consisted of two additive terms: a categorical term for vessel, and a "smooth" function of time of day (average of set and retrieval times) estimated using the *loess* scatterplot smoother (Chambers and Hastie 1992). Due to the short duration of the at-sea hake fishery (3-4 wk), a seasonal effect was not considered necessary to include in the model. The additive part of this model is log-linear; that is, $\mu(\boldsymbol{x}_i) = \exp[\eta]$, where η is the additive predictor. Separate models were fit for the 1991-95 seasons. A span width (fraction of the data used by *loess* to estimate local linear regressions) was fixed at 0.3 based on a series of trial models in which the span width was

varied systematically. A span width of 0.3 provided enough flexibility to capture the diel trend while at the same time excluding higher frequency variation from the smooth term.

Statistical Models of Vessel Movement

Although the focus of this analysis is to determine the factors leading to the decision to leave a mesoscale aggregation of fish, without an extensive acoustic survey conducted at the same time as the fishery, it is difficult to know with certainty when this decision is made. Consequently, it was necessary to use some easily measurable proxy for this decision. If a critical distance between successive trawling locations is chosen appropriately, it should be possible to partition the inter-trawl movements into those within an area and those representing a transit between areas. For this research, an distance of greater than 30 km between haul retrieval locations was selected as the criterion for moving to a new area. This criterion was based on the examination of Pacific hake spatial patterns during the 1992 and 1995 acoustic surveys reported in the results, which suggests that strong spatial correlations do not extend beyond ~25-35 km. Consequently, the dependent variable in the statistical model is the geometric distance between successive haul retrieval locations re-coded as 0-1 variable, where 0 denotes a distance of less than 30 km, and 1 denotes movement of greater than 30 km. Mean trawling distance, assuming the vessel travels in a straight line for the duration of the haul, was 16.2 km during 1991-95, which is roughly one-half the range of spatial correlation of 30 km.

Logistic regression is the primary statistical model for analyzing binary response

data. Logistic regression predicts the probability of an event (movement greater than 30 km) based on a set of covariates. Since the Arditi and Dacorogna (1988) model suggests that a threshold catch rate triggers the decision to move, a flexible regression technique, the GAM described above, was used for the statistical analyses. The expectation and variance for logistic regression are

$$E[y_i] = \pi(\boldsymbol{x}_i)$$

$$Var[y_i] = \pi(\boldsymbol{x}_i)[1 - \pi(\boldsymbol{x}_i)] ,$$

where y_i is the 0-1 response variable, $\pi(\boldsymbol{x}_i)$ is the probability of moving to a new area following the *i*th haul as a function of a vector of covariates $\boldsymbol{x}_i$. In a GAM, the linear predictor of logistic regression is replaced by an additive predictor with the general form $\eta = f_1(x_1) + f_2(x_2) + \ldots + f_p(x_p)$, where $f_i(x_i)$ is a smooth function of x_i. As with the Poisson model, this "smooth" function is estimated with local linear regressions. The probability of the event is linked to the additive predictor by the logistic function, $\pi(\boldsymbol{x}_i) = \exp(\eta)/[1 + [\exp(\eta)]$. Potential covariates examined using this modeling framework were the catch rate residual for the *i*th haul, an exponentially weighted average of the catch residuals for previous hauls within 30 km, and the number of other vessels fishing nearby, where "nearby" is defined as the number of vessels within 30 km over the previous 6 hrs. Separate models were fit for the 1991-95 seasons. This model and the

Poisson regression model for catch rates were fit using the statistical modeling language S-Plus (StatSci 1993).

RESULTS

Spatial Analysis

In 1992 and 1995 NMFS acoustic surveys, areas of high Pacific hake density were found mostly in a narrow N-S band close to the continental shelf break (Fig. 2.2). Consequently, the E-W dimensions of the area where the fishery can operate are much narrower than its N-S dimensions. Interspersed regions of high and low density extend along the entire coast. Certain features along the shelf break tend to support higher densities of Pacific hake (e.g., Heceta Bank off central Oregon and Juan de Fuca Canyon off Cape Flattery), but high Pacific hake densities are not confined to these areas. In 1992, densities in excess of 635 kg ha^{-1} represented 8.9% of the surveyed area north of 41° N lat. and east of 127° W long., but 18.2% of the area within the 150-600 m bottom depth range, where most fishing occurs. In 1995, the percentages are 4.8% and 11.4%, respectively, for the surveyed area, and the area within the 150-600 m bottom depth range. The decrease in the area of high fish density from 1992 to 1995 may be due to an estimated 23% decline in the total biomass within these depth and geographic boundaries. A relationship between overall abundance and the proportion of potential habitat that is occupied has been observed for many fish populations (MacCall 1990).

The spatial correlograms support the depiction of hake spatial pattern in Figure 2.2. The E-W directional correlogram for the 1992 survey declines from 0.56 at a

distance of 0-2.5 km to near zero at ~25 km (Fig. 2.3). The N-S directional correlogram is similar to the E-W correlogram at larger distances (> 8 km) where comparison is possible. Despite differences in overall abundance and the location of the higher density areas in the 1995 survey, the directional correlograms for the 1995 survey show a similar pattern to the 1992 correlograms (Fig. 2.3). As with the 1992 correlograms, the E-W and N-S directional correlograms for the 1995 acoustic survey are similar at lag distances where comparison is possible. There is a slight positive correlation (~0.025) extending from 30 to 60 km in the 1995 survey that does not appear in the 1992 correlograms, but this correlation is only about 5% the correlation at a range of 0-2.5 km.

The data used to estimate the N-S correlation for the smallest lag distance (0-10 km) were collected along transects in the Juan de Fuca Canyon-La Perouse region, the only area where the transect spacing was 5 nmi. in both the 1992 and 1995 surveys. Since this a bathymetrically complex region--with a narrow steep-walled canyon and a large offshore bank--the correlation structure in this region may differ from other locations along the West Coast where the bathymetry is less complex. Additional acoustic data collected along transects oriented at angles to the usual survey grid are needed to adequately assess anisotropy. Although Figure 2.2 suggests the presence of larger scale N-S structure; that is, higher densities in the Heceta Bank and Juan de Fuca canyon area and lower densities elsewhere, the spatial statistics interpret these patterns as N-S trends rather than as a spatial correlation (Swartzman et al. 1992). From the perspective of the fishing vessel, the key spatial characteristics of the hake population would appear to be 1) a narrow elongated region of potential occurrence, and 2) transient fishable aggregations

of 20-30 km in size that can be fished on multiple times.

The directional structure functions for the 1992 and 1995 NMFS acoustic surveys are shown in Figure 2.4. The E-W and the N-S structure functions are similar for both surveys. The structure functions for 1992 and 1995 show similar patterns, with a conditional probability of 0.5-0.4 of finding high fish densities at short distances (< 2.5 km) and a rapid decline to baseline levels at 25-35 km. This decline is slightly steeper than the decline in the correlograms. As distance increases, the conditional probability for finding high fish density approaches the unconditional probability (~ 0.10 in 1992 and ~ 0.05 in 1995).

The estimated structure functions are fairly robust to the choice of a threshold density in the range of plus or minus 25% of 635 kg ha^{-1}. At higher threshold densities, there is a tendency for the conditional probability of high fish density to decline more rapidly than at lower thresholds, so that baseline levels are reached at ~20 km rather than 30 km. Consequently, inaccuracies of this magnitude in the length-TS relationship for hake or in the assumed 50% capture efficiency of midwater trawls would not cause a severe bias. These results suggest that if a vessel moves more than ~30 km away from its current fishing location, its probability of encountering high densities of hake is similar to a location chosen at random within potential hake habitat. Consequently, these results provide the rationale for the statistical analysis of vessel movement, where a movement of greater than 30 km between trawling locations is assumed to represent a decision by the fishing vessel to leave a local area of high fish density.

Catch Rate Model

Since the objective of fitting the Poisson regression model to the catch rates was to obtain a set of catch rate residuals for additional analysis, only general features of the model are presented. For each year 1991-95, both terms in the model, vessel and time of day, are highly significant ($p<0.001$). The high significance level indicates that vessel and time of day are important influences on the catch rate, but this result is at least partly due to the large amount of observational data available for fitting the model (Table 2.1). The GAM analogue to the coefficient of determination (1.0 minus the ratio of the model deviance to the deviance for a null (mean) model (Swartzman et al. 1992)) ranged from 25.5% in 1991 to 43.9% in 1993. The relatively low r^2 values suggest that there is considerable variation in catch rates not explained by the model. Model results are best interpreted by looking at model predictions rather than by directly examining the model coefficients. Most vessels tended to have similar predicted noon catch rates, although in each year, several vessels had predicted catch rates that were more than twice the rest of the fleet (Fig. 2.5). Figure 2.5 shows only the predicted catch rates for 1993; however, the pattern for the other years was similar. In particular, vessels with higher catch rates in 1993 consistently experienced higher catch rates than the rest of the fleet throughout 1991-95. These variations may be explained by differences in vessel or net characteristics, variation in fishing skill, or differences in fishing strategy. For example, some vessels may spend more time searching, but target only the highest densities they encounter while searching.

The GAM smooth term for time of day (mean of set and retrieval times) generally

shows an increase in catch rate at ~06:00, and a decline at ~18:00 (all times are Pacific Daylight Time, UTC+7) (Fig. 2.5). Sunrise and sunset at 1 May at 45° N lat. 125° W long., the approximate location of Heceta Bank off central Oregon, occurs at 06:11 and 20:24 PDT, respectively, suggesting that the diel variation in catch rates is closely coupled to ambient light levels. In 1992, fishing was prohibited during nighttime (from midnight to one hour after official sunrise) to reduce the bycatch of chinook salmon. The GAM smooth term for that year does not show an increase in the predicted catch rate at sunrise shown by GAM smooth terms for other years. In 1991, 1992, 1994 and 1995 catch rates peaked in mid-morning (~10:00), but in 1993, for reasons that are unclear, catch rates peaked in the afternoon instead. Figure 2.5 shows only the predicted diel pattern in the catch rate for a representative vessel in all years. Since the additive predictor for logistic regression is log-linear, the pattern for other vessels would simply be scaled upwards or downwards by a multiplicative factor. The mean catch rates for the entire factory trawler fleet were similar in 1991-93 and 1995, while in 1994 the catch rate was 43% higher than the average for the other years (Table 2.1).

The catch rate residuals ($cr_i - \hat{cr}_i$) have a nearly symmetric distribution, with a mean of zero (as expected) and a median of -7.16 t hr^{-1}. There are a few extremely large positive residuals (maximum 1628.0 t hr^{-1}) suggesting some skewness is present. However, only 1% of the residuals are larger than 218.5 t hr^{-1}. A plot of the mean catch rate residual versus inter-trawl distance provides additional support for the use of a 30 km inter-trawl distance to indicate the decision to move to a new area (Fig. 2.6). For inter-trawl distances less than ~30 km, the mean catch rate residual decreases with increased

inter-trawl distance, while at distances greater than ~30 km, the mean catch rate residuals are strongly negative, and show no consistent relationship with inter-trawl distance. This suggests that the pattern of spatial correlation detected in the acoustic survey data is perceived in a similar way by fishing vessels.

GAM Models of Vessel Movement

The sequence of terms assessed in the models consisted of the following: 1) the catch rate residual for the most recent haul, 2) an weighted average of previous hauls within 30 km, including an assessment of the appropriate exponential weighting coefficient to use, and finally, 3) the number of other vessels operating nearby. This order was established so that the most recent information on the target species would be assessed first, while information that is less recent, or less sure (in the case of information on the activity of other vessels) would be addressed subsequently. Trial models with a term for the number of vessels added first showed smaller declines in deviance than models with a term for the catch rate residuals added first. This suggests that the order in which terms were evaluated was a reasonable approach.

Prior to fitting models, several exploratory data analyses were conducted. Figure 2.7 shows the path of a single vessel during a 28-day opening in 1994, constructed by connecting the haul retrieval positions with straight lines. Searching behavior between hauls would, of course, not appear on this figure. The distribution of between-trawl move distances during 1991-95 has a mean of 14.2 km, a median of 8.0 km, and is skewed significantly to the right (Fig. 2.8). Out of a total of 6914 valid observations for 1991-95,

530 (7.7%) consisted of move distances greater than >30 km, the criterion assumed to indicate a decision to move to a new area.

A comparison of models with linear term for the catch rate residual of the immediately preceding haul and a smooth term for the catch rate residual evaluated whether there was significant non-linearity between the catch rate residual and the probability of movement. A span width of 0.5 was selected for the smooth term by fitting a series of trial models with varying span widths for the 1994 data, and choosing a span width that provided enough flexibility to capture the non-linearity in the data, but did not result in an excessive amount of roughness in the smooth term. The addition of a smooth term for the catch rate residual for the immediately preceding haul was significant at α = 0.05 in the GAM models for four out of the five years (Table 2.2). P-values based on likelihood ratio tests (Hastie and Tibshirani 1990) for adding the non-linear smooth term ranged from <0.001 in 1991 to 0.128 in 1993. The smooth term for the catch rate residual for each year consistently shows an increase in the probability of movement with declining catch rates (Fig. 2.9). Although there are some differences between years, in general the predicted probability of movement is low when the catch rate residual is positive, increases relatively rapidly when the catch rate residual becomes negative, then remains stable at higher levels with further decreases in the catch rate residual. To address whether these results were being driven by the behavior of only a few vessels, models with individual terms for vessel were fit for 1993 and 1994 using regular logistic regression. Patterns of increasing probability of movement with declining catch rates were consistent for all vessels, although there was considerable variation in the slope and the inflection point of

the logistic curves.

To model the role of earlier information on the decision to leave an area, it was necessary to consider which hauls will be used and how much influence they should have. Certainly, recent hauls that are nearby should receive the most weight, but during the course of a fishing season a vessel will move several times, and often return to a location that was fished earlier in the season. The particular summary of previous experience used for this analysis was an exponentially weighted average, x_j, of previous hauls, such that the catch rate residual for most recent haul receives a weight of 1.0, and previous hauls within 30 km of that haul receive progressively less weight the further back in time that they occurred;

$$x_j = \frac{\sum_{k=1}^{j} (cr_k - \hat{cr}_k)\, i_j(k)\, e^{-rt_j(k)}}{\sum_{k=1}^{j} i_j(k)\, e^{-rt_j(k)}},$$

where $i_j(k)$ is an indicator function that takes the value 1.0 if the kth haul is within 30 km of the jth haul and zero otherwise, $t_j(k)$ is the time in days from the kth haul to the jth haul, and r is an exponential coefficient that governs the rate that the catch rate residuals from earlier hauls get down-weighted relative to the most recent haul. This summary of previous fishing experience was calculated on a vessel-by-vessel basis, not for the fleet as a whole.

The key parameter in this approach to modeling past information is the exponential coefficient, r. To gain some insight into the appropriate choice for r, deviance profiles

across r were obtained for each year by varying r incrementally from 0.5 to 10 in steps of 0.5. Although there were differences between years in the shape of r profile, in each year there was a value of r which resulted in a lower deviance than the model which used only the most recent catch rate residual (Fig. 2.10). The minimum deviance r values were generally in the range of 2.0-6.5 (which imply half weights of 2.5-8 hrs). The value of r with minimum deviance for all years was 3.5, which results in a half-weight of 4.8 hrs; that is, a haul retrieved 4.8 hrs before the current haul receives half the weight in the weighted average. The average time between haul retrievals on a factory trawler is usually about 5 hrs (mean haul duration 2.5 hrs, mean time between hauls 2.5 hrs). This suggests that the decision to leave an area is based on information only from the most recent 1-2 hauls. The change in deviance for $r = 3.5$ ranged between 3.1 in 1993 and 14.1 in 1995 (Table 2.2); however no attempt was made to associate p-values with these changes in deviance. Determining the appropriate degrees of freedom for the likelihood ratio test is difficult because of correlation in the catch rates of successive hauls, and the choice of the exponential coefficient r used in the weighted average.

The influence of local fishing activity on the decision to leave an area was examined next. Similar issues regarding the choice of an appropriate spatial and temporal frame to summarize information on local fishing activity must be addressed. The summary of local fishing activity used for this analysis was a simple count of the number of unique vessels (both catcher processors and catcherboats delivering to motherships) within 15 km that had conducted trawling operations within the previous 6 hrs. Fifteen kilometers is an approximation of the range of sight from a vessel at sea. This summary of local fishing

activity ranged from 0 to 12 vessels, with a mean of 2.6 vessels (Fig. 2.11). Nineteen percent of the time there were no other vessels within 15 km. The GAM smooth terms for local fishing density show a decrease in the probability of movement with increasing local fishing density (Fig. 2.12). The smooth terms are fairly linear throughout their range. The smooth terms are significant at $\alpha = 0.05$ in all years except 1994 (Table 2.2).

DISCUSSION

The analysis of acoustic survey data found that the spatial correlation extended to 25-35 km. These results are generally comparable with other research on similar species. Sullivan (1991) found that spatial correlations of spawning pollock in Shelikof Strait, Alaska, extended to about 30 km. Other analyses of survey or fishery data reporting spatial-correlation ranges are Polacheck and Vølstad (1993), haddock on Georges Bank, range - 9 nmi.; and Vignaux (1996a), hoki off New Zealand, range - 11 nmi. The factors which produce spatial correlation in fish populations are poorly understood. Ultimately, the physical oceanography of the summer feeding habitat of Pacific hake probably determines its correlation structure. Instability in the California Current mean flow produces mesoscale meanders and eddies that are sites of enhanced primary production (Abbott and Zion 1987) and create fronts which concentrate zooplankton, including euphausiids, the primary food of Pacific hake (Mackas et al. 1991, Rexstad and Pikitch 1986). The spatial scale of these mesoscale oceanographic features is determined by the baroclinic Rossby radius of deformation, which is ~25 km in mid-latitudes off the west

coast (Thomson et al. 1992). If Pacific hake concentrate in areas of high zooplankton density, aggregations may occur in association with these mesoscale oceanographic features. However, this is an area of active research, and additional work is needed to elucidate the biophysical linkages between the physical environment and regions of high fish abundance.

The geostatistical analyses of Pacific hake spatial structure demonstrates the importance of considering the spatial characteristics of fish populations when interpreting vessel movement patterns. Other research on fishing behavior has usually imposed ad hoc models of decision-making by looking at movement between arbitrary geographic blocks or statistical reporting areas, which may be unrelated to how fishermen perceive their environment (Hilborn and Ledbetter 1979, Gillis et al. 1993, Vignaux 1996b). Eales and Wilen (1986), however, examined fishing location choice in a shrimp fishery where the potential fishing area was divided into smaller regions based on fishing patterns. The structure function illustrates how the foraging landscape would be perceived by a fishing vessel that requires a threshold fish density in order to operate profitably. To estimate the structure function, however, it was necessary to link fishery catch rates with acoustically measured fish densities by making some fairly crude assumptions regarding the capture efficiency of commercial fishing gear. Independent information is needed on level of fish density that can support fishing activity, such as might be obtained by placing a calibrated echo sounder on a commercial fishing vessel.

The results of the GAM models of vessel movement showed that there is a low probability that a vessel will leave a foraging area when its catch rate is higher than its

expected catch rate. The probability of moving increases sharply when catch rate residuals become negative. This result generally agrees with the Arditi and Dacorogna (1988) prediction of a threshold prey density that triggers movement by the forager. However, the results also suggest that there may be additional factors involved in the decision to move. Although the probability of moving is clearly a non-linear function of the catch rate residual on a logistic scale, there is no evidence of a discontinuity. This may in part be due to the GAM approach to modeling, which estimates smooth terms in an additive predictor. In addition, the probability of movement for negative catch rate residuals is between 0.05 and 0.15, which indicates that fishing vessels still have a fairly low probability of leaving an area when their catch rates are below average. Since factory trawlers usually target their midwater nets on acoustically detected aggregations of fish, the ability to locate a suitably dense aggregation may play an important role in the decision to move.

The GAM models of vessel movement showed that an exponentially-weighted average of previous hauls with a half-weight of approximately 4.8 hours was more successful at predicting movement than when only the catch rate residual of the most recent haul was considered. This result suggests that vessels base their decisions on relatively short time frames. Evaluating different frame lengths is a new approach to interpreting fishing behavior, but a similar approaches have been used with bumblebees in artificial foraging environments (Real 1991). Previous research on fishing behavior has assumed an arbitrary time window over which experience is averaged, typically one day (Eales and Wilen 1986, Vignaux 1996b) or one week (Hilborn and Ledbetter 1979, Gillis et al. 1993). The time frame which the vessels use to evaluate fishing success may be

related to the temporal persistence of hake aggregations and also to the inherent stochastic variation in the catch rates. If hake aggregations are extremely transient, earlier information would rapidly become useless as a predictor of current conditions. A fishing vessel which used an inappropriate weighting scheme would remain too long in an area where the fishing is no longer good, or conversely would leave too soon and spend an excessive amount of time in transit between areas.

The tendency for vessels to be less likely to leave an area if there are other vessels nearby is an advantageous strategy from two perspectives. First, the presence of other vessels fishing in an area suggests that high fish densities are located in the area. Information on the local density of fishing vessels can be collected easily and quickly in comparison to surveying an area acoustically or by test fishing. Second, each vessel fishing in the same area can be certain that no other vessel has a higher catch rate on average than its catch rate. This is particularly important in a fishery that is managed with a fleet-wide quota. If only a few days remain to the close of season, a risk-averse strategy such as fishing near other vessels will guarantee that the remaining quota will be shared equally among vessels. Searching for a new area with higher catch rates runs the risk that the season will close before higher catch rates can compensate for the time spent searching or in transit. Since the north-south variance in trawling locations in the at-sea fishery typically decreases towards the close of the season, there is some evidence that the spatial distribution of fishing activity is affected by these considerations.

Vignaux (1996b) conducted a similar analysis of fishing behavior in a trawl fishery for hoki off New Zealand. Instead of using a GAM model to predict vessel movement as

a function of catch rates, Vignaux (1996b) tested for differences in the probability of movement when the catch rates were below and above average. Results similar to those in this chapter were obtained regarding the effect of low catch rates, suggesting that this may be common characteristic of fishing behavior. The GAM models for vessel movement developed in this chapter offer advantages over the more ad hoc approaches that have been used up to now to study fishing behavior. GAM models allow a more detailed examination of vessel response. For example, the evaluation of non-linearity in the response to declines in catch rates in this chapter would have been difficult using conventional approaches. GAM models also provide a unified framework for evaluating different sources of information and other attributes of the catch in addition to the catch rate.

One of the initial objectives of this research was to investigate vessel responses to salmon and rockfish bycatch. In addition to the catch rate of the target species, decision-making may depend on the amount of bycatch, and other attributes of the catch, such as the mean size or sex ratio of the target species. However, it became evident that current observer sampling procedures and record-keeping do not provide sufficient information to conduct such an analysis. Since bycatch estimates are often derived from a small sample of the catch, sampling variability may occasionally result in unrealistic bycatch estimates for individual hauls. This sampling variability is not a problem when the objective is to estimate the bycatch for the entire fleet, but it does present difficulties for the statistical models developed in this chapter, where accurate information is needed for each haul. In addition, observers sample only a subset of hauls for species composition, ranging from 35

to 70%. Consequently, it is difficult to assess decision-making based on more than one haul. The cumulative bycatch over a number of hauls may be a more important predictor of vessel response than bycatch from a single haul.

The spatial structure of salmon and rockfish distribution is also likely to occur at different scales than Pacific hake. An analysis of the spatial correlation of bycatch species is a prerequisite for developing models of vessel response to bycatch. Methods developed by Vignaux (1996a) using fishery data to analyze spatial structure in the distribution of the target species may also be applicable to bycatch species. Since observers record only the retrieval locations of hauls, the spatial resolution of the observer database is not adequate to examine spatial correlation and vessel movement at smaller scales than those examined in this chapter. Once the spatial scale of the bycatch species has been identified, vessel responses at this spatial scale could be explored using the techniques developed in this chapter. Since bycatch is an important concern in managing the Pacific hake fishery, expanded data collection procedures in the Pacific hake fishery should be considered.

Table 2.1. Number of factory trawlers and mean catch rates in the 1991-95 Pacific hake fishery.

Year	Number of factory trawlers	Number of hauls	Average catch rate (t/hr)
1991	9	1940	41.8
1992	14	1743	43.4
1993	13	1227	44.2
1994	7	1192	60.5
1995	9	954	39.6

Table 2.2. Analysis of deviance for logistic regression GAMs for the probability of vessel movement in 1991-95.

Year	Model [a]	Residual Df	Residual Dev.	Δ Df [b]	Δ Dev.	P-value [c]
1991	null	1908.0	1046.1	---	---	---
	+ linear CR	1907.0	1013.3	1.0	32.8	0.000
	± smooth CR	1902.2	991.1	4.8	22.2	0.000
	± AVGCR	1902.3	983.9	-0.2	7.2	No test
	+ NVESS	1898.1	933.8	4.2	50.1	0.000
1992	null	1680.0	1052.4	---	---	---
	+ linear CR	1679.0	1037.9	1.0	14.4	0.000
	± smooth CR	1673.6	1025.6	5.4	12.3	0.039
	± AVGCR	1673.7	1012.5	-0.1	13.2	No test
	+ NVESS	1670.4	970.7	3.3	41.8	0.000
1993	null	1201.0	533.9	---	---	---
	+ linear CR	1200.0	527.8	1.0	6.1	0.014
	± smooth CR	1194.9	519.1	5.1	8.7	0.128
	± AVGCR	1195.0	516.1	-0.1	3.1	No test
	+ NVESS	1191.3	497.7	3.7	18.4	0.001
1994	null	1176.0	468.2	---	---	---
	+ linear CR	1175.0	464.8	1.0	3.4	0.065
	± smooth CR	1170.0	446.1	5.0	18.7	0.002
	± AVGCR	1170.2	442.0	-0.2	4.1	No test
	+ NVESS	1166.8	435.2	3.4	6.7	0.107

Table 2.2. Continued

Year	Model [a]	Residual Df	Residual Dev.	Δ Df [b]	Δ Dev.	P-value [c]
1995	null	943.0	603.1	---	---	---
	+ linear CR	942.0	582.1	1.0	21.1	0.000
	± smooth CR	937.5	570.5	4.5	11.6	0.030
	± AVGCR	937.4	556.1	0.1	14.4	No test
	+ NVESS	932.9	537.6	4.5	18.5	0.002

a. Terms in additive predictor: null - intercept term only; linear CR - linear term for catch rate residual of the most recent haul; smooth CR - smooth term for catch rate residual; AVGCR - smooth term for the weighted average of catch rate residuals within 30 km using an exponential coefficient of 3.5; NVESS - smooth term for the number of vessels operating within 15 km over the previous 6 h. Terms were added to the models in the order they occur in the table. The "+" symbol indicates that the term has been added to the model, while the "±" symbol indicates that the term replaces the previous term.

b. The degrees of freedom for smooth terms quantify the degree of "smoothness" of the term (Hastie and Tibshirani 1990).

c. P-values (from a $\chi^2_{\Delta df}$ distribution) are for a likelihood ratio test of the change in deviance between models.

Figure 2.1. Schematic of the Arditi and Dacorogna (1988) optimal foraging model. The threshold density partitions the habitat into areas of two types, areas in which it is optimal to forage, and areas where the optimal strategy is to transit as quickly as possible.

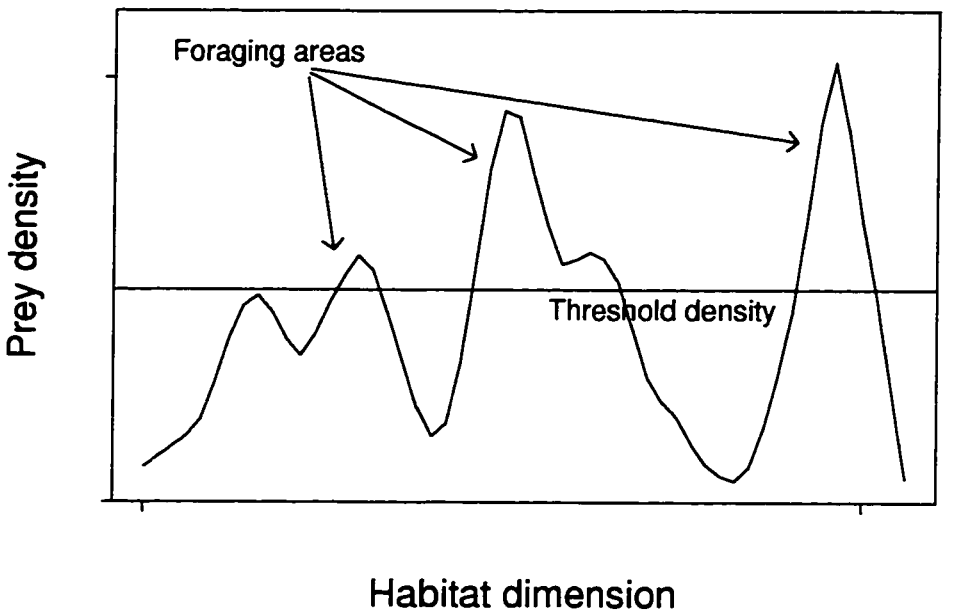
Foraging areas
Threshold density
Prey density
Habitat dimension

Figure 2.2. Pacific hake density by 0.5 nmi. transect segment for the 1992 and 1995 NMFS acoustic surveys. To show both surveys, data for the 1992 survey is offset to the west by 2° longitude. Transect segments where the Pacific hake density was greater than 635 kg ha^{-1}, the nominal density required to support fishing activity, were marked with a vertical bar. The 300 m isobath and survey transects are also shown.

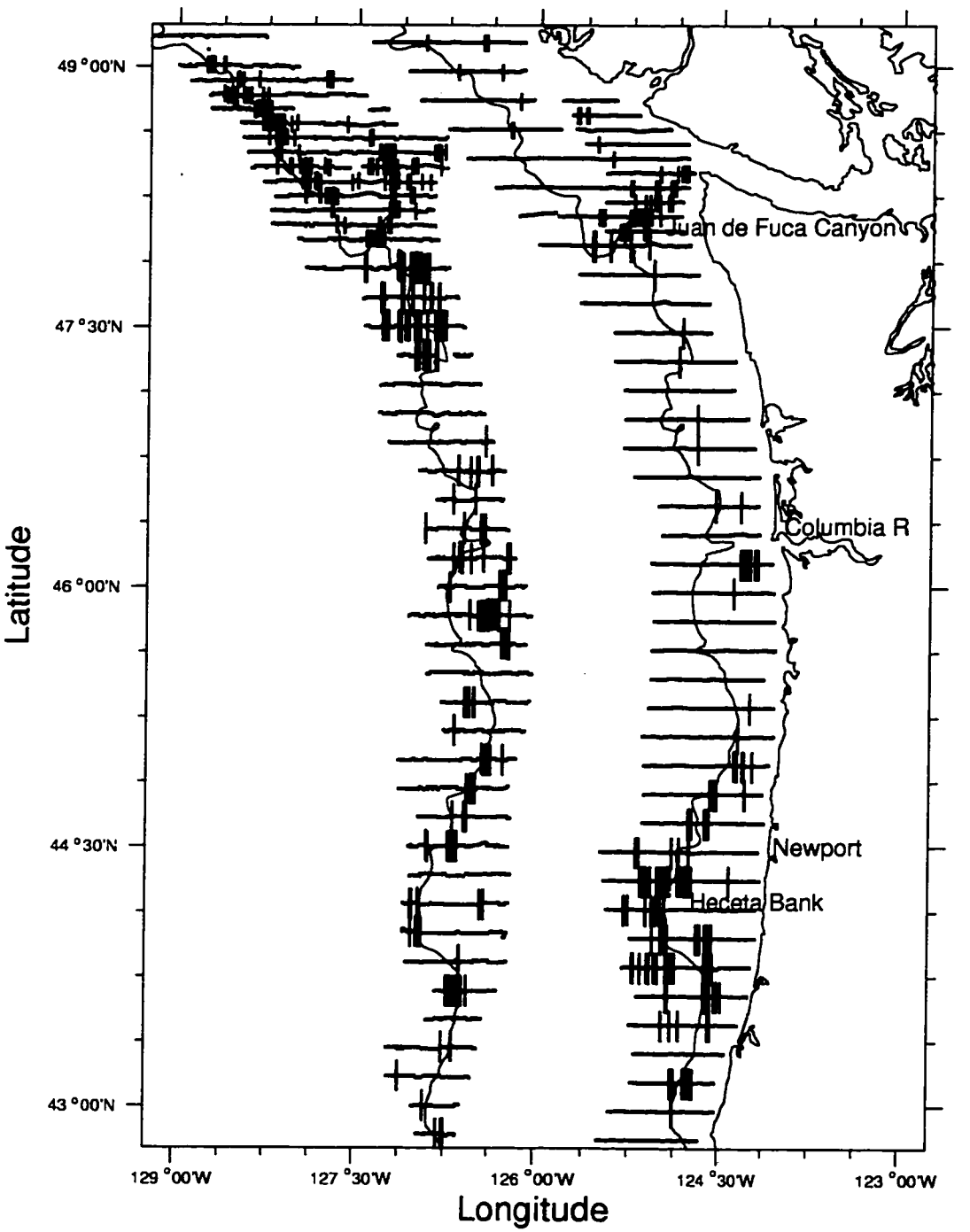
49 °00'N
47 °30'N
46 °00'N
44 °30'N
43 °00'N
Latitude
129 °00'W
127 °30'W
126 °00'W
124 °30'W
123 °00'W
Longitude
Juan de Fuca Canyon
Columbia R
Newport
Heceta Bank

Figure 2.3. Directional correlograms for the 1992 (left panel) and 1995 (right panel) NMFS acoustic surveys of Pacific hake.

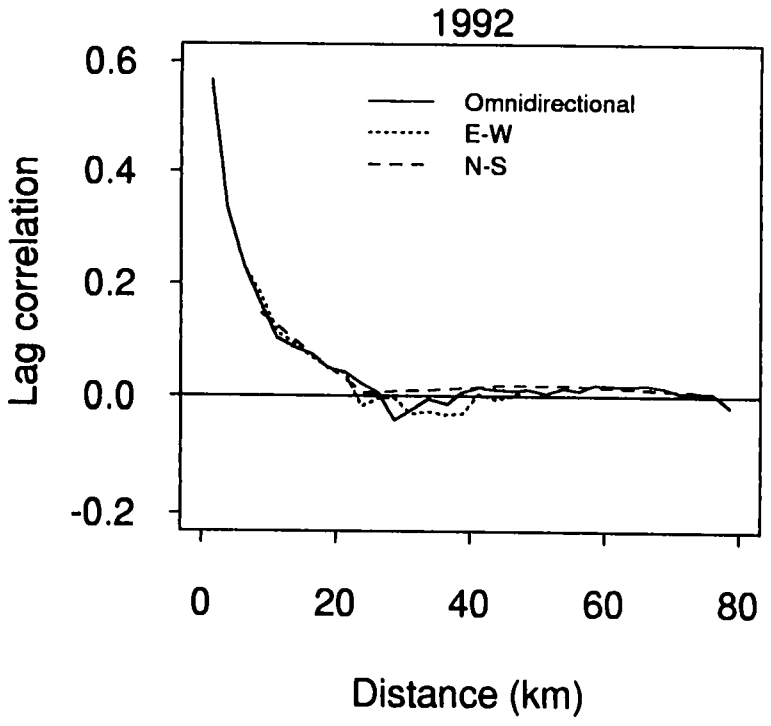
1992
Omnidirectional
E-W
N-S
Lag correlation
0.6
0.4
0.2
0.0
-0.2
0
20
40
60
80
Distance (km)

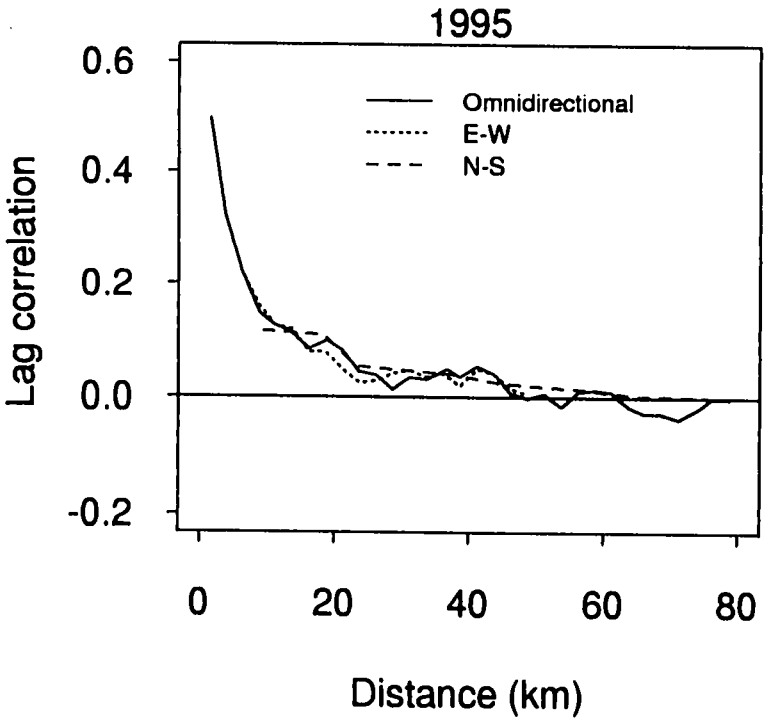
1995
Omnidirectional
E-W
N-S
Lag correlation
0.6
0.4
0.2
0.0
-0.2
0
20
40
60
80
Distance (km)

Figure 2.4. Directional structure functions for the 1992 (left panel) and 1995 (right panel) NMFS acoustic surveys of Pacific hake. Only the first part of the structure function is shown; that is, the conditional probability of finding hake densities higher than the threshold density at vector distance $\boldsymbol{h}$ away, given that the density is higher than the threshold at the current location.

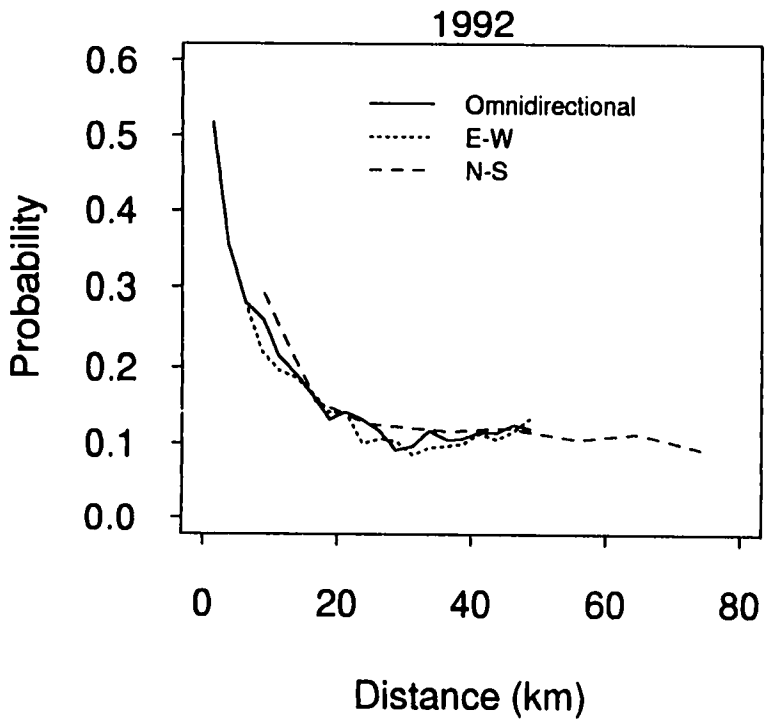
1992
Probability
0.6
0.5
0.4
0.3
0.2
0.1
0.0
Omnidirectional
E-W
N-S
0
20
40
60
80
Distance (km)

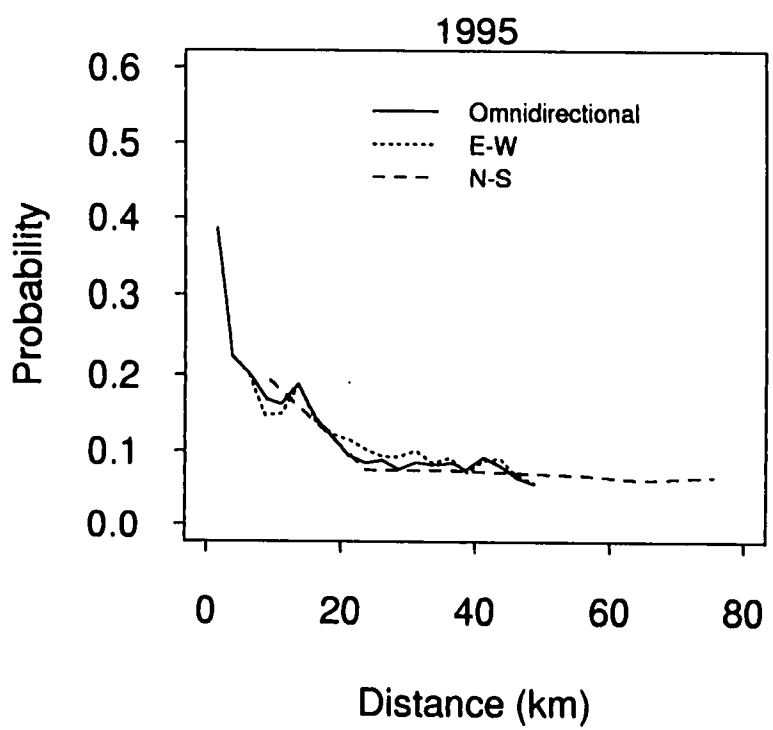
1995
Probability
0.6
0.5
0.4
0.3
0.2
0.1
0.0
Omnidirectional
E-W
N-S
0
20
40
60
80
Distance (km)

Figure 2.5. Poisson catch rate regression predictions for noon catch rate by vessel in 1994 (left panel) and time of haul (right panel) for 1991-95 for a single vessel which fished in all years.

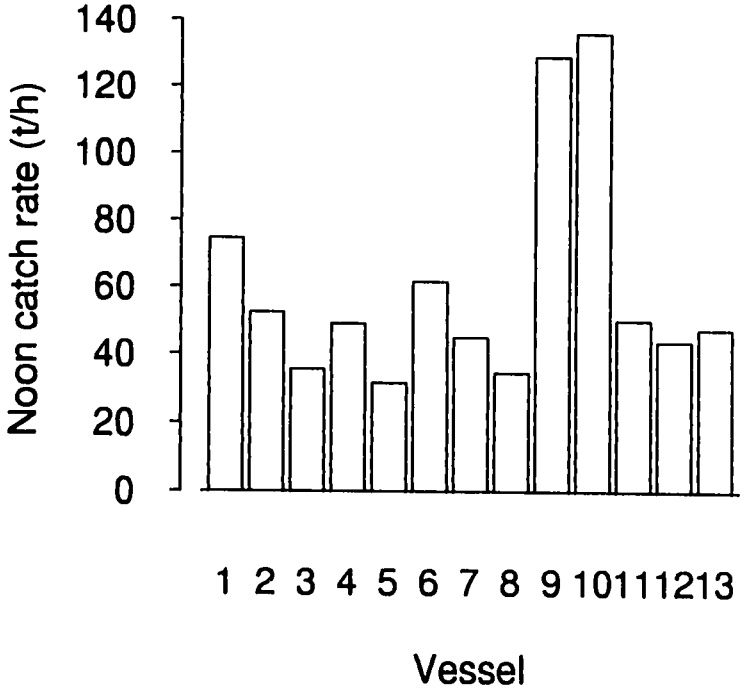
Noon catch rate (t/h)
140
120
100
80
60
40
20
0
1 2 3 4 5 6 7 8 9 10 11 12 13
Vessel

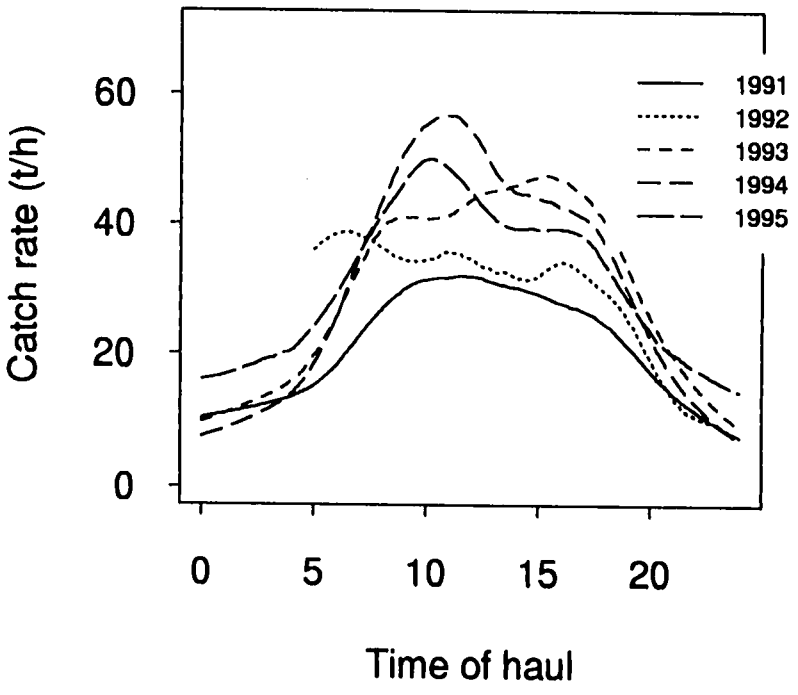
Catch rate (t/h)
60
40
20
0
0
5
10
15
20
Time of haul
1991
1992
1993
1994
1995

Figure 2.6. Mean catch rate residual versus inter-trawl distance (distance between successive haul retrieval locations) for factory trawlers during 1991-95.

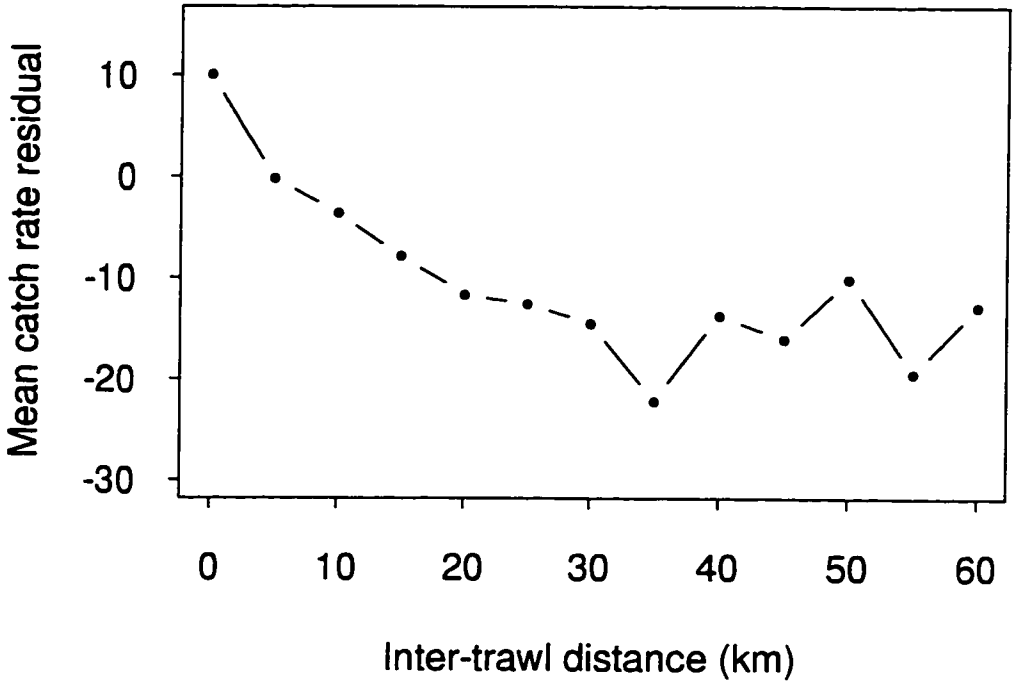
Mean catch rate residual
10
0
-10
-20
-30
0
10
20
30
40
50
60
Inter-trawl distance (km)

Figure 2.7. Path of a single factory trawler during a 28-day opening in 1994, constructed by connecting the haul retrieval positions with straight lines. Solid lines connect consecutive haul retrieval locations less than 30 km apart; while dashed lines connect those greater than 30 km apart. The E-W scale on this figure has been expanded to better depict the fine-scale structure of the path. The box in the figure is 30 km square.

Latitude N
Longitude W

Figure 2.8. Frequency distribution of the distances between successive haul retrieval positions for factory trawlers in the Pacific hake fishery in 1991-95. The final bar of the histogram includes all distances greater than 100 km.

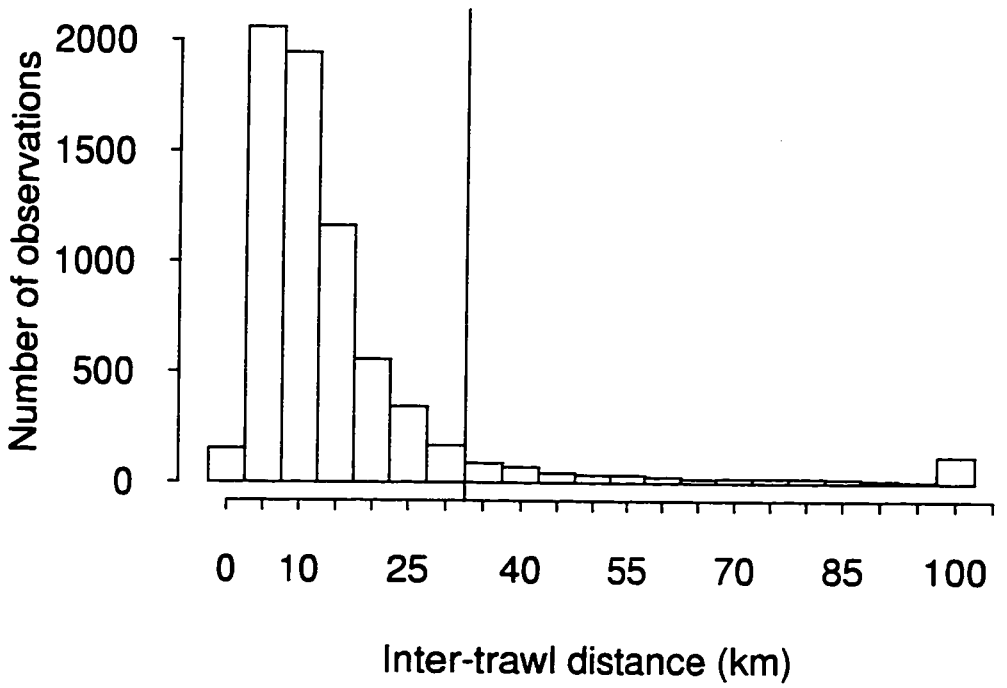
Number of observations
2000
1500
1000
500
0
0
10
25
40
55
70
85
100
Inter-trawl distance (km)

Figure 2.9. Generalized additive model (GAM) predictions of the probability of movement as a function of the catch rate residual for the most recent haul. The upper and lower limits of the x-axis are the 0.05 and 0.95 quantiles of the catch rate residual.

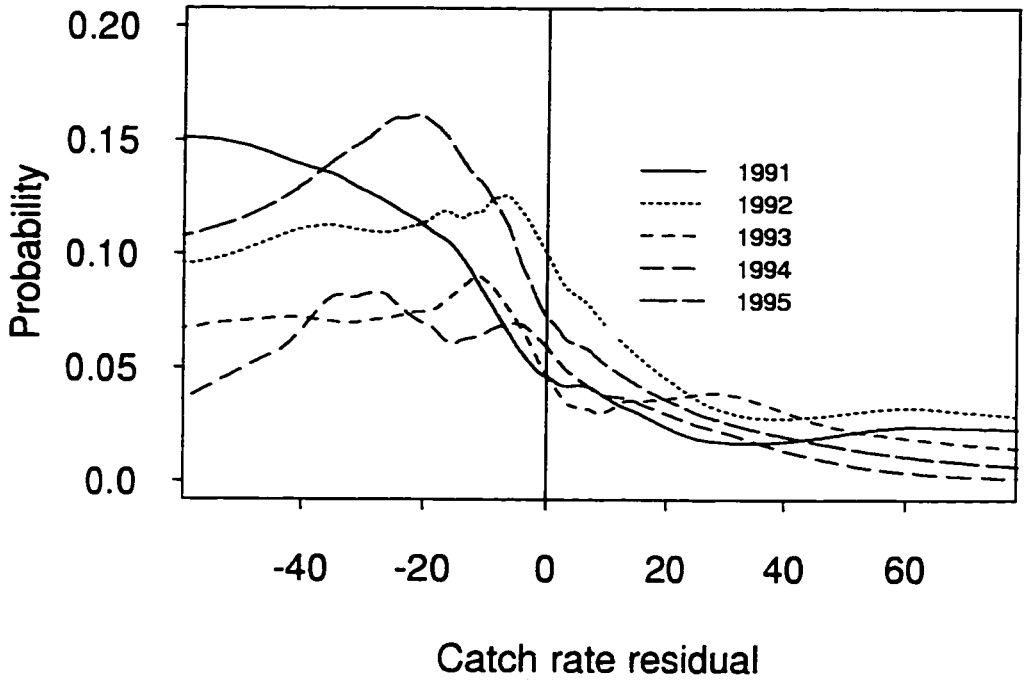
0.20
0.15
0.10
0.05
0.0
Probability
1991
1992
1993
1994
1995
-40
-20
0
20
40
60
Catch rate residual

Figure 2.10. Deviance profiles for 1991-95 of the exponential coefficient (r) in the exponential average summarizing previous fishing experience. The furthest right point of the profile is the deviance for a model with only the most recent haul. The bold line is mean for all years.

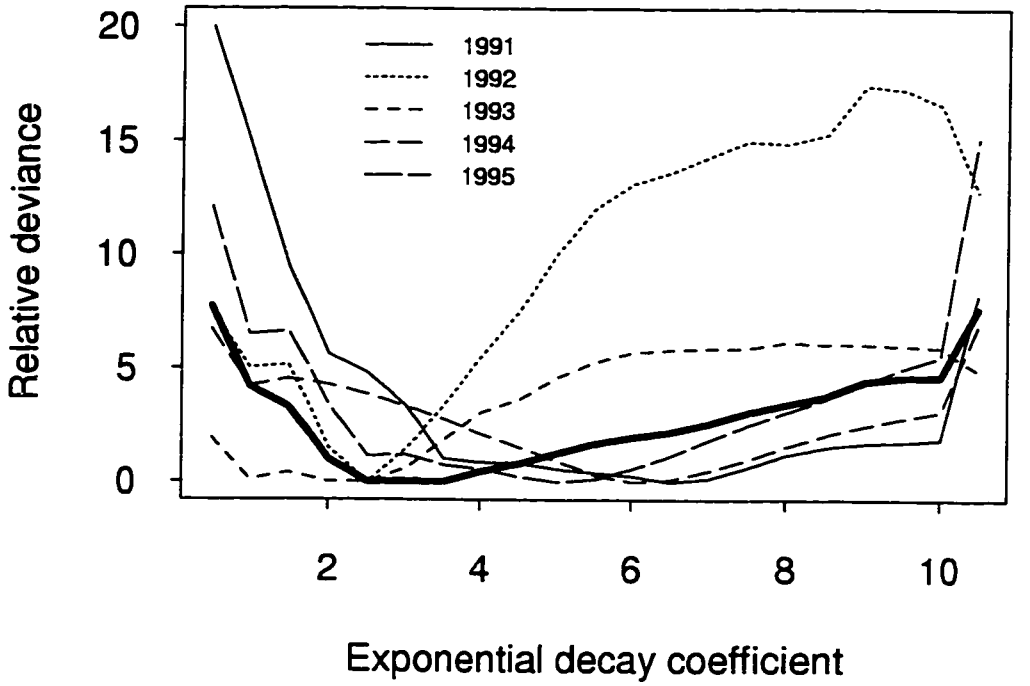
Relative deviance
20
15
10
5
0
1991
1992
1993
1994
1995
2
4
6
8
10
Exponential decay coefficient

Figure 2.11. Frequency distribution of local fishing density during 1991-95 (the number of vessels fishing within 15 km over the previous 6 hrs)

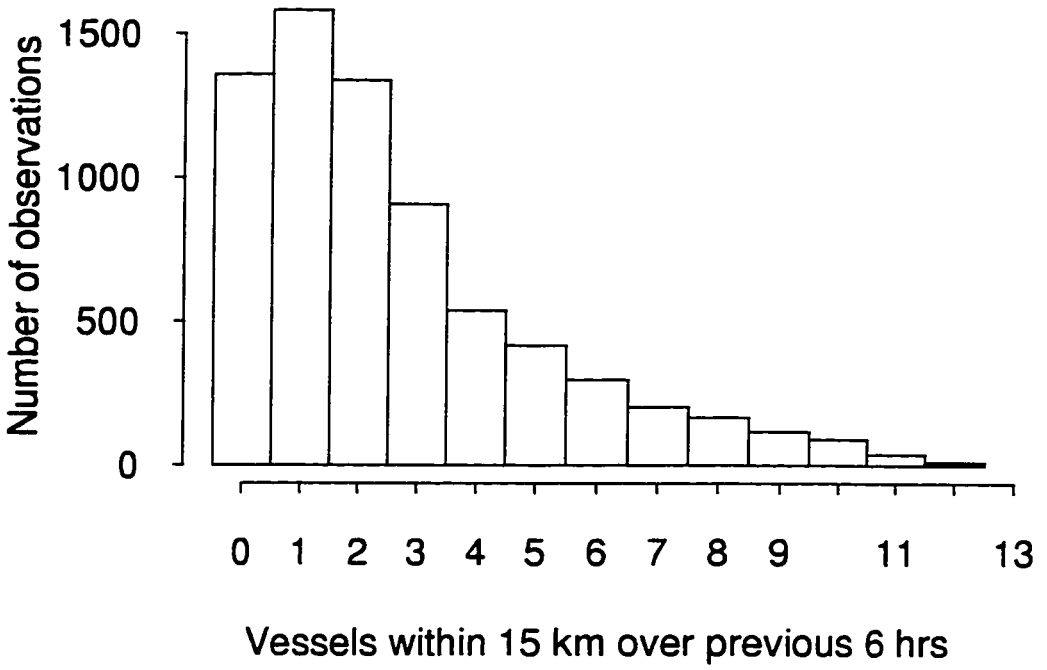
Number of observations
1500
1000
500
0
0 1 2 3 4 5 6 7 8 9 11 13
Vessels within 15 km over previous 6 hrs

Figure 2.12. Generalized additive model (GAM) predictions of the probability of movement as a function of local fishing density for 1991-95. Predictions are for a model with two terms: an exponential average of the catch rate residuals for previous hauls and local fishing density. The catch rate residual term was fixed at zero to produce the model predictions.

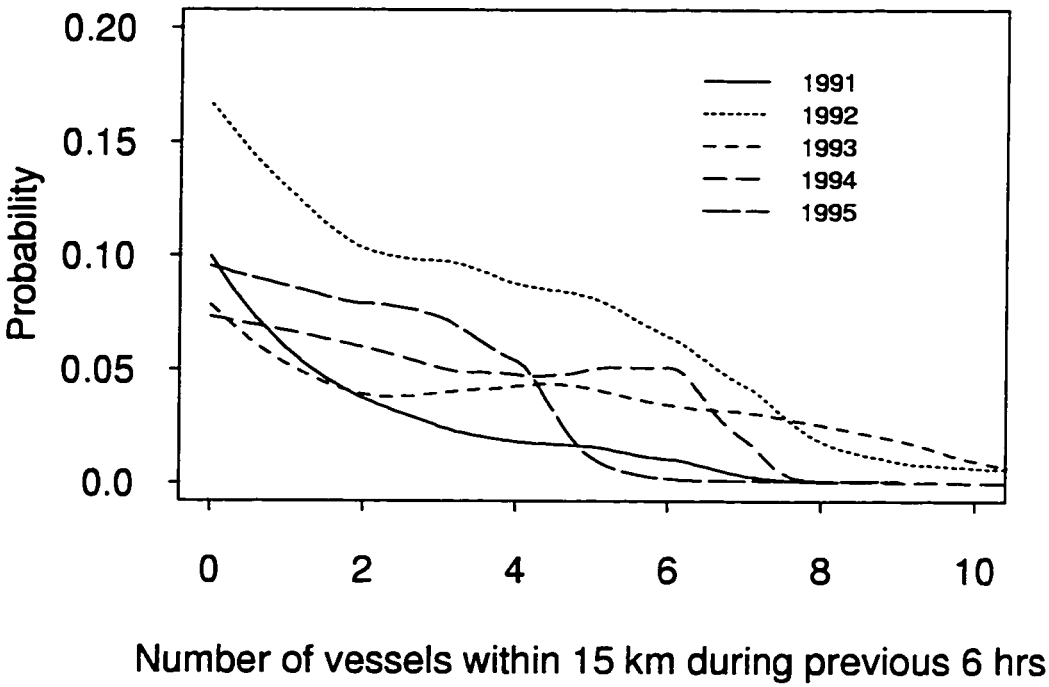
0.20
0.15
0.10
0.05
0.0
Probability
1991
1992
1993
1994
1995
0
2
4
6
8
10
Number of vessels within 15 km during previous 6 hrs

CHAPTER 3 - FISHING BEHAVIOR OF INDIVIDUAL FACTORY TRAWLERS: A HIERARCHICAL MODEL OF INFORMATION PROCESSING AND DECISION MAKING

INTRODUCTION

Historically, fishery catch and effort data have been collected principally to estimate abundance indices for stock assessment. Although fishing is undeniably a rich source of information about a fish population, both experience and theoretical models have demonstrated that simple abundance indices derived from fishery catch and effort data (e.g., catch per unit effort, or CPUE) are not reliable indicators of population trends. (See review by Walters and Maguire (1996) for a discussion of CPUE trends prior to the Northern cod collapse, and reviews by Peterman and Steer (1981) and Bannerot and Austin (1983) for a description of factors that could give rise to a non-linear relationship between CPUE and abundance). Recognition of these limitations has led to the current emphasis on standardized resource surveys of marine ecosystems that support significant commercial fisheries.

Rather than to ignore the information content of fishing experience entirely, this chapter promotes the view that the preferable response to the limitations of CPUE abundance indices is to conduct research into fishing behavior. Such research can provide

a better understanding of the appropriate use of catch and effort data in stock assessment, and may result in new approaches to monitor population trends (Hilborn 1985). Research into fishing behavior is also important to improve communication between fishery scientists and the fishing industry. If management agencies do not acknowledge the validity of fishing experience, they risk alienating the fishing industry, whose participation is essential to the fisheries management process. Research into fishing behavior may also be able to tap into the rapidly developing information technologies that are transforming fishing practice. Most modern fishing vessels are equipped with global positioning systems (GPS) and microcomputers running navigation and plotting software that give vessel operators the ability to plot fine-scale trawl trajectories over bathymetry and real-time environmental data. The usefulness of these new information sources to monitor population trends and to study the fine-scale distribution patterns of target species has not yet been evaluated.

In this chapter, a simulation model is developed for an individual factory trawler conducting fishing operations off the west coast of North America in the Pacific hake fishery. The simulation model is used to explore several concepts that provide new insight into fishing behavior. A central theme of the model is the role of decision-making at different spatio-temporal scales. Decision-making occurs at two spatio-temporal scales: 1) choosing an area within which fishing will be conducted, and 2) scheduling haul setting and retrievals while fishing within an area. These decisions are considered to be state-dependent, with the state consisting of both the internal state of the vessel, such as the amount of fish in holding bins and the amount of fish already in the net, and the external

state of the environment, such as density of the prey species in the area. Since vessel operators will not have certain knowledge about the state of the environment, their foraging decisions must be based on uncertain information about the environment obtained by searching and fishing.

A novel feature of the model is a procedure for modeling expert knowledge about local fish densities gained by fishing and searching. Geo-referenced information about local fish density is processed by the fisherman, and retained in memory as a spatial representation, or a "map." Associated with the map is a quantitative measure of accuracy of the local abundance estimates, and a procedure for updating those estimates. Although the spatial structure of the map and the updating procedures are quite simple in the model presented in this chapter, the concept is general and can easily be extended to other kinds of information available to the fisherman about local fish densities. The procedure for updating maps of local abundance is based on the Kalman filter (Harvey 1990); however an experimental approach is adopted whereby the Kalman filter is "de-calibrated" to explore how net revenue is affected by changes in the filtering algorithm.

The simulation model developed in this chapter can generally be classified as an optimal foraging model, a branch of behavioral ecology that investigates the foraging decisions made by animal predators. Optimal foraging models have three main components: a currency to be optimized, a set of constraints that impose limits on amount of the currency that can be obtained, and, lastly, a decision variable which is under the animal's control (Krebs and Davies 1991). Usually optimal foraging models use some intermediary currency, such as the rate of energy intake, but ultimately the animal is

assumed to be maximizing its fitness, that is, the contribution of its genes to future generations. For fishing vessels, of course, this ultimate objective is not appropriate, though the intermediary currencies used in optimal foraging models for animals are still appropriate, at least up to scaling factor. Depending on the complexity of the model and its stochastic assumptions, the optimal decision-making rules can be obtained analytically, using stochastic dynamic programming (Lane 1989, Gillis et al. 1995a, 1995b) or using simulation techniques, the approach used in this study.

The marginal value theorem (Charnov 1976) is the prototype optimal foraging model. The marginal value theorem applies to a situation where a predator is foraging in a environment consisting of patches where prey are found at differing densities. The predator encounters food within a patch, and spends time traveling between patches. The rate of energy intake declines with time spent in a patch. The question addressed is the following: How long should a the predator remain in a patch so as to maximize its long term rate of energy intake? The solution, the marginal value theorem, states that a predator should leave a patch when the marginal capture rate in the patch drops to the average capture rate in the environment. The marginal value theorem is a deterministic model where the forager is assumed to have perfect knowledge of the environment. Although these unrealistic assumptions have been relaxed in the model developed in this chapter, conceptual framework of the marginal value theorem is helpful to understand the simulation results.

Other ecological models have been used to investigate how fleets of fishing vessels distribute their effort between statistical areas (Hilborn and Ledbetter 1979, Abrahams and

Healey 1990, Gillis et al. 1993). The ideal free distribution predicts how a population of predators distributes itself among patches of varying productivity (Fretwell and Lucas, 1970). Each predator is assumed to move to the patch where it experiences the highest rate of food intake and is assumed to have perfect knowledge of prey densities in all patches. An equilibrium distribution of predators between patches results when the rate of food intake is equal across all patches. No predator can experience higher gains by moving to another patch. In an equilibrium distribution, the most productive patches can support a higher density of predators. In a recent example, Gillis et al. (1993) used catch and effort data in the Hecate Strait trawl fishery to investigate whether the ideal free distribution explained observed patterns of vessel distribution and catches.

In this chapter, the focus on decision-making by individual vessels, and the primary objective of model analysis is to distinguish between advantageous decision-making rules and rules which perform poorly. In addition to finding the rules which maximize net revenue, the simulation approach can also be used to study how profitability is affected when decision rules deviate from the optimal controls. The key aspects of decision-making that are investigated are the following:

1. What threshold prey density should be used to decide when to leave an area in which the vessel is currently fishing (i.e., the question addressed by the marginal value theorem)?
2. When the prey density in an area is variable and unknown, how should recent information on catch rates be combined with older information as the basis for decisions about whether to continue fishing an area?

3. How much time should be spent searching a new area before deciding whether or not to start fishing in the area?

In addition, the model is used to explore the relationship between mean fish density and vessel production (i.e., the vessel's functional response curve), the vessel's allocation of time to different activities, and standard CPUE abundance indices. These relationships are then used to evaluate the usefulness of indices derived from factory trawler data to monitor population trends.

METHODS

The general structure of the simulation model is described by a simple conceptual model of intra-seasonal decision-making for an individual factory trawler (Fig 3.1). (From a modeling perspective, it is reasonable to view the fishing vessel as a single agent--though it is, of course, a complex machine operated by a crew). The conceptual model describes two linked cycles. One cycle describes the events taking place aboard the fishing vessel, the other cycle describes the events taking place in the environment--the local population dynamics of the prey species. The two cycles are linked by the act of fishing. On the vessel, the sequence of events consists of: 1) observing the state of the vessel and the environment; 2) making a decision based on the observed state; 3) implementing the decision, i.e., fishing, not fishing, searching, or transiting; 4) incurring revenues and costs; and, finally, 5) updating the vessel state to the start of the next step. The environmental

cycle consists of the spatially-explicit population dynamics of the prey population, and potentially could include such processes as mortality due to fishing and natural causes, recruitment, diffusion, and aggregation. In the model developed in this chapter, an empirical approach is adopted by modeling the local population dynamics as a first-order autoregressive process, rather than modeling each biological process separately.

Modeling the dynamics of fish density

The Pacific hake fishery in the U.S. management zone is conducted from 42° N to 48.5° N lat. A prohibition of at-sea processing south of 42° N latitude establishes the southern limit of this region, while the northern limit is the border between the U.S. and Canadian management zones. This region of potential fishing activity was modeled as a linear habitat divided into 25 contiguous areas, each spanning 30 km in the north-south direction. Spatial analyses of acoustic survey data suggest that the spatial correlation of Pacific hake does not extend further than about 30 km (Dorn 1997). Consequently, mean fish density in each area was modeled as independent (but autocorrelated) random variable. During the 1991-95 hake fishery, mean towing distance (assuming straight-line trawling trajectory) was ~16 km, which is roughly one-half the north-south length of an area.

The density of hake in each area was modeled as first-order autoregressive process,

$$X_t = \phi X_{t-1} + \varepsilon_t ,$$

where X_t is the mean density of hake (kg/ha) at time step t (time is incremented in steps of 15 min duration), and ε_t is a gamma random variate with mean μ and variance σ^2. Since the model considers only the foraging behavior of a single vessel, it is reasonable to assume to a first approximation that fishing does not affect the density of fish in an area.

Parameter values used to simulate local population dynamics were estimated from at-sea fishery catch rates during 1991-95 (Dorn 1997), and acoustic data collected by the NOAA research vessel *Miller Freeman* during resource assessment surveys in July-September of 1992 and 1995 (Dorn et al. 1994; Wilson and Guttormsen 1997). Fishery catch rates were analyzed to obtain an estimate of the autoregressive parameter. Standardized catch rate residuals were obtained by fitting a generalized additive model (GAM) to fishery catch rates using time of day and vessel as predictor variables (Dorn 1997). The lag correlogram (Rossi et al.(1992) was estimated using the catch rate residuals for pairs of hauls separated by less than 30 km, where the elapsed time between the pairs was calculated as the difference in retrieval times recorded for the two hauls. The estimated autoregressive parameter, $\phi = 0.989$, was obtained fitting the model $\rho_t = \rho_0 \phi^t$ to the lagged correlations using non-linear least squares.

The inferences from fishery catch rates to the temporal persistence of hake densities at small spatial scales are admittedly indirect; however, no other source of information is available. The correlogram is still quite irregular even though the amount of

data used to estimate the lagged correlations is large (no. of pairs = 175,000). The fitted model is reasonable as a first-order approximation, and indicates that positive correlations decline to near zero after 3-4 d. There is a small negative correlation at lags greater than 4 d, which is consistent with localized depletion of higher fish densities (Fig 3.2).

To obtain the mean and the variance of the random innovations in the local population dynamics, hake surface densities (integrated over the vertical dimension) by 1 nmi transect segments for 1992 and 1995 NOAA acoustic surveys of Pacific hake were used. Transect segments within the latitudinal bounds of 42° to 48.5° N lat. and depth ranges of 150-600 m were used to limit the analysis to the region where the at-fishery typically operates. The acoustic surface densities were averaged by 30 km latitudinal blocks. The mean and variance for ε_t was obtained from the mean and variance of 30 km block averages by the relations $\mu = \bar{s}\,(1-\phi)$, and $\sigma^2 = Var(s_i)(1-\phi^2)$, where s_i is the mean surface density in area i. Implicit in this procedure is the assumption that the "snapshot" of spatial variability obtained from the NOAA acoustic survey approximates the temporal variability of density within a single area. Estimates of $\bar{s} = 292.3$ *kg/ha* with a CV of 0.780 were obtained. Quantile-quantile plots suggest that a gamma probability density function for the random innovations is a reasonable assumption. Because of the skewness of the gamma distribution and the high level of auto-correlation in the time series, the simulated time series of mean hake density within an area tends to show sharp increases followed by relatively slow declines (Fig. 3.3).

Vessel state dynamics

When conducting fishing operations within an area, the vessel followed the internal state dynamics of Markov decision process (MDP) model in Dorn (1998). The model was configured to increment time in 15 min steps, giving the model sufficient resolution to capture the pattern of net setting, fishing, and net retrieval that make up the daily schedule on a factory trawler. For a MDP model, time is modeled discretely, the sequence of events that occur at each time step follows a fixed pattern. First, the state of the vessel and the environment is observed. Based on the observed state, a decision is made. Next, random variables are generated according to given probability distributions (conditional on the state and the decision at that time step). Revenues and costs are then calculated and added to previous revenues and costs. Finally, the state equations update the vessel state to the start of the next step. If the next step is the final period, the terminal reward is added to the previous rewards and the process stops; otherwise, the same sequence of events is repeated for the next time step.

The internal state of the fishing vessel consists of three variables: the weight of unprocessed fish on board, the weight of fish currently in the net, and a ship status indicator variable, which keeps track of the current activity of the vessel. The internal state variables are assumed to be observable at each time step, implying that fish bins can be monitored periodically, and that the vessel can monitor the catch already in the net while trawling. This assumption is reasonable because net telemetry on a factory trawler typically includes headrope-mounted side-scan sonar, which detects fish entering the net, and net tension indicators, which trigger as the net fills with fish. The cycle of setting the

net, fishing, and retrieving the net is modeled using the ship status indicator variable (Fig. 3.4). Retrieving the net takes place over two time steps, and the vessel is committed to completing the sequence once it starts retrieving the net. With these dynamics, the catch is added to the fish in the bins 45 min after the decision to stop fishing. Fish begin entering the net 15 min following the decision to start fishing. In each time step, the weight of fish in the bins decreases by the quantity the factory processes in a time step. While the vessel is fishing, the weight of fish in the net increases by a catch increment drawn from a non-negative probability distribution. The state variables for the weight of fish in the bins and the net are subject to constraints determined by the maximum bin and net capacity. Additional details are provided in Dorn (1998).

The reward per time step is the value of surimi and fish meal produced during that time step, minus costs incurred during that time step. The positive part of the reward is the processing rate multiplied by conversion factor, which converts raw fish weight to product value. It is assumed that product value does not depend on the intrinsic characteristics of the fish (i.e., size or sex), or on how long the fish have been held before processing. The activity costs of the vessel depend on vessel status. There are three different costs: a cost per time step while fishing, a cost per time step while not fishing, and a cost per time step while the vessel is setting or retrieving the net.

At this level of detail, decision-making entails deciding when to start trawling based on the amount of fish remaining in the bins, and deciding when to stop trawling based on the amount of fish in the net and the bins. The MDP solution gives the optimal decision of when to continue fishing or stop fishing for every possible combination of bin

level and catch level. In this chapter, a simpler "rule of thumb" strategy was modeled, consisting of a bin and catch threshold strategy. A bin and catch threshold strategy is the following: start fishing when the weight of fish in the bins is $\leq$ x tons, and stop fishing when the weight of fish in the net is $\geq$ y tons. This strategy was obtained by abstracting the most important characteristics of the optimal control into a simple set of rules. Dorn (1998) shows that a large fraction of potential yield can be obtained using this strategy across a range of mean catch rates. These fine-scale controls are embedded in the simulation model, which is primarily concerned with higher-level aspects of decision-making.

Fishing

The catch per time step is a random variable, y_t, with expected value equal to the mean density in an area times a catchability coefficient that converts hake density in kg/ha to a random catch increment in tons per 15 minute time step,

$$E(y_t) = qX_t \ .$$

Catchability in this context is determined by the width of the net opening, trawling speed, and the proportion of fish in the water column that are captured by the net. Of these three elements, the first two can be obtained from observer records, while the third component requires some guesswork. Average towing speed in the at-sea hake fishery is 4.0 knots, while the average net opening is 90 m, so that a trawl filters 16.7 ha of surface area in 15

min. As a first approximation, it seems reasonable to assume that a midwater trawl captures all the fish in the water column, resulting in the estimate $q = 0.0167$, so that a mean hake density of 292.3 kg/ha would result in an expected catch of 4.9 t in 15 min.

Following the approach in Dorn (1998), the random catch increments were modeled with a Δ-distribution, which specifies the probability of a zero catch and models the nonzero values with a log-normal distribution (Pennington 1983). The CV and probability of a zero catch were obtained by calculating these statistics for the hake density by 1 nmi acoustic survey transects segments (approximately equal to 15 min of trawling) *within* the 30 km blocks described above. Since fishing is not random within the area where the fishery operates, this approach may misrepresent the distribution of potential catch increments. However, out of the limited alternatives available, this method was considered to be the most reliable. With this procedure, the CV was estimated as 1.165, and probability of a zero catch as 0.114. An evaluation of the relationship between the CV, the probability of a zero catch, and mean density for a 30 km block revealed no obvious trends. Consequently, during a simulation run, the expected catch rate was generated from the stochastic population dynamics model, while the CV and the probability of a zero catch were assumed to remain constant at the above values. For the Δ-distribution, holding constant the CV and the probability of a zero catch maintains the shape (i.e., the skewness) of the distribution as the mean changes. Conversion formulas in Pennington (1983) were used to obtain the mean and standard deviation of the log-normal distribution for the non-zero part of the distribution.

Transit and search

To give the vessel the ability to transit between areas and to search a new area, two additional states were added the ship status indicator variable. These states can potentially occur after the completion of a haul back, and give the vessel the ability to exit the fine-scale pattern of conducting fishing operations, transit to a new area, and search the new area (Fig. 3.4). There are two points in this transit and search cycle where decisions are made. The first occurs when the net is brought on board, when the vessel decides whether to remain in the same area or transit to a new area. The second point occurs after having searched a new area, when the vessel decides whether to start fishing in that area, or move on to the next area. The transit and search states are forced to be recursive for a fixed number of steps, since several time steps are required to transit between areas and to search a new area. Since it is not obvious *a priori* how much time a vessel should spend searching before deciding whether to fish in an area, the time spent searching is considered a control variable, and effect of varying the search time is evaluated in simulation runs.

Since the spatial structure of the model consists of a linear habitat divided into 25 areas with independent local population dynamics, an obvious movement strategy would be to simply move to the adjacent area. The factory trawler fleet is based in Seattle, Washington, at the north end of the linear habitat, so the simulation model starts the vessel in the northernmost area. If the vessel decides to leave that area, it moves to adjacent area to the south, and searches that area. Then the vessel decides whether to fish in that area, or move to the next area to the south. This pattern of movement is fairly consistent with

what is observed in the factory trawler fleet. If the vessel reaches the southernmost area, it then switches directions and works its way back north. Transiting between adjacent areas is assumed to require 1 hr (4 time steps).

For each time step searching an area, an index of abundance is obtained with same mean and probability distribution as fishing, but with a smaller CV to model the increased rate that information becomes available during searching. Searching for Pacific hake aggregations is usually accomplished by running a search pattern over potential trawling grounds and examining the echograms obtained from the echosounder. Since running speed is approximately three times trawling speed, searching is assumed to yield an index of abundance equal to $\sqrt{1/3}$ the CV of fishing.

Maps, updating procedures, and movement decision rules

The prey distribution map is a model for the dynamic mental image which fishermen use to track fluctuations in their catch rates, and thus is distinct from the model for local population dynamics already described. The procedure for updating local abundance estimates is based on the Kalman filter (Harvey 1990), a recursive procedure for estimating the state of the environment at time t, based on the information available up to time t - 1. Do fishermen use a Kalman filter to catch fish? Although the mathematics of the Kalman filter would be difficult for non-scientists to appreciate, updating is an intuitive process of combining a previous abundance estimate with new information. Fishermen may update estimates of local abundance using relatively *ad hoc* procedures, but it is difficult to see how they can avoid making estimates and updating them with new

information. The net revenue earned by the vessel would likely be affected by the method used to update abundance estimates. Since the Kalman filter has optimal properties as an estimator, the decision-making behavior of fishermen may take on these optimal characteristics as they become more knowledgeable about local population dynamics and variability in catch rates.

A map is a time series vector of predicted catch rates, $\hat{x}_t$, where the ith element of the vector is the predicted catch rate in area i at time step t. To use the Kalman filter, the equations for the local population dynamics and fishing/searching must be re-cast as a state-space model. The following equations describe the state transition equation and the observation equation for a state-space model of the catch rate in a single area. Under the assumption that the state transitions are independent in each area, the Kalman filter can be applied to each area independently with the observations from fishing and searching in that area. Let x_t be the mean catch rate (t/15 min) in an area, and y_t be an observed catch rate obtained either by fishing or by searching. The state transition and observation equations are:

$$x_t = \phi x_{t-1} + \mu + \varepsilon^*_t ,$$

$$y_t = x_t + \delta_t ,$$

where ε_t and δ_t are random variables with zero mean and variances σ^2 and τ_t^2 respectively. Since the observations obtained by searching have lower variance than those obtained by fishing, the observation variance, τ_t^2, is subscripted by time t. Note also that the catchability coefficient has been dropped from the observation equation because the fisherman will be interested in estimating the catch rate in an area and not hake density. There are two steps to the Kalman filter, a prediction step and an updating step. Hats (^) are used to indicate predicted values, while primes (′) indicate updated values for the state and its variance, P_t. The prediction step runs the process forward one step based on the state transition equation:

$$\hat{x}_t = \phi\, x'_{t-1} + \mu,$$

$$\hat{P}_t = \phi^2\, P'_{t-1} + \sigma^2.$$

The updating step is a weighted average of the prediction and the new observation, with weights equal to the inverse of their respective variances:

$$x'_t = \frac{\hat{P}_t y_t + \tau_t^2 \hat{x}_t}{\hat{P}_t + \tau_t^2},$$

$$P_t' = \frac{\hat{P}_t \, \tau_t^2}{\hat{P}_t + \tau_t^2} .$$

These equations describe a situation where new information is available for that time step. Since the vessel can occupy only one area in a given time step, for all other areas the projections must be made without new information. In such cases, the updating step is omitted. Without new information, the predicted catch rate gradually reverts to the unconditional mean catch rate, $\mu/(1-\phi)$, while the variance increases to the unconditional variance, $\sigma^2/(1-\phi^2)$.

To correctly use the Kalman filter, a fisherman will need to "know" the following parameters: the autocorrelation coefficient, ϕ, the transition and observation variances, σ^2 and τ_t^2, and the mean catch rate, $E(x_t) = \mu/(1-\phi)$. He must also initialize the filter with estimates of x_0 and P_0 for each area. For the analysis presented in this chapter, the Kalman filter was initialized with the unconditional mean and variance, and the filtering parameters used are the correct values based on the population dynamics model. Although the Kalman filter can be used to derive likelihood equations to estimate these parameters, such refinements fall outside the simulation modeling emphasis of this chapter. Experienced fishermen may have an intuitive sense of many these quantities, since they describe the fundamental characteristics of fishing experience.

The importance of using the correct parameter values in the filtering equations was assessed experimentally by "de-calibrating" the filter and evaluating the effect on net

revenue. The Kalman filter was de-calibrated by changing the level of transition variance assumed by the fisherman, while keeping the value of fishing/search variance constant at the "correct" value, i.e., the value used to simulate the process. This procedure has the effect of altering the relative weight given to the projected estimate and the new observation in the updating step of the Kalman filter. Although other Kalman filter parameters could also be evaluated in this way, the ratio of transition variance to fishing variance was considered to the most important aspect of filtering for the foraging environment encountered by fishermen in the Pacific hake fishery. The hake population is characterized by rapid temporal changes in abundance at local spatial scales, and the absence of persistent regions of high density. Other Kalman filter parameters may be more important in other fisheries, such as the priors for the Kalman filter in fisheries for sessile organisms.

At the two points in the transit and search cycle where decisions are made, the vessel will have available a predicted catch rate of hake in the area from the Kalman filter, based on information about local abundance gained from fishing and searching. The control rule for these decisions is the following: if the abundance estimate is above a threshold value, the vessel stays and continues to fish within the same area. If the abundance estimate is lower than the threshold, the vessels leaves. The same criterion is used to decide whether to start fishing in an area where search operations have been conducted. The use of a threshold value for the decision to leave an area has considerable theoretical justification, including the marginal value theorem (Charnov 1976), and other models of animal foraging in more realistic environments (Arditi and Dacorogna 1985,

1988). Analyses of observer data from the at-sea hake fishery in Dorn (1997) indicate that there is a low probability that a vessel will leave a foraging area when its catch rate is higher than its expected catch rate, but that probability of moving increases sharply when catch rate residuals become negative.

A complete listing of the parameters used to configure the simulation model is given in Table 3.1.

RESULTS

Primary model behavior

To understand the basic behavior of the simulation model, the time paths of state variables were obtained for a simulation run where the vessel fished within a single area only. The time paths for the variables tracking the internal state of the vessel during a three day period for this simulation are shown in Figure 3.5. During the three day period, the fish density (expressed as an expected catch rate in tons per 15 min time increment) begins at relatively low levels, increases sharply due to a large value for the gamma random variable in the state transition equation, and then gradually declines to low levels again. In general, the state variables indicating the weight of fish in holding bins and the net show fairly realistic behavior over time. When the fish density is low, the vessel must spend nearly all its time actively fishing, while during the period when fish density is high, the vessel becomes inactive (Vessel state 3) between hauls until the bin level drops below 100 tons. Then, as fish density decreases, it becomes increasingly difficult to keep the

amount of fish in bins above 100 t, and the vessel must start fishing immediately after retrieving a haul.

The non-spatial model was also used to demonstrate how different assumptions for the transition variance affect the Kalman filter predictions of mean fish density (Fig. 3.5). Since the ratio of transition variance to observation variance determines the relative weight given to the projection and the new observation in the Kalman filter updating equation, increasing the transition variance by a factor of 10 is equivalent to decreasing the observation variance by one tenth. When high transition variance is assumed, the estimated fish density becomes highly variable, while when low transition variance is assumed the estimate stays close to the unconditional mean fish density. These differences correspond to well-known personality traits, contrasting the individual who stubbornly clings to prior beliefs in the face of conflicting evidence (low transition variance), with the individual who continually changes opinions based on the latest trends (high transition variance).

Optimal decision rules for a spatial model

To identify the combination of parameter values which maximized daily net revenue, a numerical search was conducted over the three decision parameters controlling vessel movement between areas. The three parameters consisted of: 1) the catch rate threshold (as estimated by the Kalman filter) for leaving an area (MTHRESH), 2) the multiplier for Kalman filter transition variance (KMULT), and 3) the number of steps to search a new area (SRCHSTEP). MTHRESH was varied from one to ten (t/15 min) in

increments of 0.5, SRCHSTEP was varied from zero to five steps in increments of one, and KMULT was varied from e^{-5} to e^{5} in even increments on a log scale. For each set of parameter values, 500 replicate simulations were conducted. Each replicate simulation continued for 21 days (2016 time steps of 15 min), the approximate duration of a Pacific hake opening. The results from the replicate simulations were averaged. To assess how the optimum parameter values were affected by changes in mean density, this analysis was conducted for a baseline mean fish density (expected catch rate = 4.87 t/15 min), and for a mean fish density 50% higher (expected catch rate = 7.305 t/15 min.). For this analysis, the correct values for the other Kalman filter parameters at each mean fish density were assumed to be "known" by the fisherman. Since catchability and mean fish density are confounded, comparing different mean fish densities also addresses the sensitivity of model results to the assumed catchability coefficient.

For the baseline fish density, the optimal combination of parameter values was to use a movement threshold of 4.5 t/15 min. (MTHRESH=4.5 t/15 min), to search for a single time step (SRCHSTEP = 1.0). The Kalman filter transition variance which resulted in the maximum net revenue was the correct value (i.e., KMULT=1.0). When the fish density was increased by 50%, giving an expected catch rate of 7.3 t/15 min, the optimum values for SRCHSTEP and KMULT remain the same, but the movement threshold increases to 6.0 (MTHRESH=6.0 t/15 min), suggesting that the optimum controls for searching and information processing are independent of mean fish density.

After locating the general region of the parameter space where mean daily net revenue was maximized, interactions between parameter values were assessed by

generating contour plots with one parameter value held constant at its optimum value, and varying the other two parameters across a range of values. In general, there were no alternate parameter combinations which yielded nearly as much net revenue as the optimal combination (Fig. 3.6). It was possible to identify a strategy with KMULT < 1 and a high movement threshold as a poor strategy, because vessel spends all its time searching for high densities, but never believes the information that indicates a high density aggregation has been encountered. The converse strategy with KMULT > 1 and a low movement threshold does not substantially reduce net revenue, and consists of a strategy of being overly-credulous about information received from searching and fishing, but not acting on the information until it indicates that fish density is very low. Vessels have more flexibility to spend longer periods of time searching (SRCHSTEP > 1), and to be overly-credulous (KMULT > 1) without net revenue being substantially reduced, than the reverse (i.e., SRCHSTEP = 0, KMULT < 1).

The effect of changing mean fish density on fishing strategies was explored further by doing a numerical search for the best movement threshold for a full range of fish densities, with both the search time and the Kalman filter transition variance multiplier held constant (SRCHSTEP=1, KMULT = 1). At low fish densities, there is a relatively sharp maximum in net revenue as a function of the movement threshold. However, as mean density increases, net revenue becomes positive over a wider range of movement thresholds, and the slope near the maximum becomes flatter, indicating that the choice of movement threshold is less critical at high fish densities (Fig. 3.7). The optimum movement threshold is close to mean fish density at low fish densities, however as fish

density increases, the relative rate of increase of the optimum movement threshold is slower, so that the optimum movement threshold is lower than the mean fish density at higher fish densities (Fig. 3.8).

The major results of the simulation runs can be summarized as follows. 1) Searching before fishing an area is advantageous, however relatively short search times produce higher net revenue than longer search times. 2) The Kalman filter performs best when the transition variance is specified correctly, though the net revenue is fairly insensitive to different assumptions of transition variance over a fairly broad range. 3) At low fish densities, the optimum catch rate threshold for moving to a new area is close to mean fish density, however as fish density increases, the movement threshold is lower than the mean fish density.

Relationship between fish density and vessel performance statistics

The functional response (i.e., the relationship between the fish density and daily catch) for a factory trawler was obtained for a sequence of models with increasingly complex and realistic assumptions about the temporal dynamics of fish density and its spatial structure. First, transition variance and autocorrelation were added to the local population dynamics for a vessel fishing in a single area. Then, the full spatial structure included in the model, and the effect movement on the functional response curve was assessed. Two movement strategies were evaluated: 1) an adaptive threshold catch rate for movement to a new area that adjusts to changes in mean fish density as shown in Figure 3.8, and 2) a constant threshold catch rate (4.5 t/15). Note that these decision

thresholds are applied to the Kalman filter estimates of the catch rate, and not the observed catch rates.

In comparison to a model where the mean fish density is constant, including transition variance in the state transition equation has a minor effect on the shape of the functional response (Fig. 3.9). However, when autocorrelation is included, the slope of the functional response is flattened considerably, although the asymptote remains the same At a constant fish density with an expected catch rate of 5 t/15 min, slightly higher than the factory production capacity of 4 t/15 min, net revenue is close to the maximum attainable, while for the model with autocorrelation, daily net revenue remains negative. Because of the autocorrelation in the local population dynamics, even when the mean catch rate is high enough to keep the processing factory running full time, there will still be periods when fishing is poor, and the vessel runs out of fish to process.

When spatial structure is included in the model, the ability of the vessel to move to a different area when catch rates decline compensates for the autocorrelation in the population dynamics within an area (Fig. 3.9). For a vessels with a constant movement threshold strategy, the functional response curve has a sigmoidal shape, since the vessel spends most of its time searching rather than fishing when the mean fish density is below the threshold. However, the functional response curves for the constant and adaptive movement strategies are very similar when mean fish density increases above the constant threshold (4.5 t/15 min expected catch rate).

As mean fish density increases, there are changes the proportion of time that a factory trawler allocates to different activities (Fig. 3.10). Both vessels with a constant

movement threshold and those with an adaptive movement threshold show an increase in proportion of time that the vessel is inactive and a decrease in the proportion of time transiting and searching. The most significant difference between constant and adaptive threshold strategies is that the vessel with the adaptive threshold spends nearly all its time fishing at low fish densities, while the vessel with the constant threshold spends nearly all its time searching and transiting, and only begins to fish when mean fish densities raise to near the level of the threshold.

There are two common methods of estimating CPUE abundance indices from fishery data (Richards and Schnute 1992):

1. Mean of the CPUE for individual hauls: $\Sigma\ (catch_i\ /\ duration_i)/n$,
2. Ratio estimator: $\Sigma catch_i\ /\ \Sigma duration_i$.

Simulated abundance indices were estimated using these two methods across a range of fish densities (0.5-20.0 t/15 min expected catch rate) by averaging the results of 500 replicate runs of 21 days for each level of fish density. Abundance indices were obtained for both vessels with a constant movement threshold (4.5 t/15 min.), and those with a movement threshold that adapts to changes in fish density.

For each movement strategy, the haul average (CPUE estimator 1) was higher than the ratio estimator (CPUE estimator 2) at all levels of fish density, but the relationship between fish density and the abundance index were similar for both estimators (Fig. 3.11). Since the vessel uses a catch threshold for determining when to retrieve a net, tows with

high catch rates tend to be of shorter duration than those with low catch rates. When a simple average is calculated, the shorter tows are given equal weight as the longer tows, and thus average tends to be higher than the ratio estimate. All of these abundance indices are non-linear close to the origin, indicating that assumption of proportionality between the index and stock abundance would lead to erroneous conclusions about stock status at low abundance levels. The abundance indices for an adaptive movement threshold strategy tend to be fairly linear throughout the range of fish density, while the abundance indices for constant movement threshold are highly non-linear at low fish density. This rather surprising result suggests that the general properties of the index will depend on the fishing strategy of the vessels involved in the fishery.

DISCUSSION

Several recent simulation and optimization models of fishing behavior (Mangel 1988, Butterworth 1988, Lane 1989, Gillis et al. 1995a, 1995b) share with this chapter an emphasis on modeling the behavior of individual fishing vessels. This emphasis reflects the growing recognition that classical approach of treating fishing effort as an aggregate of uniform units (i.e., vessel-days) (as in Caddy 1975, Hilborn and Walters 1987, Anganuzzi 1995) is, at best, an incomplete characterization. The most significant benefit of the individual-based approach is the ability to more accurately model actual fishing experience. This chapter and the other papers cited above promote the view that fishing is, fundamentally, a decision process based on uncertain information about a stochastic

environment. State-dependent decision making and information processing, consequently, are central to understanding fishing behavior, and ultimately the impact of fishing on exploited populations.

Although the state-dependent nature of decision-making is a key element of the simulation model in this chapter, this aspect of decision-making has not been treated in a systematic way by previous researchers. In other simulation models of fishing, the decision rules have usually been assumed to be independent of the state (Butterworth 1988, Mangel 1988). Markov decision process (MDP) models, which explicitly address the state-dependent characteristics of decision-making, have been applied to simplified fishery problems to obtain optimum decision rules (Lane 1989, Gillis et al. 1995a, 1995b). Although MDP models are a general approach to decision-making in stochastic dynamic systems, these models quickly become unwieldy for realistic systems, greatly increasing the difficulty of obtaining and interpreting solutions (Walters 1986). Furthermore, as demonstrated by this chapter and Dorn (1998), additional insight can be gained by studying how profitability is affected when decision rules deviate from the optimal controls, an approach that requires the use of simulation techniques.

Because of the simple spatial structure of the model and uncertainty in the parameter values used to configure the model, the combination of decision parameters that maximizes net revenue should be viewed as a fairly provisional indication of an optimal strategy for a factory trawler in the actual hake fishery. The most important results of the simulation runs with different values for the decision parameters are the non-monotonic relationship between each decision parameter and net revenue and the existence of a well-

defined maximum. This plausible model behavior suggests that the decision making and information processing aspects of the model are important elements of fishing behavior.

The nearly one-to-one relationship between the optimum catch rate threshold for moving to a new area (MTHRESH) and mean fish density, suggests that the marginal value theorem (Charnov 1976) is relatively robust. The lower movement threshold at high fish densities may due to the functional response of a factory trawler, since net revenue is constrained by processing capacity at higher fish densities. In the simulation model, local prey density is stochastic, autocorrelated, and not known with certainty. Since the unconditional mean catch rate is the same in each area, moving to another area is advantageous only because of the autocorrelation in catch rates. These results suggest that autocorrelation in catch rates (regardless of the mechanism which produces the autocorrelation) is the fundamental problem that is addressed by a movement strategy.

Since a vessel will move to another area only because its catch rate within an area has declined, moving between areas is a critical time for a fishing vessel. The vessel may have already run out of fish in the holding bins to process, or be in immanent danger of doing so. The simulation result that the vessel should search a new area only for a single time step (SRCHSTEP = 1) before deciding whether to start fishing should be viewed in this context. Of course, the longer that a vessel searches the more precise its estimate of the catch rate will be. However, the benefit of this increased precision has to be weighed against the higher probability of running out of fish to process and thus lowering net revenue.

Because searching behavior is not routinely recorded in observer and logbook

databases, modeling searching behavior can be a data-limited exercise in speculation by the modeler. It is quite likely that fishing and search within an area is not random, as is assumed by the model. Recent technological developments in acoustic/GPS recording systems may make it possible to record continuous-time measurements of acoustic backscatter intensity and vessel location on factory trawlers in the Pacific hake fishery. These data could be integrated with the observer database and the vessel logbooks, so that it would be possible to identify trawl starting and ending locations. The complete data set could be used to characterize searching behavior and decision making in relation to acoustic backscatter intensity. A study of fine-scale searching and fishing behavior using an acoustic/GPS logger is a high priority for new research into this system. The modeling is also limited our understanding of fine-scale spatial structure in the fish populations. A model consisting of spatial cells is probably overly simplistic. Information on fine-scale spatial structure would require transects at a finer spatial scale and at different orientations to supplement the standard acoustic survey design of parallel, evenly-spaced transects.

The major methodological innovation of the simulation model is the use of the Kalman filter to model the fisherman's view of environment as a map with estimates of local abundance. To my knowledge, a virtual fisherman has never before been equipped with a Kalman filter. Mangel and Clark (1983) consider a situation where fishermen use Bayesian updating, but their model assumes that mean fish abundance within an area does not vary. Lane (1989) uses a Bayesian procedure for updating information in a dynamic system in a general model of salmon migration and fishing behavior. Although the Markov decision process model in Lane (1989) uses a discretized state vector, state

transition probabilities, and discrete observation probabilities, the process of updating indices of abundance in a dynamic system are similar to the Kalman filter.

Because the probability distributions for the fish density dynamics and the observations (fishing and searching) are not Gaussian, not all of the optimal characteristics of the Kalman filter will apply to filtering problem considered here. Harvey (1990) notes that in the non-Gaussian case there is no assurance that the Kalman filter will give the conditional mean of the state vector; however the Kalman filter is still optimal in the sense that it is the minimum mean square error estimator among linear estimators. The interest in the Kalman filter in this chapter stems from the need for a simple updating procedure to evaluate as a general strategy for information processing by the vessel. It is possible that relatively small declines in net revenue for KMULT > 1 (high transition variance, or, equivalently, low observation variance) could be due the skewness of the probability distributions for the local population dynamics and the fishing process.

The Kalman filter is used in this chapter to model the local aspects of uncertainty and information processing. Since the overall mean fish density and the Kalman filter parameters are assumed known by the fisherman, the problem of global uncertainty was not explicitly addressed. For example, although consequences of incorrectly specifying the transition variance was evaluated, the problem of how to estimate the transition variance was not considered. A more significant limitation may be that the fisherman was assumed to know the overall mean density. Knowing the mean is important because the optimum movement threshold is strongly related to the mean density, and because the mean is used in the Kalman filter prediction equations. An estimate based on fishing

experience during the previous year may provide a sufficiently accurate overall mean for local decision-making. A procedure for estimating the overall mean could be developed using the Kalman filter. Alternatively, information processing algorithms that do not require as much knowledge to implement could be tested. For example, experimentation with a Kalman filter for a random walk with measurement error, which does not require an estimate of the overall mean density, gave similar results as the Kalman filter derived from the population dynamics model.

The objective of the simulation model was to examine the primary processes using a relatively simple model for a single vessel. Consequently, no attempt was made to model interactions between vessels. It is recognized that information transfer between vessels may influence decision-making. The information processing framework of the Kalman filter can easily be generalized to include the inferences about local fish densities from the observed distribution of other vessels and reports of less than complete reliability from other fisherman. However, adding information exchange between vessels would increase the complexity of the model and its analysis, and would require a level of speculation about how information transfer takes place would that is difficult to justify at the current state of knowledge. Furthermore, the effect of fishing on the population dynamics within an area can not be ignored in a model of the entire fishery. Despite some intriguing experimentation with a model of interacting vessels by Allen and McGlade (1986), simulating an entire fishery is mostly unexplored territory for the individual-based modeling approach.

Mangel (1988) proposes that an index of abundance should have the following

characteristics: 1) consistency, such that changes in the index are always be in the same direction as changes in population abundance; 2) linearity, such that the relationship between the index and population abundance is linear with a zero intercept; and 3) small variability. The conventional CPUE indices calculated from the simulated factory trawler data satisfy the first criterion, but not the second, since some non-linearity is present in both indices. The third criterion was not addressed in this study, since this would require modeling the entire fishery from which the CPUE data was collected. Because information exchange between vessels would tend increase the correlation between their respective catch rates, the variability of an abundance index from a fleet of interacting vessels may be higher than if each vessel fished independently.

The simulation results suggest that standard CPUE indices calculated from factory trawler catch and effort data should not be used directly as an index of abundance for stock assessment Without a better understanding of how targeting on small-scale aggregations affects catch statistics, it would be premature to make recommendations about alternatives to the standard CPUE indices. One possibility would be to use simulation modeling to obtain the general form of the relationship between the index and population abundance (which need not be linear), and then estimate the parameters of that relationship while fitting the stock assessment model. For example, the relationship between fish density and daily catch in Figure 3.9 is clearly an asymptotic function, with an inflection point close to the production capacity of the factory trawler.

Simulation results also suggested that the general properties of an abundance index will depend on the fishing strategy of the vessels involved. For example, the severity of

the non-linearity between the CPUE index and fish density will depend on whether vessels adjust their movement thresholds in response to changes in abundance. Statistical analyses of CPUE data typically treat fishing effort as a random variable (Richards and Schnute 1992). When fishing is considered an activity in which decision making plays a central role, effort should be regarded as a control variable. In the simulation model, where a catch threshold is used for deciding when to retrieve the net, the variance in catch rates is converted into variance in haul durations, while the total catch per haul is relatively constant. It may be enlightening to consider CPUE data as a censored sample of the distribution of potential catch rates. Censoring occurs at least two levels in the model: 1) on the level of a fine-scale decision-making in deciding when to retrieve a haul, and 2) in the choice of an area in which to conduct fishing operations. The nature of censoring will depend on the fishing strategy of the vessel, i.e., the set of decision rules which govern its behavior.

Table 3.1. Parameter values used in factory trawler simulation model.

Parameter	Parameter value	Source
	Fish density dynamics	
Time increment	15 min	---
Autoregressive parameter	0.989	Correlogram of catch rate residuals (Fig. 2)
Probability distribution	Gamma	QQ plot
Baseline mean hake density	292.3 kg/ha	Mean acoustic density by 30 km blocks
Hake density CV	0.780	CV of acoustic density by 30 km blocks
	Vessel state dynamics	
Catch threshold	50 t	"Rule of thumb" in Dorn (1998)
Bin threshold	100 t	"Rule of thumb" in Dorn (1998)
Processing rate	4 t/15 min	Dorn (1998)
Conversion of tons to dollars	260 $/t	Freese et al. 1995
Bin capacity	200 t	Unpublished observer data
Net capacity	160 t	Unpublished observer data
Per time step cost of setting and retrieving the net	$880	Freese et al. 1995
Per time step cost of not fishing and running	$800	Freese et al. 1995
Per time step cost of fishing	$840	Freese et al. 1995

Table 3.1. Continued.

Parameter	Parameter value	Source
	Fishing	
Catchability (q)	0.0167	Mean net width, trawling speed, and capture efficiency
Probability distribution	Δ-distribution	Dorn (1998)
Fishing CV	1.165	CV of 1 nmi acoustic transect segments *within* 30 km areas
Probability of zero catch	0.114	Probability of zero density for 1 nmi acoustic transect segments *within* 30 km blocks
	Transit and Search	
Number of time steps to transit to new area	4 (1 hr)	Running speed of 12.0 knots
Search CV	0.673	$\sqrt{1/3}$ * Fishing CV
	Updating parameters for the Kalman filter	
Autoregressive coefficient, ϕ	0.989	Correlogram of catch rate residuals (Fig. 2)
Initial filter estimate, $\hat{x}_0$	4.87 t/15 min.	Unconditional mean, $E(x_t)$
Initial filter variance, $\hat{P}_0$	14.49	Uncond. variance, $Var(x_t)$
Linear term, μ	0.0537	$E(x_t)\,(1-\phi)$
Transition variance, σ^2	0.317	$Var(x_t)\,(1-\phi^2)$
Observation variance, τ_t^2	32.3 (while fishing) 10.8 (while searching)	$[(Fishing\ CV)\ E(x_t)]^2$

Figure 3.1. Conceptual model of intra-seasonal decision-making on a commercial fishing vessel (adapted from Lane 1989).

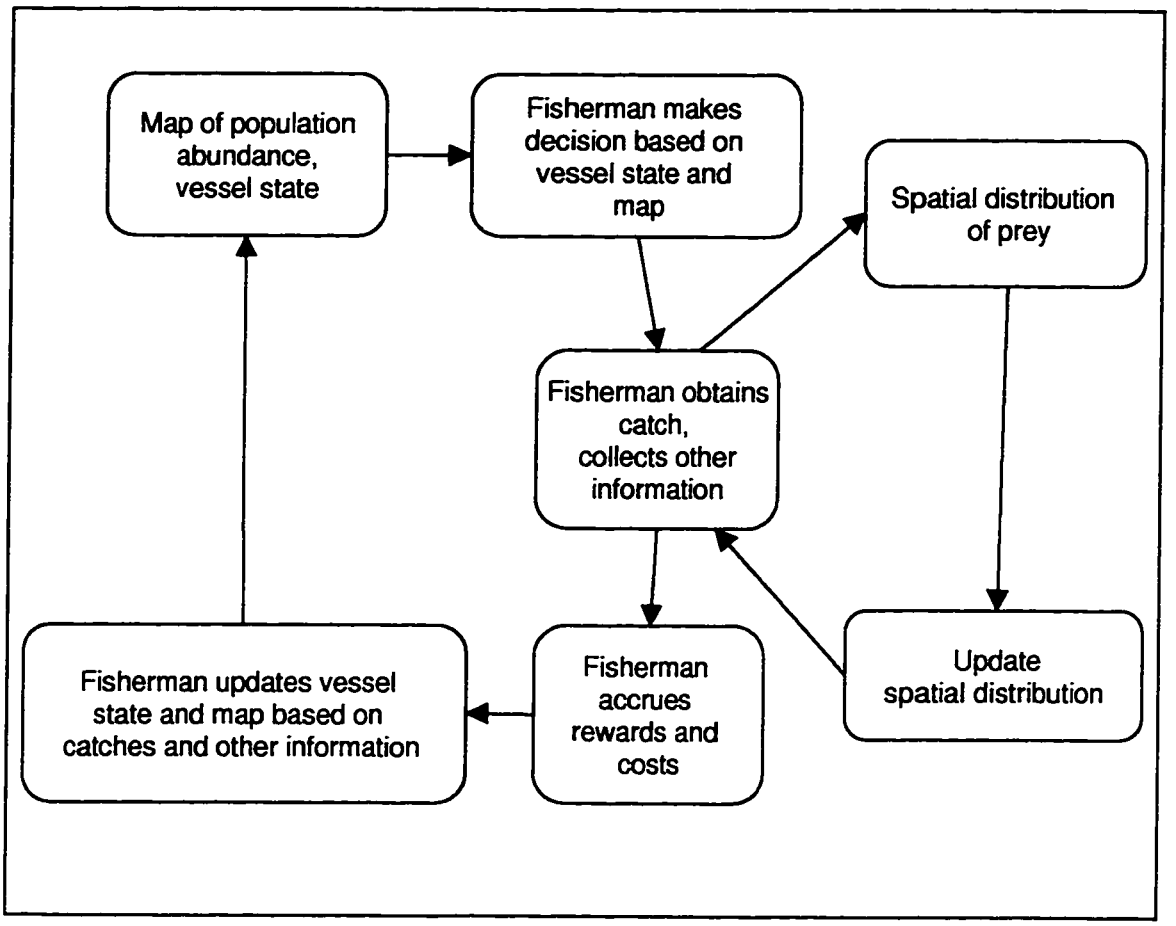
Map of population abundance, vessel state
Fisherman makes decision based on vessel state and map
Spatial distribution of prey
Fisherman obtains catch, collects other information
Update spatial distribution
Fisherman accrues rewards and costs
Fisherman updates vessel state and map based on catches and other information

Figure 3.2. Temporal correlation of catch rate residuals separated by less than 30 km (Dorn 1997) and predicted correlation from the model $\rho_t = \rho_0 \phi^t$.

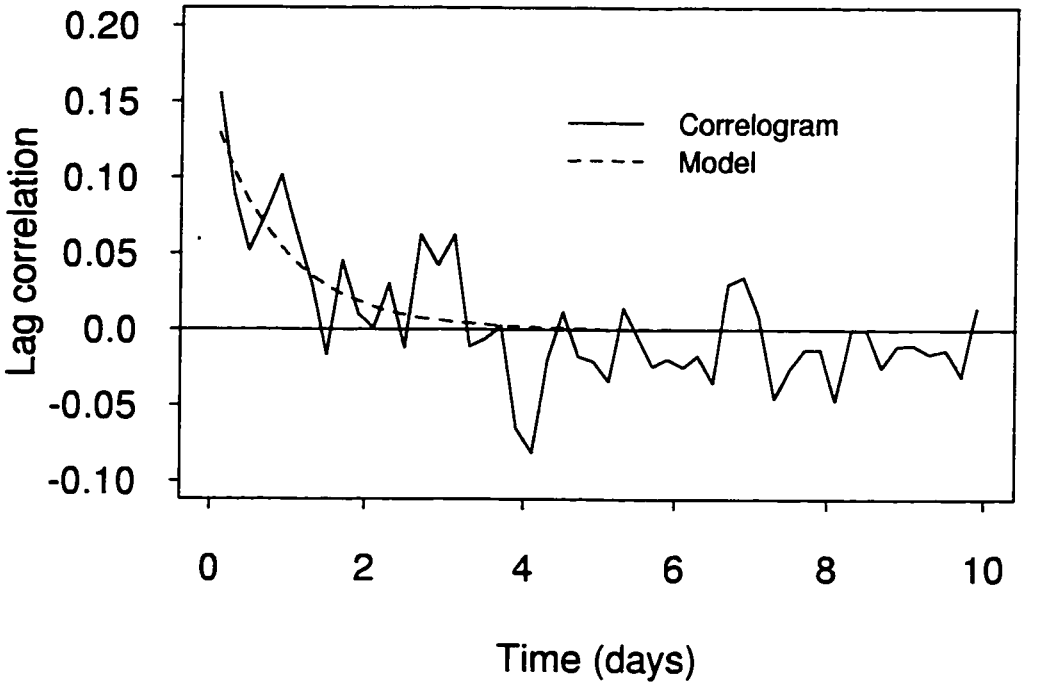
0.20
0.15
0.10
0.05
0.0
-0.05
-0.10
Lag correlation
Correlogram
Model
0
2
4
6
8
10
Time (days)

Figure 3.3. Simulated time series of mean surface density for a single area during 21 d for a first-order autoregressive process with gamma random innovations.

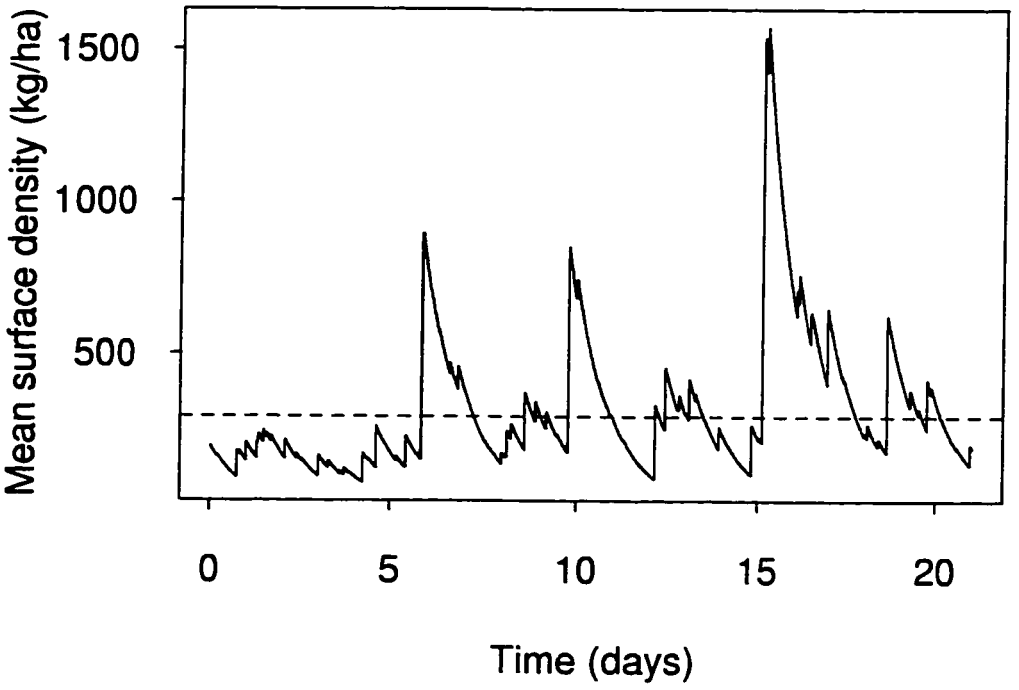
Mean surface density (kg/ha)
1500
1000
500
0
5
10
15
20
Time (days)

Figure 3.4. State transitions for the vessel status indicator variable.

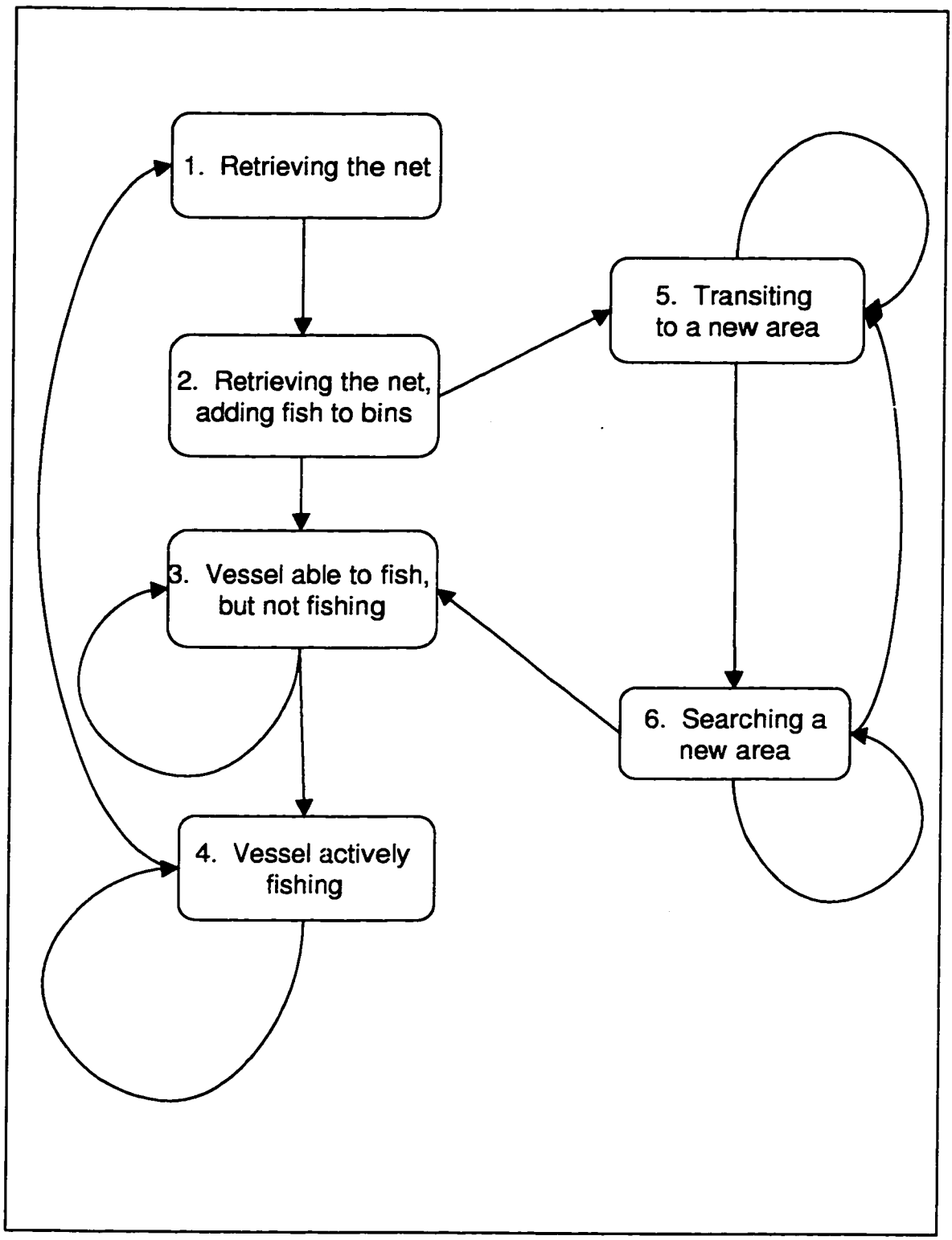
1. Retrieving the net
2. Retrieving the net, adding fish to bins
3. Vessel able to fish, but not fishing
4. Vessel actively fishing
5. Transiting to a new area
6. Searching a new area

Figure 3.5. Time path of state variables during 3 d for a vessel fishing in a single area. (A) Weight of fish in holding bins and in the net. The thick broken line across the top of the graph indicates whether or not the vessel is actively fishing. (B) Kalman filter estimates of the mean catch rate for the same 3 d period for different assumptions for the transition variance in the Kalman filter updating equation. High and low estimates were obtained by assuming the transition variance is 10 times and one tenth the true transition variance in the population dynamics model.

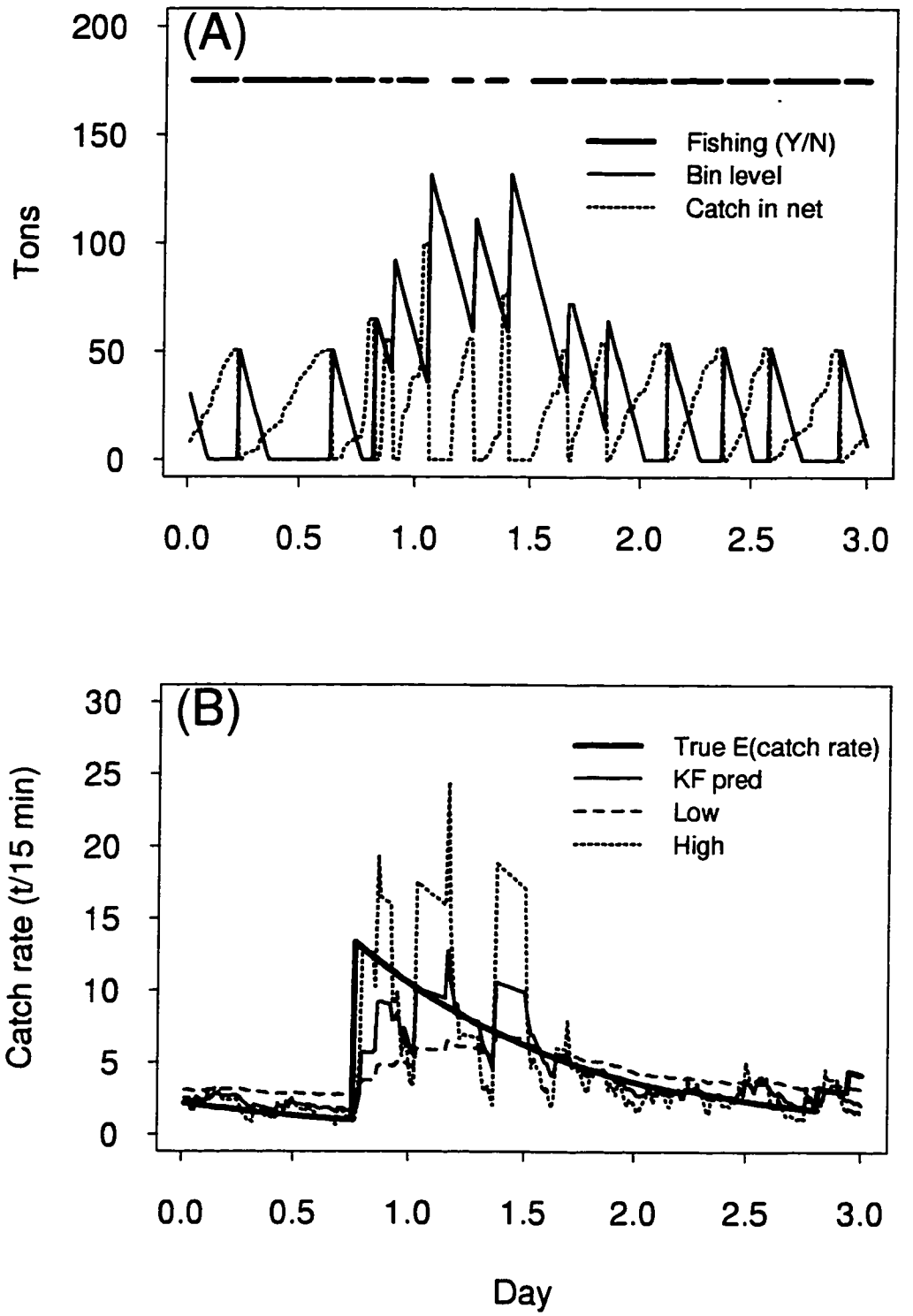
(A)
200
150
100
50
0
Tons
Fishing (Y/N)
Bin level
Catch in net
0.0
0.5
1.0
1.5
2.0
2.5
3.0
(B)
30
25
20
15
10
5
0
Catch rate (t/15 min)
True E(catch rate)
KF pred
Low
High
0.0
0.5
1.0
1.5
2.0
2.5
3.0
Day

Figure 3.6. Contour plots of daily net revenue ($ 1,000) at two levels of mean fish density for the movement threshold (MTHRESH), transition variance multiplier (KMULT), and the number of time steps to search a new area (SRCHSTEP). Contour plots were obtained by varying two parameters with the third parameter held constant at its optimum value. (Baseline fish density: expected catch rate = 4.87 t/15 min; high fish density: expected catch rate = 7.305 t/15 min.)

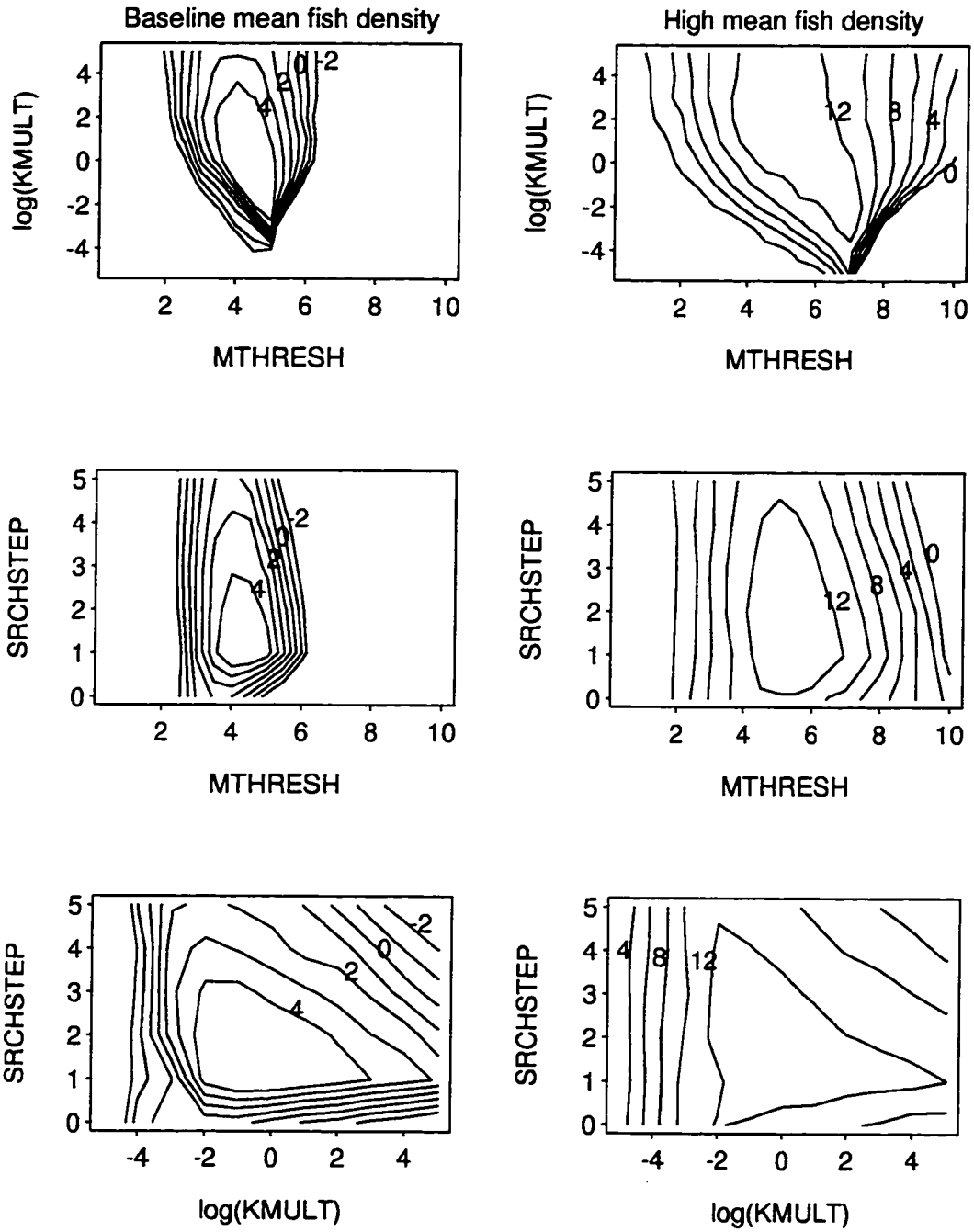
Baseline mean fish density
High mean fish density
log(KMULT)
MTHRESH
SRCHSTEP
log(KMULT)

Figure 3.7. Daily net revenue ($1,000) for an individual factory trawl at different levels of mean fish density (FD, expected catch rate in t/15 min) as a function of the threshold for moving to a new area (MTHRESH).

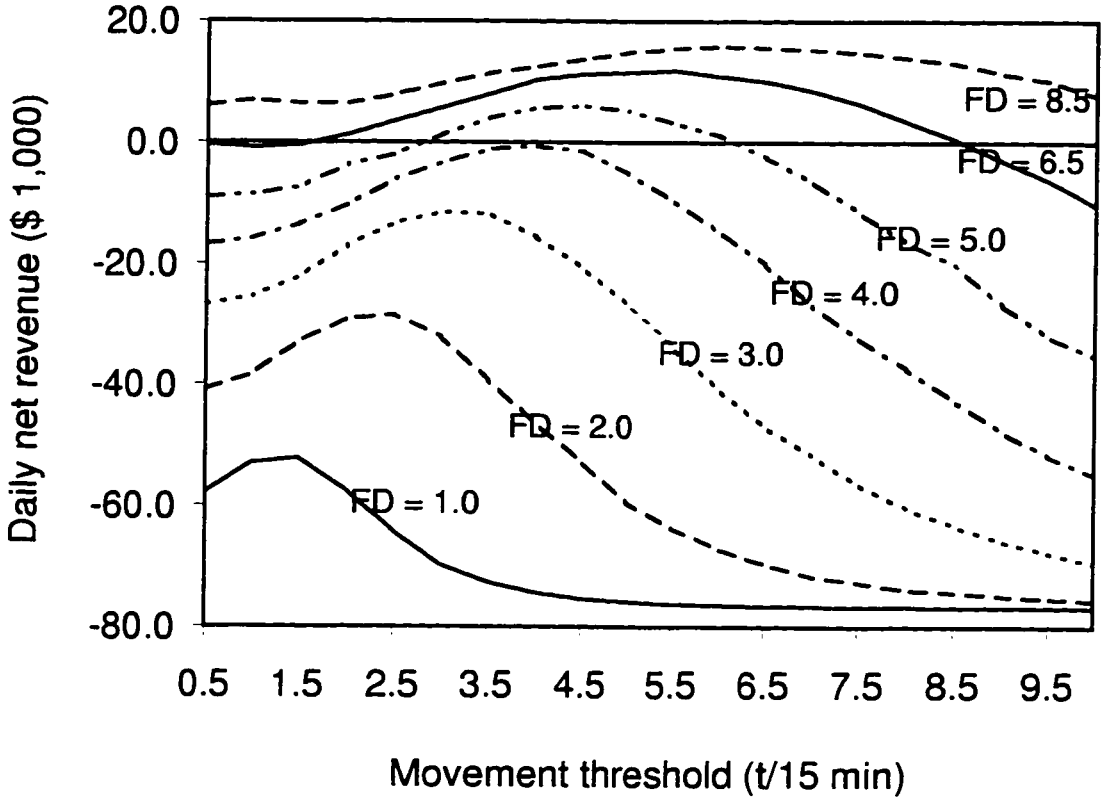
20.0
0.0
-20.0
-40.0
-60.0
-80.0
Daily net revenue ($ 1,000)
FD = 8.5
FD = 6.5
FD = 5.0
FD = 4.0
FD = 3.0
FD = 2.0
FD = 1.0
0.5
1.5
2.5
3.5
4.5
5.5
6.5
7.5
8.5
9.5
Movement threshold (t/15 min)

Figure 3.8. Relationship between mean fish density (expected catch rate in t/15 min) and the movement threshold which maximizes daily net revenue.

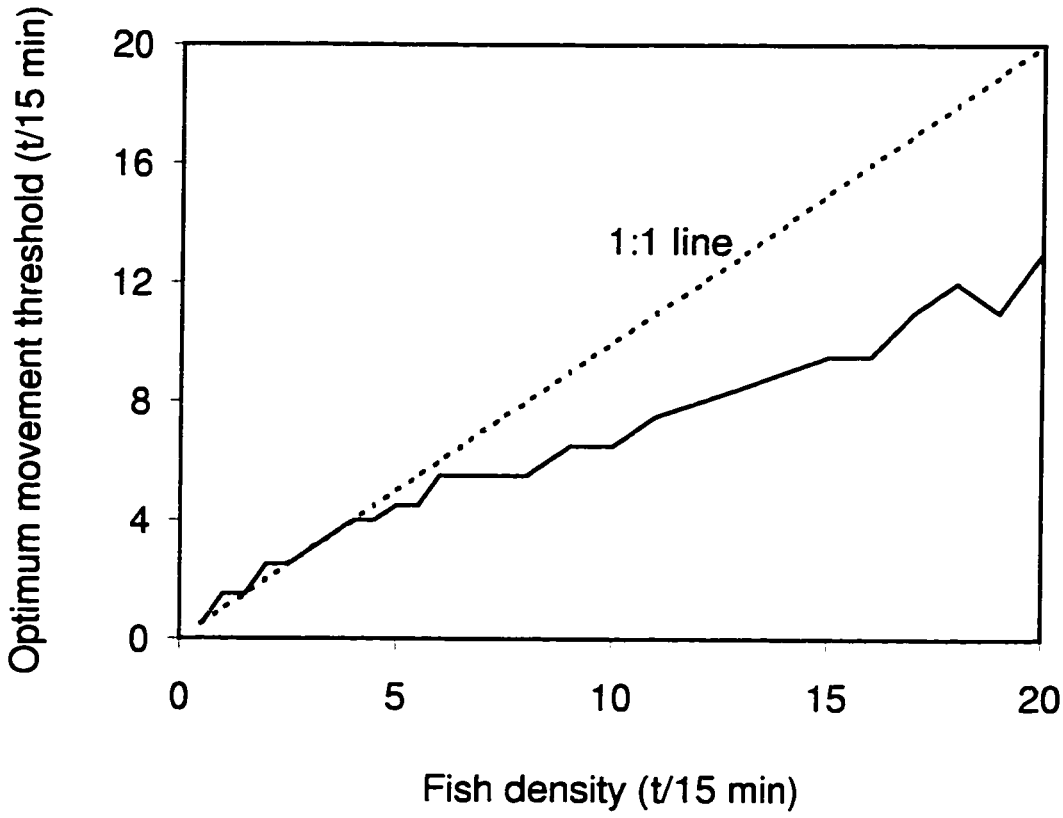
Optimum movement threshold (t/15 min)
20
16
12
8
4
0
1:1 line
0
5
10
15
20
Fish density (t/15 min)

Figure 3.9. Functional response of a factory trawler (catch (t) per day as a function of fish density) for models with a constant mean density, variance in the state transition equation, both variance and autocorrelation in the transition equation, and movement between areas (with both transition variance and autocorrelation). For the model with movement between areas, the functional response curves are shown for vessels with constant and adaptive movement thresholds.

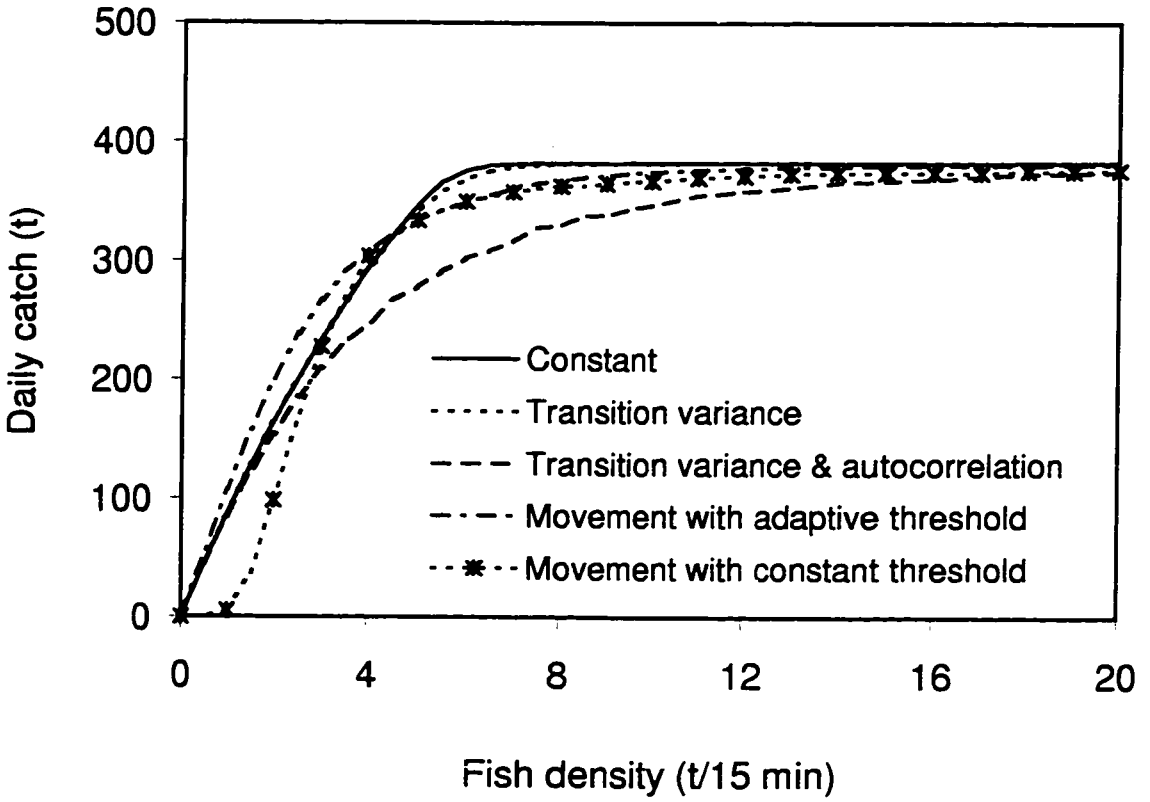
500
400
300
200
100
0
Daily catch (t)
0
4
8
12
16
20
Fish density (t/15 min)
Constant
Transition variance
Transition variance & autocorrelation
Movement with adaptive threshold
Movement with constant threshold

Figure 3.10. Proportion of time allocated to different activities by a factory trawler as a function of mean fish density. (A) For vessel with adaptive movement threshold that adjusts in response to changes mean fish density as in Fig. 9. (B) For vessel with constant movement threshold of 4.5 t/15 min.

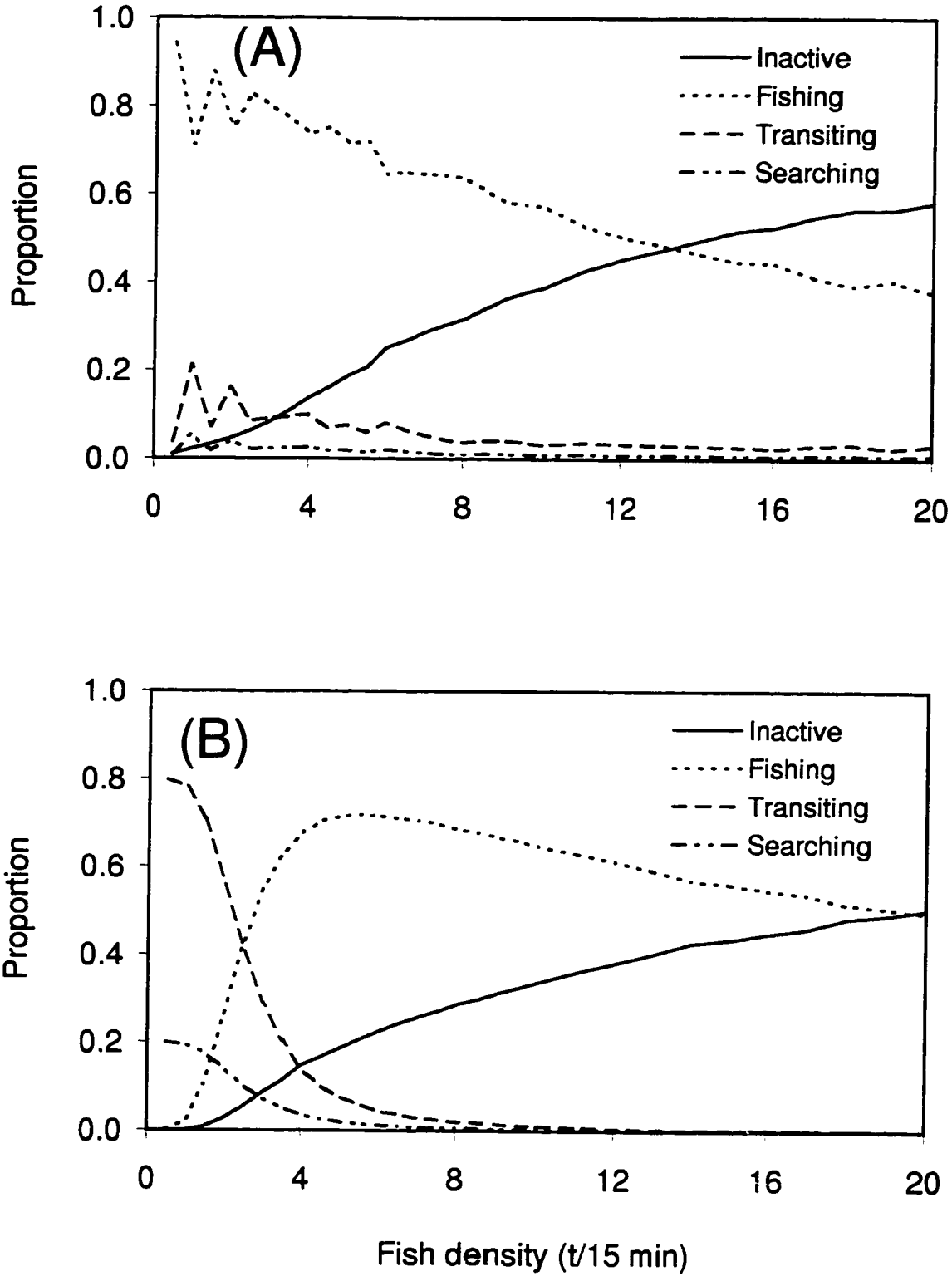
(A)
Inactive
Fishing
Transiting
Searching
Proportion
1.0
0.8
0.6
0.4
0.2
0.0
0
4
8
12
16
20
(B)
Inactive
Fishing
Transiting
Searching
Proportion
1.0
0.8
0.6
0.4
0.2
0.0
0
4
8
12
16
20
Fish density (t/15 min)

Figure 3.11. Relationship between fish density and standard CPUE abundance indices for vessels with constant and adaptive movement thresholds.

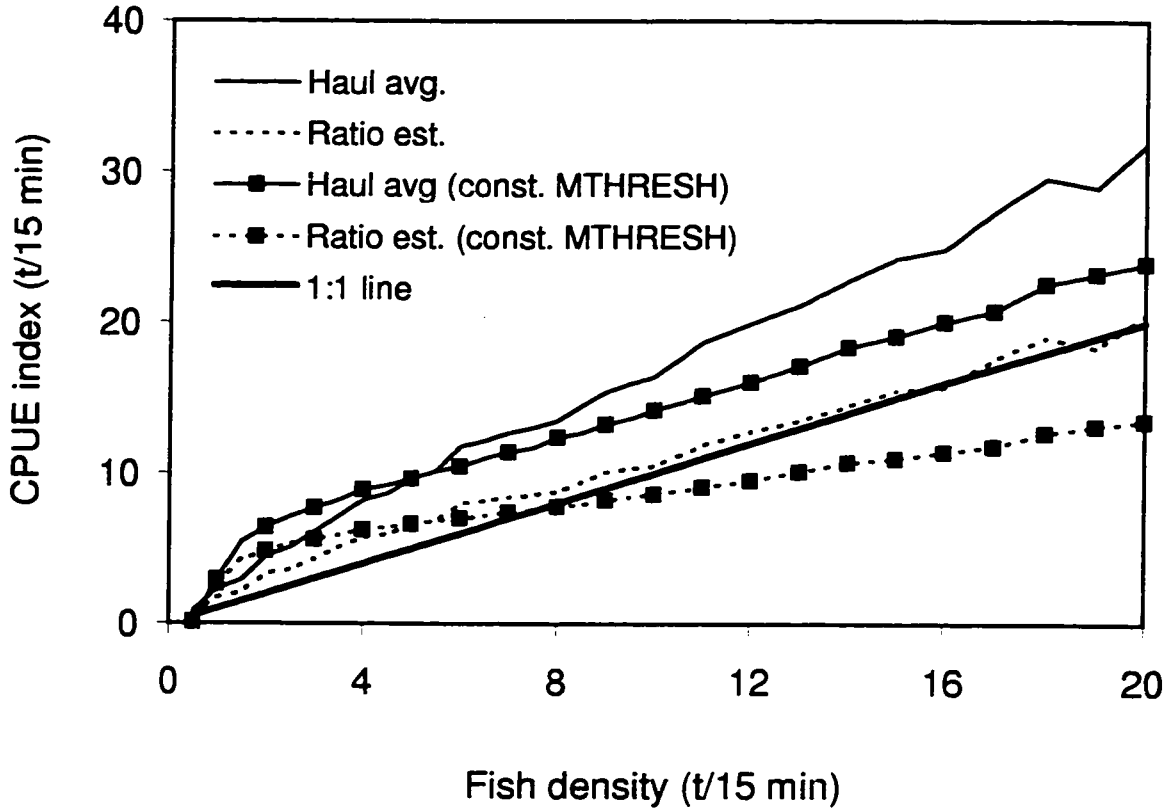
40
30
20
10
0
CPUE index (t/15 min)
Haul avg.
Ratio est.
Haul avg (const. MTHRESH)
Ratio est. (const. MTHRESH)
1:1 line
0
4
8
12
16
20
Fish density (t/15 min)

REFERENCES

Abbott, M. R., and P. M. Zion. 1987. Spatial and temporal variability of phytoplankton pigment off northern California during Coastal Ocean Dynamics Experiment 1. J. Geophys. Res. 92:1745-1756.

Abrahams, M.V., and M. C. Healey. 1990. Variation in the competitive abilities of fishermen and its influence on the spatial distribution of the British Columbia salmon troll fleet. Can. J. Fish. Aquat. Sci. 47:1116-1121.

Allen P. M., and J. M. McGlade. 1986. Dynamics of discovery and exploitation: the case of the Scotian Shelf groundfish fisheries. Can. J. Fish. Aquat. Sci. 43: 1187-1200.

Anganuzzi, A. A. 1995. An aggregate model of effort distribution. Second FAO expert consultation on interactions of Pacific tuna fisheries. Paper No: 5-7.

Arditi, R., and B. Dacorogna. 1985. Optimal foraging in nonpatchy habitats. I. Bounded one-dimensional resource. Math. Biosci. 76:127-145.

Arditi, R., and B. Dacorogna. 1988. Optimal foraging on arbitrary food patches and the definition of habitat patches. Am. Nat. 131:837-846.

Bannerot , S. P. and C. B. Austin. 1983. Using frquency distributions of catch per unit effort to measure fish-stock abundance. Trans. Amer. Fish. Soc. 112:608-617.

Bertsekas, D.P. 1987. Dynamic programming: deterministic and stochastic models. Prentice-Hall, Inc., Englewood Cliffs, N. J. 07632. 376 p.

Bodolt, H., H. Nes, and H. Solli. 1989. A new echo sounder system. Proceedings of the Institute of Acoustics 11:123-130.

Butterworth, D. S. 1988. A simulation study of krill fishing by an individual Japanese trawler. Selected Scientific Papers, Part 1, p 1-108. Commission for the Conservation of Antarctic Marine Living Resources, Hobart (Australia).

Caddy, J. F. 1975. Spatial model for an exploited shellfish population, and its application to the Georges Bank scallop fishery. J. Fish. Res. Board Can. 32:1305-1328.

Chambers, J.M., and Hastie, T.J. 1992. Statistical Models in S. Wadsworth and Brooks, Pacific Grove, CA. 608 p.

Charnov, E. L. 1976. Optimal foraging, the marginal value theorem. Theor. Pop. Biol. 9:129-136.

Clark, C. W. and M. Mangel. 1979. Aggregation and fishery dynamics: a theoretical study of schooling and the purse seine tuna fisheries. Fishery Bull. 77: 317-337.

Dorn, M. W., E. P. Nunnallee, C. D. Wilson and M. E. Wilkins. 1994. Status of the coastal Pacific whiting resource in 1993. U.S. Dep. Commer., NOAA Tech. Memo. NMFS-AFSC-47, 101 pp.

Dorn, M.W. 1997. Mesoscale fishing patterns of factory trawlers in the Pacific hake (Merluccius productus) fishery. Calif. Coop. Oceanic Fish. Invest. Rep. 38:77-89.

Dorn, M. W. 1998. Fine-scale fishing strategies of factory trawlers in a midwater trawl fishery for Pacific hake (Merluccius productus). Can. J. Fish. Aquat. Sci. 55.

Eales, J., and J.E. Wilen. 1986. An examination of fishing location choice in the pink shrimp fishery. Mar. Res. Econ. 2:331-351.

Fisher, F. W. 1994. Past and present status of Central Valley chinook salmon. Conserv. Biol. 8:870-873.

Foote, K. G., H. P. Knudsen, R. J. Korneliussen, P. E. Nordbo, and K. Roang. 1991. Postprocessing system for echo sounder data. J. Acoust. Soc. Am. 90:37-47.

Freese S., Glock J., and Squires D. 1995. Direct allocation of resources and cost-benefit analyses in fisheries, an application to Pacific whiting. Marine Policy 19:199-211.

Fretwell, S. D. and H. J. Jr. Lucas. 1970. On territorial behavior and other factors influencing habitat distribution in birds. Acta Biotheor. 19: 16-36.

Garcia, S. M., and C. Newton. 1995. Current situation, trends and prospects in world capture fisheries. Conf. on Fisheries Management. Global Trends, Seattle (USA), 14-16 Jun. 1994. FAO, Rome (Italy), 63 pp.

Gillis, D. M., R. M. Peterman, and A. V. Tyler. 1993. Movement dynamics in a fishery: application of the ideal free distribution to spatial allocation of effort. Can. J. Fish. Aquat. Sci. 50: 323-333.

Gillis, D. M., R. M. Peterman, and E. K. Pikitch. 1995a. Implications of trip regulations for high-grading: a model of the behavior of fisherman, Can. J. Fish. Aquat. Sci. 52:402-415.

Gillis, D. M., E. K. Pikitch, and R. M. Peterman. 1995b. Dynamic discarding decisions: foraging theory for high-grading in a trawl fishery. Behav. Ecol. 6:146-154.

Harvey, A.C. 1990. Forecasting, structural time series models and the Kalman filter. Cambridge: Cambridge University Press. 554 p.

Hastie, T., and R. Tibshirani. 1990. Generalized additive models. Chapman and Hall, London. 289 pp.

Hilborn, R., and M. Ledbetter. 1979. Analysis of the British Columbia salmon purse-seine fleet: dynamics of movement. J. Fish. Res. Board Can. 36: 384-391.

Hilborn, R. 1985. Fleet dynamics and individual variation: why some people catch more fish than others. Can. J. Fish. Aquat. Sci. 42: 2-13.

Hilborn, R. and C. J. Walters. 1987. A general model for simulation of stock and fleet dynamics in spatially heterogeneous fisheries. Can. J. Fish. Aquat. Sci. 44: 1366-1369.

Holling, C.S. 1992. Cross-scale morphology, geometry, and dynamics of ecosystems. Ecol. Monog. 62:447-502.

Kareiva, P., Morse, D.H., and Ecceleston, J. 1989. Stochastic prey arrivals and crab spider giving-up times: simulations of spider performance using two simple "rules of thumb". Oecologica 78:542-549.

Krebs, J. R. and N. B. Davies. 1991. Behavioral ecology, 3rd. Ed. Blackwell Scientific Publications. Cambridge, MA.

Lane, D.E. 1989. A partially observable model of decision making by fishermen. Oper. Res. 37: 240-254.

Lawless, J. F. 1987. Negative binomial and mixed Poisson regression. Can. J. Stat. 15:209-225.

Lilliefors, H.W. 1967. On the Kolmogorov-Smirnov test for normality with mean and variance unknown. J. Amer. Statist. Assoc. 62:399-402.

MacCall, A. 1990. Dynamic geography of marine fish populations. Univ. of Washington Press, Seattle, WA. 153 p.

Mackas, D. L., L. Washburn, and S. L. Smith. 1991. Zooplankton community pattern associated with a California Current cold filament. J. Geophys. Res. 96:14781-14797.

McCullagh, P., and J. A. Nelder. 1983. Generalized linear models. Chapman and Hall, London. 261 p.

McNamara, J. M., and A. I. Houston. 1985. Optimal foraging and learning. J. Theor. Biol. 117: 231-249.

Mangel, M. 1988. Analysis and modeling of the Soviet Southern Ocean krill fisheries. Selected Scientific Papers, p 127-221. Commission for the Conservation of Antarctic Marine Living Resources, Hobart (Australia).

Mangel, M., and C. W. Clark. 1983. Uncertainty, search, and information in fisheries. J. Cons. int. Explor. Mer, 41:93-103.

Mangel, M., and Clark, C.W. 1988. Dynamic modeling in behavioral ecology. Princeton Univ. Press, Princeton, New Jersey. 308 p.

Mangel, M., and F. R. Adler. 1994. Construction of multidimensional clustered patterns. Ecology 75:1289-1298.

National Marine Fisheries Service. 1996. Our living oceans. Report on the status of U.S. living marine resources, 1995. U.S. Dep. Commer., NOAA Tech. Memo. NMFS-F/SPO-19, 160 p.

Nunnallee, E. P. 1991. An investigation of the avoidance of Pacific whiting (Merluccius productus) to demersal and midwater trawl gear. Int. Coun. Explor. Sea., Paper/B:5,sess. U., Fish Capture Meeting 26 Sep - 4 Oct 1991, La Rochelle, France.

Pelletier, D., and A. M. Parma. 1994. Spatial distribution of Pacific halibut (*Hippoglossus stenolepis*): An application of geostatistics to longline survey data. Can. J. Fish. Aquat. Sci. 51:1506-1518.

Pennington, M. 1983. Efficient estimators of abundance, for fish and plankton surveys. Biometrics 39:281-286.

Polacheck, T., and J. H. Vølstad. 1993. Analysis of spatial variability of Georges Bank haddock (*Melanogrammus aeglefinus*) from trawl survey data using a linear regression model with spatial interaction. ICES J. Mar. Sci. 50:1-8.

Real, L. 1991. Animal choice behavior and the evolution of cognitive architecture. Science 253:980-986.

Rexstad, E. A., and E. K. Pikitch. 1986. Stomach contents and food consumption estimates of Pacific hake, *Merluccius productus*. Fish. Bull., U.S. 84:947-956.

Richards, L. J. and J. T. Schnute. 1992. Statistical models for estimating CPUE from catch and effort data. Can. J. Fish. Aquat. Sci. 49: 1315-1327.

Rossi, R. E., D. J. Mulla, A. G. Journel, and E. H. Franz. 1992. Geostatistical tools for modeling and interpreting ecological spatial dependence. Ecol. Monog. 62:277-314.

Smith, S. J. 1990. Use of statistical models for the estimation of abundance from groundfish trawl survey data. Can. J. Fish. Aquat. Sci. 47:894-903.

Smith, T.D. 1988. Stock assessment methods: the first fifty years. Fish population dynamics. Edited by J.A. Gulland. J. Wiley and Sons, New York. pp. 1-33.

Squires, D., and Kirkley J. 1991. Production quota in multiproduct Pacific fisheries. J. Environ. Econ. Manage. 21:109-126.

Sullivan, P. J. 1991. Stock abundance estimation using depth-dependent trends and spatially correlated variation. Can. J. Fish. Aquat. Sci. 48:1691-1703.

StatSci. 1993. S-Plus for DOS reference manual. Statistical Sciences Inc., Seattle, Wash.

Swartzman, G., C. Huang, and S. Kaluzny. 1992. Spatial analysis of Bering Sea groundfish survey data using generalized additive models. Can. J. Fish. Aquat. Sci. 49:1366-1378.

Thomson R. E., M. C. Healey, J. F. T. Morris, and G. A. Borland. 1992. Commercial troll fishing vessel distribution of Vancouver Island during July 1988: relation to observed physical oceanography. Can. J. Fish. Aquat. Sci. 49:820-832.

Traynor, J. J. 1996. Target-strength measurements of walleye pollock (*Theragra chalcogramma*) and Pacific whiting (*Merluccius productus*). ICES J. Mar. Sci. 53:253-258.

Vignaux, M. 1996a. Analysis of spatial structure in fish distribution using commercial catch and effort data from the New Zealand hoki fishery. Can. J. Fish. Aquat. Sci. 53:963-973.

Vignaux, M. 1996b. Analysis of vessel movements and strategies using commercial catch and effort data from the New Zealand hoki fishery. Can. J. Fish. Aquat. Sci. 53:2126-2136.

Walters, C. 1986. Adaptive management of renewable resources. Macmillan Publishing Company, New York.

Walters, C. and J. J. Maguire. 1996. Lessons for stock assessment from the northern cod collapse. Rev. Fish. Biol. Fish.:6:125-137.

Waples, R. S., R. P. Jones, B. R. Beckman, and G. A. Swan. 1991. Status review for Snake River fall chinook salmon. U.S. Dep. Commer., NOAA Tech. Memo. NMFS F/NWC-194, 81 pp.

Wilson, C. D., and M. A. Guttormsen. 1997. Echo integration-trawl survey of Pacific whiting, *Merluccius productus*, off the west coasts of the U.S. and Canada during July-September 1995. U.S. Dep. Commer., NOAA Tech. Memo. NMFS-AFSC-74, 70 p.

VITA

Name: Martin William Dorn

Birth Place: Seattle, Washington

Birth Date: April 24, 1955

Parents: John and Natalie Dorn

Education:

1976-1979	University of Washington Seattle, Washington B.S. Fisheries
1985-1989	University of Washington Seattle, Washington M.S. Biomathematics
1991-1998	University of Washington Seattle, Washington Ph.D. Fisheries

IMAGE EVALUATION
TEST TARGET (QA-3)

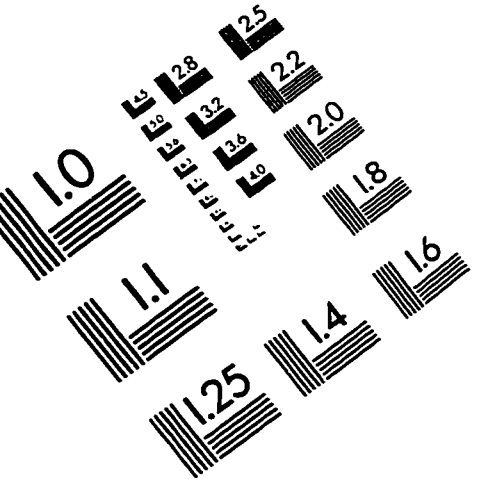

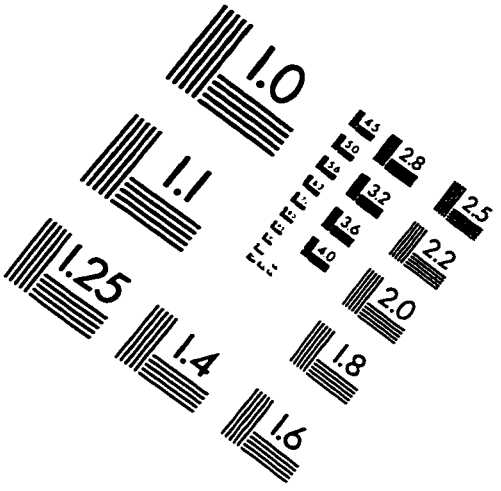

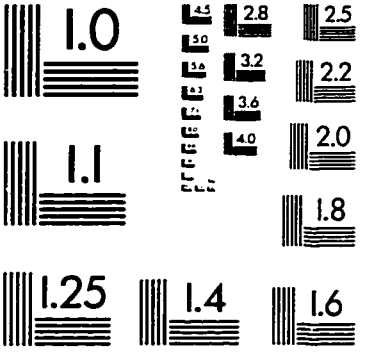

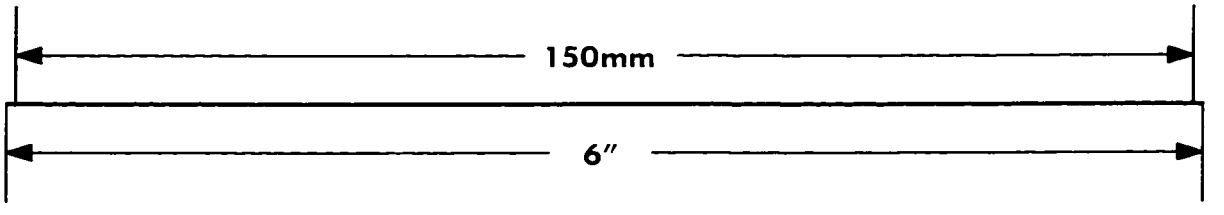

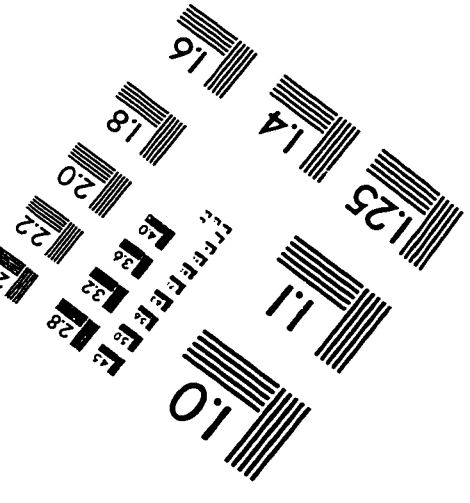

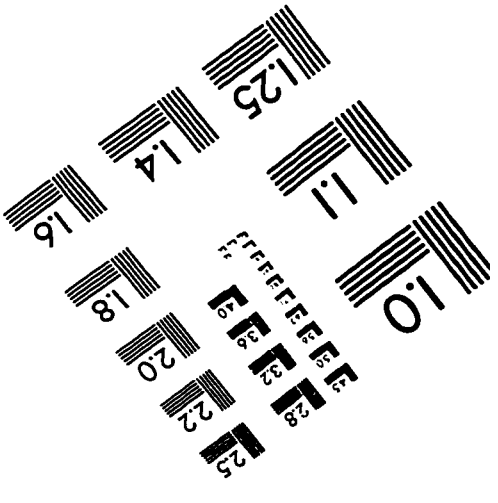

APPLIED IMAGE, Inc
1653 East Main Street
Rochester, NY 14609 USA
Phone: 716/482-0300
Fax: 716/288-5989